

AFRL-SN-RS-TR-2006-21
Final Technical Report
January 2006



**DEVELOPMENT OF A 94 GHZ RADAR SYSTEM
FOR DEDICATED BIRD DETECTION AT
AIRPORTS AND AIRFIELDS**

WaveBand Corporation

APPROVED FOR PUBLIC RELEASE; DISTRIBUTION UNLIMITED.

**AIR FORCE RESEARCH LABORATORY
SENSORS DIRECTORATE
ROME RESEARCH SITE
ROME, NEW YORK**

STINFO FINAL REPORT

This report has been reviewed by the Air Force Research Laboratory, Information Directorate, Public Affairs Office (IFOIPA) and is releasable to the National Technical Information Service (NTIS). At NTIS it will be releasable to the general public, including foreign nations.

AFRL-SN-RS-TR-2006-21 has been reviewed and is approved for publication

APPROVED: /s/

DAVID B. BUNKER
Project Engineer

FOR THE DIRECTOR: /s/

RICHARD G. SHAUGHNESSY, Chief
Rome Operations Office
Sensors Directorate

REPORT DOCUMENTATION PAGE

Form Approved
OMB No. 074-0188

Public reporting burden for this collection of information is estimated to average 1 hour per response, including the time for reviewing instructions, searching existing data sources, gathering and maintaining the data needed, and completing and reviewing this collection of information. Send comments regarding this burden estimate or any other aspect of this collection of information, including suggestions for reducing this burden to Washington Headquarters Services, Directorate for Information Operations and Reports, 1215 Jefferson Davis Highway, Suite 1204, Arlington, VA 22202-4302, and to the Office of Management and Budget, Paperwork Reduction Project (0704-0188), Washington, DC 20503

1. AGENCY USE ONLY (Leave blank)		2. REPORT DATE JANUARY 2006	3. REPORT TYPE AND DATES COVERED Final Sep 02 – Jan 05	
4. TITLE AND SUBTITLE DEVELOPMENT OF A 94 GHZ RADAR SYSTEM FOR DEDICATED BIRD DETECTION AT AIRPORTS AND AIRFIELDS			5. FUNDING NUMBERS C - F30602-02-2-0119 PE - 62805F PR - 4770 TA - SN WU - P2	
6. AUTHOR(S) Lawrence A. Klein and Lev Sadovnik				
7. PERFORMING ORGANIZATION NAME(S) AND ADDRESS(ES) WaveBand Corporation 17152 Armstrong Avenue Irvine California 92614			8. PERFORMING ORGANIZATION REPORT NUMBER N/A	
9. SPONSORING / MONITORING AGENCY NAME(S) AND ADDRESS(ES) Air Force Research Laboratory/SNRT 26 Electronic Parkway Rome New York 13441-4514			10. SPONSORING / MONITORING AGENCY REPORT NUMBER AFRL-SN-RS-TR-2006-21	
11. SUPPLEMENTARY NOTES AFRL Project Engineer: David B. Bunker/SNRT/(315) 330-2345/ David.Bunker@rl.af.mil				
12a. DISTRIBUTION / AVAILABILITY STATEMENT APPROVED FOR PUBLIC RELEASE; DISTRIBUTION UNLIMITED.				12b. DISTRIBUTION CODE
13. ABSTRACT (Maximum 200 Words) WaveBand, as part of a Dual Use and Science and Technology Contract in partnership with the Federal Aviation Administration and the US Air Force Research Laboratory at Rome, NY, developed a 94 GHz radar, named BIRDARTM, to detect and report bird activity at airports and airfields and thus prevent potential bird strikes with aircraft during landing and takeoff. The radar is compact, utilizing a state-of-the-art 575 mW solid state millimeter-wave power source. WaveBand's patented scanning antenna is used to transmit and receive signals that detect and track birds. The return signals are processed in a radar signal processor incorporated into a low-cost PC architecture. The integrated monitor displays the backscattered power in several ways. The primary format is backscattered power in range versus azimuth angle or transformed azimuth distance. Alternate displays of moving targets superimposed on GIS maps or two-dimensional perspective imagery, with near-photographic quality, corresponding to the backscattered power are also available. Months of testing at several venues proved the final radar design to exhibit reliable performance. Calibration, test, and evaluation sites included USAFRL Rome, NY; JFK Airport, NY; Klamath Basin, OR; El Mirage Dry Lake, CA; Salton Sea CA; Bolsa Chica Bird Reserve, CA; and DFW Airport, TX. Small bird detections were reported at distances of 1.2 to 1.3 km and large birds, such as geese, at distances of 2.3 to 2.6 km during these tests. Final testing at DFW Airport was a great success in that the radar functioned perfectly throughout and was able to detect birds of opportunity at ranges that provided data to substantiate the extrapolation of future radar designs to the detection of large bird flocks at 3 miles. Substantial coverage of the final DFW tests was provided by members of radio, TV, and the printed press.				
14. SUBJECT TERMS Bird Detection Radar, Millimeter-Wave Bird Detection Sensor, Bird Strike Prevention, Aircraft Safety			15. NUMBER OF PAGES 101	
			16. PRICE CODE	
17. SECURITY CLASSIFICATION OF REPORT UNCLASSIFIED	18. SECURITY CLASSIFICATION OF THIS PAGE UNCLASSIFIED	19. SECURITY CLASSIFICATION OF ABSTRACT UNCLASSIFIED	20. LIMITATION OF ABSTRACT UL	

TABLE OF CONTENTS

EXECUTIVE SUMMARY	1
1. PROGRAM DESCRIPTION AND RADAR DEVELOPMENT HISTORY	2
2. AFRL RADAR CALIBRATION TESTS	8
3. KLAMATH FALLS TESTS	11
4. EL MIRAGE DRY LAKE BED TESTS.....	14
5. SALTON SEA TESTS.....	17
6. BOLSA CHICA BIRD RESERVE TESTS	25
7. DFW AIRPORT TESTS	26
8. RADAR PERFORMANCE SUMMARY	28
9. LESSONS LEARNED	28
10. NEED FOR MODIFIED RADAR DESIGNS TO MEET AUTOMATIC DETECTION RANGE GOAL OF 3 MILES	29
11. RADAR DESIGN AND PERFORMANCE CONSIDERATIONS FOR BIRDAR™ WITH AUTOMATIC DETECTION FEATURE	31
11.1 RANGE RESOLUTION CELL AND NUMBER OF RANGE BINS	31
11.2 TIME BIRD REMAINS IN A RANGE RESOLUTION CELL	31
11.3 TRANSMITTED WAVEFORM	31
11.4 RF MODULATION FREQUENCY	32
11.5 NONCOHERENT INTEGRATION OF RADAR RETURNS OVER SEVERAL FRAMES	33
11.6 NONCOHERENT FRAME INTEGRATION AS A FUNCTION OF DETECTION AND FALSE ALARM PROBABILITIES	33
11.7 RADAR RANGE EQUATION EXPRESSED AS SIGNAL-TO-NOISE RATIO.....	37
11.8 MODELED DETECTION RANGE	38
11.9 REDUCED DRUM ROTATION SPEED AND SPATIAL INTEGRATION	39
11.10 ANTENNA CONFIGURATION TO REDUCE GROUND RETURN.....	40
11.11 RADAR DESIGNS FOR AUTOMATIC TARGET DETECTION	40
<i>Signal-to-noise ratio improvement.....</i>	<i>40</i>
<i>RF modulation frequency.....</i>	<i>41</i>
<i>Noise bandwidth.....</i>	<i>44</i>
<i>Noncoherent integration</i>	<i>45</i>
<i>Radar performance summary.....</i>	<i>45</i>
11.12 IMPROVED MOVING TARGET INDICATOR ALGORITHM	46
11.13 COHERENT RECEIVER DESIGN AND SIGNAL DEMODULATION	46
12. BENEFIT SUMMARY	49
13. DEVELOPMENT AND DEMONSTRATION SCHEDULE	49
13.1 TASK SUMMARY BY YEAR	51
APPENDIX A: 94 GHZ BIRD DETECTION RADAR FIELD TEST PLAN	52
APPENDIX B: PROTOCOL FOR FIELD TESTING OF THE 94 GHZ BIRD DETECTION RADAR AT THE DFW AIRPORT	74

LIST OF FIGURES

FIGURE 1-1. 94 GHZ OPERATIONAL RADAR SYSTEM TO DETECT BIRDS AT AIRFIELDS.	3
FIGURE 1-2. SIMPLIFIED BIRDARTM TRANSCEIVER BLOCK DIAGRAM.	3
FIGURE 1-3. TRANSMITTED FMCW SIGNAL.	4
FIGURE 1-4. IMPATT TRANSCEIVER.	5
FIGURE 1-5. MMIC SOLID STATE RADAR TRANSCEIVER CONFIGURATION USED AT AFRL ROME, KLAMATH BASIN, SALTON SEA, BOLSA CHICA BIRD RESERVE, AND DFW AIRPORT.	5
FIGURE 1-6. MMIC SOLID STATE TRANSCEIVER COMPONENTS.	6
FIGURE 1-7. ASSEMBLED 0.5-DEGREE X 5-DEGREE BEAMWIDTH ANTENNA AND MMIC SOLID STATE TRANSCEIVER. ..	7
FIGURE 2-1. RADAR MOUNTED IN WEATHERPROOF ENCLOSURE ON TRAILER AT AFRL, ROME, NY.	9
FIGURE 2-2. RADAR CONTROL AND SIGNAL PROCESSING EQUIPMENT.	9
FIGURE 2-3. SCENE IMAGE AS RECORDED BY VIDEO CAMERA BORESIGHTED WITH THE ANTENNA.	10
FIGURE 2-4. (A) CALIBRATION CORNER REFLECTOR TARGET. (B) GROUND AND CORNER REFLECTOR RETURNS DISPLAYED ON MONITOR.	10
FIGURE 2-5. ALUMINUM SPHERE CALIBRATION TARGET SUSPENDED FROM A TETHERED BALLOON AT AFRL, ROME, NY.	11
FIGURE 3-1. EXPERIMENTAL SETUP AT THE KLAMATH BASIN.	13
FIGURE 3-2. TEST LOCATIONS IN THE KLAMATH BASIN.	13
FIGURE 3-3. SNOW GEESE DETECTED BY BIRDAR™ AT KLAMATH BASIN.	14
FIGURE 4-1. EL MIRAGE DRY LAKE BED.	15
FIGURE 4-2. 94 GHZ RADAR AS MOUNTED IN TRAILER WITH ANTENNA IN VERTICAL POSITION AT EL MIRAGE DRY LAKE BED.	15
FIGURE 4-3. KITE WITH METAL SPHERE SUSPENDED BELOW IT (IN BLACK CIRCLE). TAIL OF KITE IS BEHIND THE KITE AND NOT AT THE SAME ALTITUDE AS THE SPHERE.	15
FIGURE 4-4. DETECTION OF TRANSMISSION WIRES AT EL MIRAGE DRY LAKE BED WITH 94 GHZ RADAR.	17
FIGURE 5-1. TEST LOCATIONS AT THE SALTON SEA.	18
FIGURE 5-2. RADAR TRAILER SETUP ALONG SHORE OF SALTON SEA NEAR RED HILL MARINA ON EVENING OF AUGUST 26, 2004. VIEW OF RADAR IS TOWARD THE SALTON SEA.	19
FIGURE 5-3. EVENING BIRD ACTIVITY – SALTON SEA AUGUST 26, 2004.	19
FIGURE 5-4. RCS OF INDIVIDUAL BIRD DETECTION AT 1.6 KM OVER SALTON SEA EVENING OF AUGUST 26, 2004.	20
FIGURE 5-5. RADAR TRAILER SETUP ALONG ROAD LEADING TO RED HILL MARINA AND SALTON SEA ON MORNING OF AUGUST 27, 2004. VIEW OF RADAR IS TOWARD THE SALTON SEA.	21
FIGURE 5-6. TYPICAL EARLY MORNING BIRD ACTIVITY – SALTON SEA AUGUST 27, 2004.	21
FIGURE 5-7. RCS OF INDIVIDUAL BIRD DETECTION AT 1.9 KM OVER SALTON SEA MORNING OF AUGUST 27, 2004.	22
FIGURE 5-8. RCS OF INDIVIDUAL BIRD DETECTION AT 2.3 KM OVER SALTON SEA MORNING OF AUGUST 27, 2004.	23
FIGURE 5-9. RCS OF BIRD FLOCK DETECTION AT 2.6 KM. BIRDS WERE FLYING TOWARD SALTON SEA MORNING OF AUGUST 27, 2004.	24
FIGURE 6-1. BOLSA CHICA BIRD RESERVE LOCATION, HUNTINGTON BEACH, CA.	25
FIGURE 6-2. GULLS AND CORMORANTS FLYING OVERHEAD AT BOLSA CHICA BIRD RESERVE, HUNTINGTON BEACH, CA JUST BEFORE SUNRISE.	26
FIGURE 7-1. RADAR CALIBRATION AT DFW AIRPORT.	27
FIGURE 7-2. RADAR OPERATOR AT CONSOLE INSIDE TRAILER.	28
FIGURE 11-1. TRANSMITTED WAVEFORMS: (A) UPSWEEP COMPONENT ONLY. (B) UPSWEEP AND DOWNSWEEP COMPONENTS.	32
FIGURE 11-2. SNR FOR DETECTION PROBABILITIES OF 0.90 AND 0.95 FOR NON-FLUCTUATING TARGETS (SOURCE: M. SKOLNIK, <i>RADAR HANDBOOK</i> , MCGRAW-HILL BOOK COMPANY, NY, 1970).	34
FIGURE 11-3. SNR FOR DETECTION PROBABILITIES OF 0.90 AND 0.95 FOR SWERLING 1 FLUCTUATING TARGETS (SOURCE: M. SKOLNIK, <i>RADAR HANDBOOK</i> , MCGRAW-HILL BOOK COMPANY, NY, 1970).	35
FIGURE 11-4. NONCOHERENT VIDEO INTEGRATION OF INDEPENDENT SIGNAL SAMPLES SHOWING REDUCTION IN VARIANCE OF NOISE AND SIGNAL PLUS NOISE. (SOURCE: L.A. KLEIN, <i>MILLIMETER-WAVE AND INFRARED MULTISENSOR DESIGN AND SIGNAL PROCESSING</i> , ARTECH HOUSE, NORWOOD, MA, 1997).	36
FIGURE 11-5. TYPE 1 AND TYPE 2 TARGET CLASSIFICATION ERRORS ARE REDUCED BY NONCOHERENT INTEGRATION AS A RESULT OF THE DECREASE IN VARIANCE OF THE NOISE AND SIGNAL PLUS NOISE. (SOURCE: L.A. KLEIN, <i>SENSOR AND DATA FUSION: A TOOL FOR INFORMATION ASSESSMENT AND DECISION MAKING</i> , SPIE PRESS MONOGRAPH 138,	36

FIGURE 11-6. 94 GHZ BIRDAR™ SNR FOR ORIGINAL AND DFW AIRPORT RADAR CONFIGURATIONS ASSUMING BIRD FLOCK TARGETS WITH RCS = 0.03M ²	38
FIGURE 11-7. TWO DIMENSIONAL ANTENNA SCANNING CONCEPT	40
FIGURE 11-8. ANTENNA ROTATION SPEED AND MODULATION FREQUENCY ANALYSIS.	41
FIGURE 11-9. SNR FOR PROPOSED 35 AND 94 GHZ BIRDAR™ RADARS ASSUMING BIRD FLOCK TARGETS WITH RCS = 0.03M ²	45
FIGURE 11-10. TRANSMITTED UP AND DOWNSWEEP WAVEFORM SHOWING DOPPLER FREQUENCY CALCULATION. (SOURCE: L.A. KLEIN, <i>MILLIMETER-WAVE AND INFRARED MULTISENSOR DESIGN AND SIGNAL PROCESSING</i> , ARTECH HOUSE, NORWOOD, MA, 1997.)	47
FIGURE 11-11. SUPERHETERODYNE TRANSCEIVER.	48
FIGURE 11-12. QUADRATURE DEMODULATION USING DIRECT IF SAMPLING AND DIGITAL I AND Q.	49
FIGURE 13-1. BIRDAR™ DEVELOPMENT AND DEMONSTRATION SCHEDULE	50

LIST OF TABLES

TABLE 1-1. RADAR OPERATIONAL CONSIDERATIONS FOR BIRD DETECTION.....	2
TABLE 1-2. 94 GHZ ORIGINAL BIRDAR™ DESIGN PARAMETERS.....	6
TABLE 1-3. 94 GHZ BIRDAR™ DESIGN PARAMETERS USED AT SALTON SEA AND DFW.....	8
TABLE 3-1. SAMPLE RADAR PARAMETER TEST MATRIX.....	12
TABLE 3-2. SOME MAJOR DETECTIONS AT THE KLAMATH BASIN TESTS.....	14
TABLE 4-1. EL MIRAGE TEST RESULTS.....	16
TABLE 4-2. INDIVIDUAL BIRD X-BAND RCS MEASUREMENT DATA FROM SEVERAL SOURCES.....	16
TABLE 5-1. SOME MAJOR DETECTIONS AT THE SALTON SEA TEST.....	21
TABLE 8-1. DEMONSTRATED RANGE DETECTION PERFORMANCE OF BIRDAR™ AT DFW AIRPORT, KLAMATH FALLS, SALTON SEA, AND EL MIRAGE DRY LAKE BED (WITH HUMAN OBSERVER FOR TARGET DETECTION).....	28
TABLE 10-1. PREDICTED RANGE DETECTION PERFORMANCE OF IMPROVED 94 GHZ AND 35 GHZ RADARS WITH HUMAN (SNR = 0 DB) AND AUTOMATIC TARGET DETECTION (SNR = 15 DB).....	30
TABLE 11-1. SNR CALCULATION FOR ORIGINAL 94 GHZ BIRDAR™ DESIGN.....	39
TABLE 11-2. ONE-WAY ABSORPTION (REF. N.C. CURRIE AND C.E. BROWN, PRINCIPLES AND APPLICATIONS OF MILLIMETER-WAVE RADAR, ARTECH HOUSE, NORWOOD, MA, 1987).....	41
TABLE 11-3. 35 GHZ BIRDAR™ DESIGN PARAMETERS.....	43
TABLE 11-4. IMPROVED 94 GHZ BIRDAR™ DESIGN PARAMETERS.....	44
TABLE 11-5. MAXIMUM NUMBER OF RETURNS NONCOHERENTLY INTEGRATED IN A 2.3 M RANGE RESOLUTION CELL WHEN THE RF MODULATION OCCURS OVER $T_M/2 = 2$ MS AND BIRDS FLY AT SPEEDS OF 20 AND 30 MI/H.....	45

EXECUTIVE SUMMARY

WaveBand, as part of a Dual Use and Science and Technology Contract in partnership with the Federal Aviation Administration and the US Air Force Research Laboratory at Rome, NY, developed a 94 GHz radar, named BIRDAR™, to detect and report bird activity at airports and airfields and thus prevent potential bird strikes with aircraft during landing and takeoff.

The radar is compact, utilizing a state-of-the-art 575 mW solid state millimeter-wave power source. WaveBand's patented scanning antenna is used to transmit and receive signals that detect and track birds. The return signals are processed in a radar signal processor incorporated into a low-cost PC architecture. The integrated monitor displays the backscattered power in several ways. The primary format is backscattered power in range versus azimuth angle or transformed azimuth distance. Alternate displays of moving targets superimposed on GIS maps or two-dimensional perspective imagery, with near-photographic quality, corresponding to the backscattered power are also available.

Months of testing at several venues proved the final radar design to exhibit reliable performance. Calibration, test, and evaluation sites included USAFRL Rome, NY; JFK Airport, NY; Klamath Basin, OR; El Mirage Dry Lake, CA; Salton Sea CA; Bolsa Chica Bird Reserve, CA; and DFW Airport, TX. Small bird detections were reported at distances of 1.2 to 1.3 km and large birds, such as geese, at distances of 2.3 to 2.6 km during these tests.

Final testing at DFW Airport was a great success in that the radar functioned perfectly throughout and was able to detect birds of opportunity at ranges that provided data to substantiate the extrapolation of future radar designs to the detection of large bird flocks at 3 miles. Substantial coverage of the final DFW tests was provided by members of radio, TV, and the printed press.

1. PROGRAM DESCRIPTION AND RADAR DEVELOPMENT HISTORY

WaveBand, as part of a Dual Use and Science and Technology Contract in partnership with the Federal Aviation Administration and the US Air Force Research Laboratory at Rome, NY, developed a 94 GHz radar to detect birds at airports and airfields that could potentially interfere with the landing and takeoff of aircraft. The requirements for the radar system are summarized in table 1-1.

TABLE 1-1. RADAR OPERATIONAL CONSIDERATIONS FOR BIRD DETECTION.

Constraint	Description
Objective	Detect and track movement of bird species in and around airports
Altitude	Up to 3,000 ft (0.91 km) AGL in airport approach and departure corridors
Radar mounting height	Function of proximity to runway
Detection range	3 statute mi (4.8 km) minimum, 5 statute mi (8 km) desired (multiple radar units can be used)
Data latency	10 seconds for newest information to appear on display

The radar system developed by WaveBand was subsequently given the name BIRDAR™. The radar system concept is illustrated in figure 1-1. BIRDAR™ detects and reports bird activity in the airspace surrounding airports in order to decrease bird encounters with aircraft.

The antenna scans a 30-degree by 2.5-degree or 30-degree by 5-degree field of view, depending on the model selected. Separate transmit and receive antennas are used to increase the isolation between the transmitted and received signals. A video camera is mounted on top of the radar to capture imagery from the scanned area. The primary purpose of this feature was to assist in assessing the performance of the radar during its development.

The transceiver consists of transmitter and a receiver sections as illustrated in figure 1-2. The transmitter produces a 94 GHz signal generated by the low phase noise signal source. The signal is amplified to its final value of 575 mW. The first stage in the receiver is a low noise amplifier, which increases the backscattered signal power captured by the receive antenna and lowers the composite noise figure of the receiver. The mixer downconverts the received energy into an intermediate frequency (IF) band that extends to approximately 5 MHz. After amplification and filtering, the IF signal is passed to the data acquisition card in the PC radar signal processor.

The magnitude of the voltage supplied to the motor inside the antenna module controls the speed of the spinning drums. Other power supplies provide the required voltages and currents to the transceiver components.

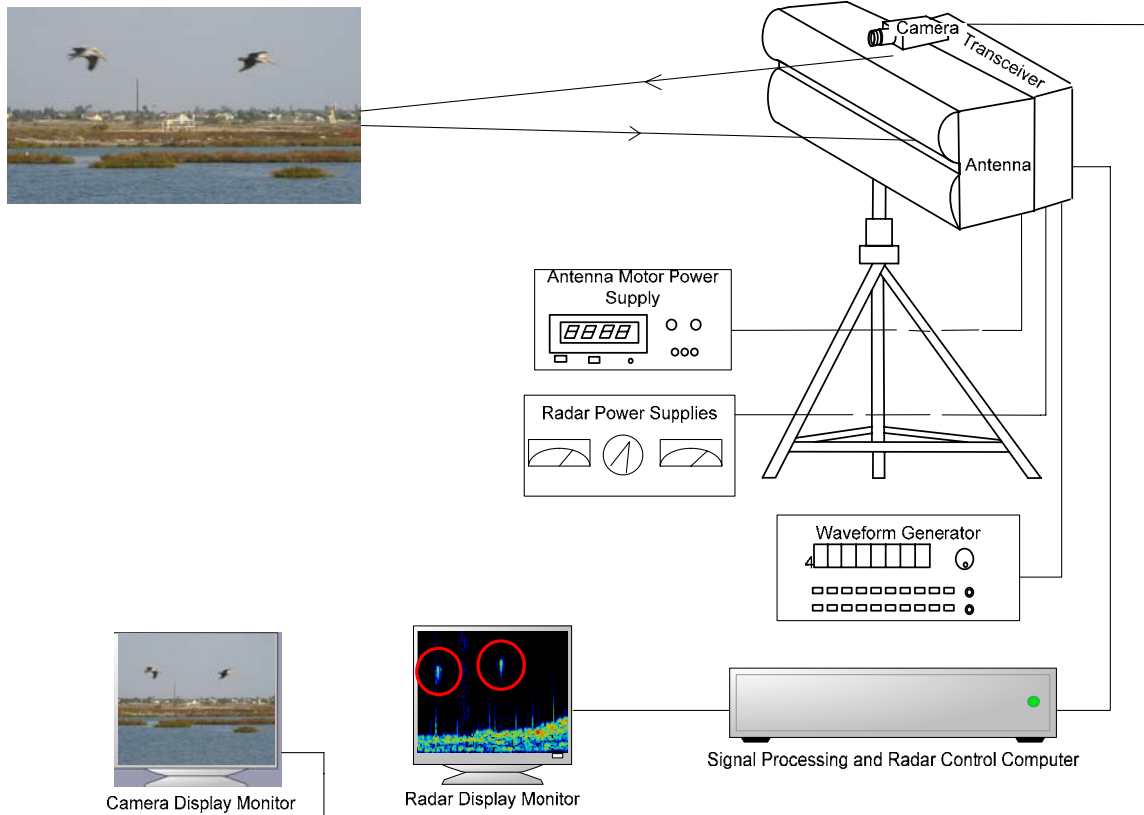


FIGURE 1-1. 94 GHZ OPERATIONAL RADAR SYSTEM TO DETECT BIRDS AT AIRFIELDS.

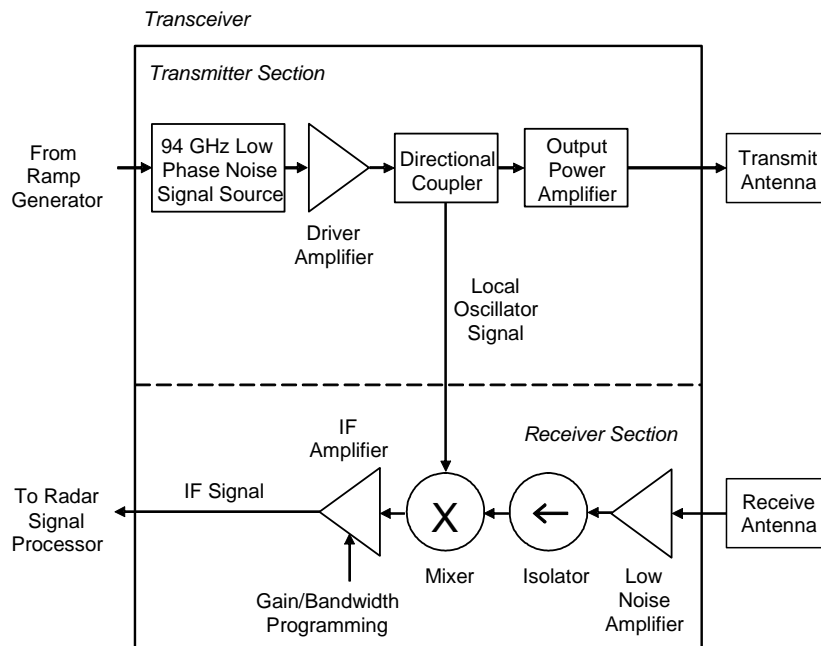


FIGURE 1-2. SIMPLIFIED BIRDARTM TRANSCIEVER BLOCK DIAGRAM.

The radar signal processor is based on a PC architecture. The PC contains a data acquisition card that digitizes the input IF signal and converts it into a frequency-domain, Fast Fourier Transform (FFT) spectrum. The FFT represents the backscattered radar power as a function of range (measured from the radar location). There is one FFT range power spectrum for each 0.5 degree beamwidth spatial resolution angle scanned by the antenna.

The BIRDAR™ models produced to date use an Agilent waveform generator, controlled through the PC bus to provide the linear voltage sweep that generates the FMCW signal. The magnitude of the voltage sweep adjusts the RF bandwidth of the transmitted signal to the required frequency deviation illustrated in figure 1-3. Future models will replace the external waveform generator with a waveform synthesis card connected to a PC bus.

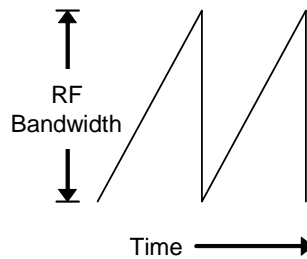


FIGURE 1-3. TRANSMITTED FMCW SIGNAL.

The radar monitor displays the backscattered power in several ways. The primary format is backscattered power in range versus azimuth angle or transformed azimuth distance. Alternate displays of moving targets superimposed on GIS maps or two-dimensional perspective imagery, with near-photographic quality, corresponding to the backscattered power are also available.

The camera monitor presents a visual image of the scene in the radar's field of view.

Several iterations of the radar were produced. The first model employed an IMPATT millimeter-wave (MMW) power source and the patented WaveBand high resolution, scanning antenna. A block diagram of this transceiver is shown in figure 1-4. Its specifications are given in table 1-2.

This version was tested locally in California and at JFK Airport. Although it initially functioned well, the antenna construction was not rugged enough to withstand the rigors of shipping to the various test sites that were utilized. Also, the IMPATT required a high voltage power supply that was awkward to transport. As a result of the antenna construction, performance suffered and the antenna was redesigned. Appendix A contains the test plan for the JFK tests.

The subsequent radar model was more robust and used a solid state MMW power source constructed from MMIC chips. The MMIC power amplifier also produced 1.3 dB more output power than the IMPATT version. The construction of the antenna was modified to simplify assembly and to seal the transmit and receive chambers from one another, increasing isolation and reducing cross talk between the transmitted and received signals. Months of testing proved this design to exhibit reliable performance. A block diagram of this transceiver and photograph

are shown in figures 1-5 and 1-6, respectively. The assembled 0.5-degree x 5-degree beamwidth antenna and transceiver are shown in figure 1-7. Another scanning antenna having a 0.5-degree x 2.5-degree beamwidth was designed and built. The advantage of this antenna was an increase in two-way antenna gain of 6 dB and improved detection range performance. The specifications for this version of the radar are given in table 1-3.

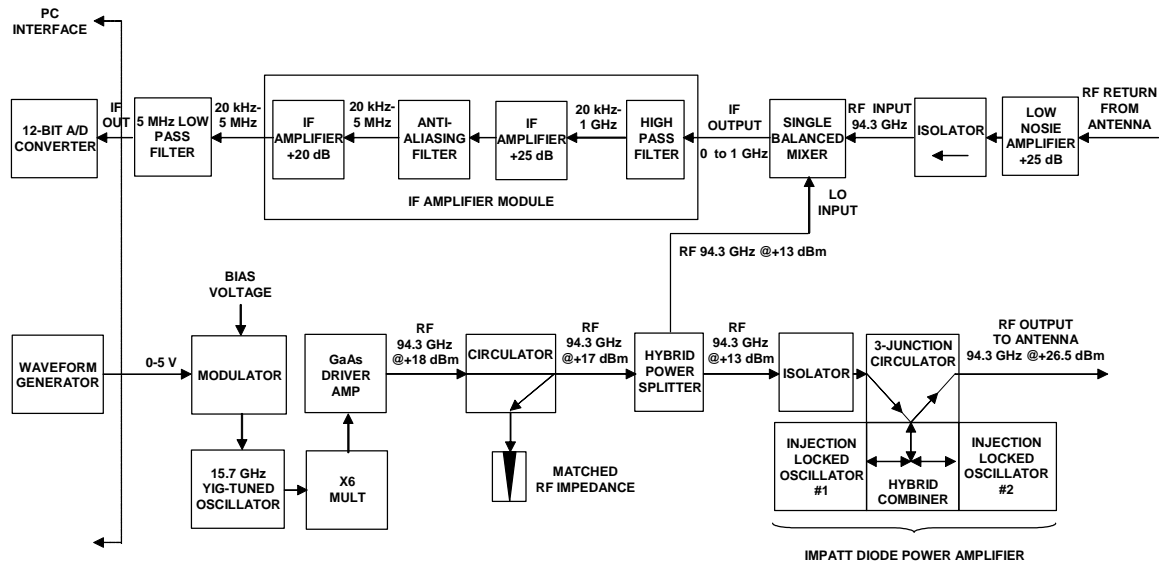


FIGURE 1-4. IMPATT TRANSCEIVER.

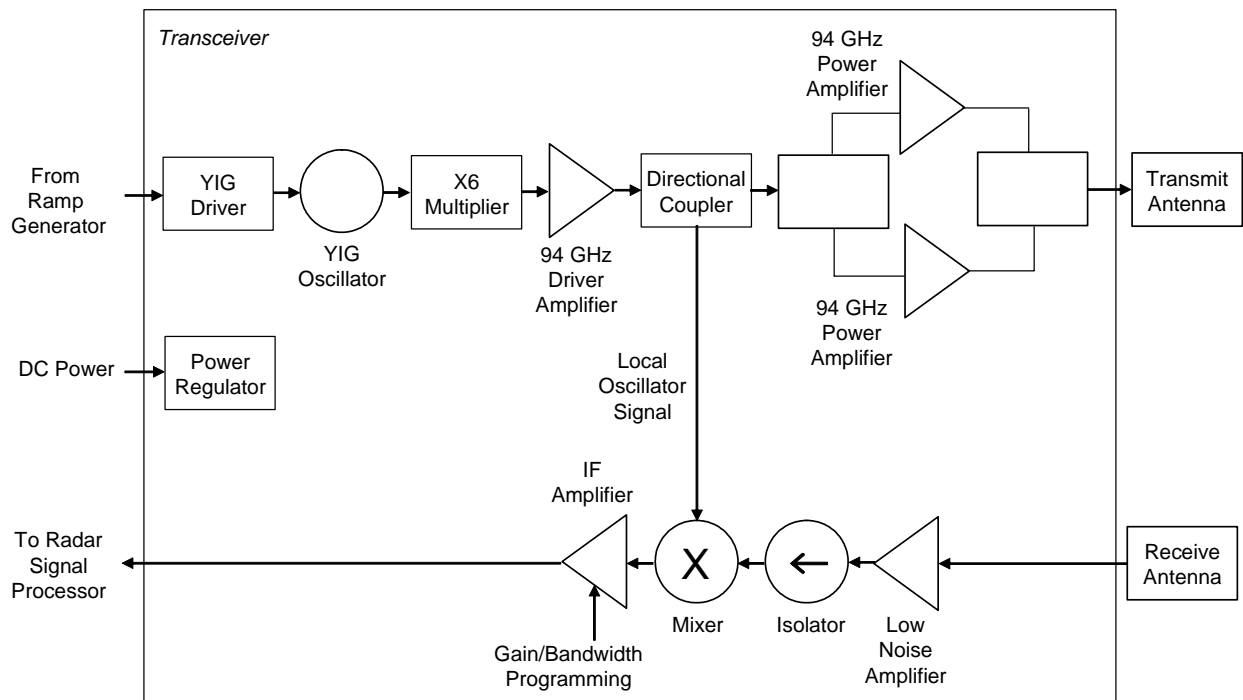


FIGURE 1-5. MMIC SOLID STATE RADAR TRANSCEIVER CONFIGURATION USED AT AFRL ROME, KLAMATH BASIN, SALTON SEA, BOLSA CHICA BIRD RESERVE, AND DFW AIRPORT.

TABLE 1-2. 94 GHZ ORIGINAL BIRDAR™ DESIGN PARAMETERS.

Parameter	Value
Center frequency	94.3 ± 0.5 GHz
Azimuth beamwidth	0.5 degree
Elevation beamwidth	5 degrees
Antenna gain (transmit and receive, each)	38 dB
Antenna polarization	Vertical (when narrow beamwidth is in azimuth direction)
Antenna losses (one way)	Less than 3 dB
Azimuth scan field of view	30 degrees
Azimuth scan time function	Linear, true continuous
Azimuth scan speed	10 scans per second
Angles/frame	60
Output power	430 mW CW
Noise figure	6 dB with low noise amplifier
IF bandwidth	5 MHz
RF modulation bandwidth	230 MHz
RF modulation period T_m	1.6 ms
Image band rejection	0 dB
IF processing	8K FFT (4K utilized giving 36 dB processing gain)
IF dynamic range	82 dB
Displayed range cells	Up to 4K per azimuth beam
Range cell size	2.1 ft (0.65 m)
Target radar cross section	0.0015 m ² for individual birds 0.03 m ² for bird flocks



FIGURE 1-6. MMIC SOLID STATE TRANSCEIVER COMPONENTS.

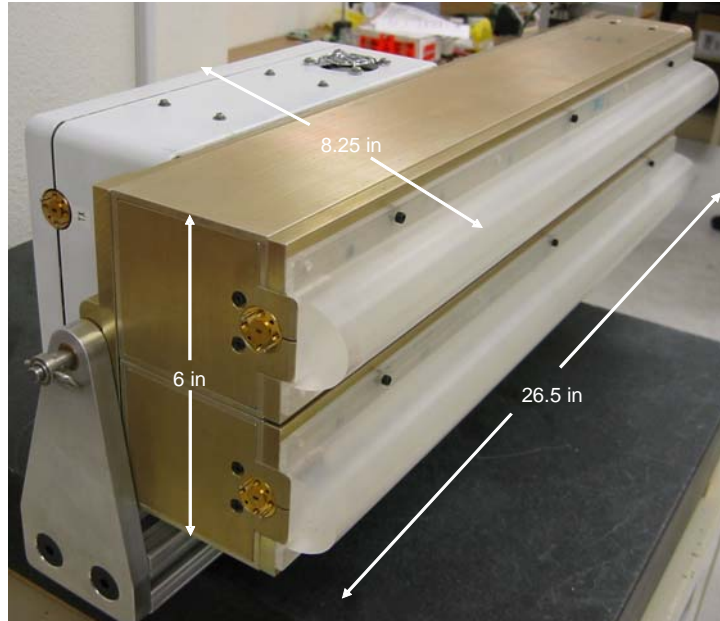


FIGURE 1-7. ASSEMBLED 0.5-DEGREE X 5-DEGREE BEAMWIDTH ANTENNA AND MMIC SOLID STATE TRANSCEIVER.

Radar analysis procedures and equations for designing and predicting radar performance are given later in Section 11.

TABLE 1-3. 94 GHZ BIRDAR™ DESIGN PARAMETERS USED AT SALTON SEA AND DFW.

Parameter	Value
Center frequency	94.3 ± 0.5 GHz
Azimuth beamwidth	0.5 degree
Elevation beamwidth	2.5 degrees
Antenna gain (transmit and receive, each)	36 dB
Antenna polarization	Vertical (when narrow beamwidth is in azimuth direction)
Total losses (FFT window, signal processing, atmospheric, waveguide)	9 dB
Azimuth scan field of view	30 degrees
Azimuth scan time function	Linear, true continuous
Azimuth scan speed	2.4 scans per second
Angles/frame	90
Output power	575 mW CW
Noise figure	6 dB with low noise amplifier
IF bandwidth	0.5 MHz
RF modulation bandwidth	65 MHz
RF modulation period T_m	4.1 ms
Image band rejection	0 dB
IF processing	4K FFT (2K utilized giving 33 dB processing gain)
IF dynamic range	82 dB
Displayed range cells	Up to 2K per azimuth beam
Range cell size	7.5 ft (2.3 m)
Target radar cross section	0.0015 m ² for individual birds 0.03 m ² for bird flocks

2. AFRL RADAR CALIBRATION TESTS

In March 2004, WaveBand conducted radar calibration tests at AFRL/SNRT in Rome, NY using spherical reflectors and trihedral retroreflectors. The transceiver shown in figures 1-3 through 1-5 was used in these tests. The antenna, transceiver, radar signal processor and controller (PC based), power supplies, and a waveform generator were mounted in a trailer provided by the Air Force. Photographs of the antenna and transceiver mounted on the outside of the trailer are shown in figure 2-1. The PC, power supplies, and waveform generator were rack mounted inside the trailer as illustrated in figure 2-2. A video monitor was also mounted in the trailer. It displayed the image, shown in figure 2-3, from a video camera boresighted with the antenna.



FIGURE 2-1. RADAR MOUNTED IN WEATHERPROOF ENCLOSURE ON TRAILER AT AFRL, ROME, NY.



FIGURE 2-2. RADAR CONTROL AND SIGNAL PROCESSING EQUIPMENT.

Trihedral corner reflectors mounted on tripods and aluminum spheres suspended from a tethered inflatable balloon were used as calibration targets. A corner reflector target and radar return data are shown in figure 2-4. The suspended metal sphere is shown in figure 2-5.

The radar performed well during these tests. However, the limited height at which the corner reflectors could be deployed and the radar return from the balloon limited the accuracy of the calibration results.

Lessons learned from the AFRL tests included the need for a better calibration procedure (metal spheres of known diameter were eventually suspended from a kite during the El Mirage tests) and the need for a trailer with more space so that the operators could be protected from the weather and have a place to store calibration and other test equipment (the University of Illinois eventually provided a larger trailer and a trailer tow vehicle).



FIGURE 2-3. SCENE IMAGE AS RECORDED BY VIDEO CAMERA BORESIGHTED WITH THE ANTENNA.



(a)



(b)

FIGURE 2-4. (A) CALIBRATION CORNER REFLECTOR TARGET. (B) GROUND AND CORNER REFLECTOR RETURNS DISPLAYED ON MONITOR.



FIGURE 2-5. ALUMINUM SPHERE CALIBRATION TARGET SUSPENDED FROM A TETHERED BALLOON AT AFRL, ROME, NY.

3. KLAMATH FALLS TESTS

The bird detection radar (BIRDAR™) system was evaluated at several other locations before the DFW Airport demonstration occurred. The first of these was in the Klamath Basin in Oregon. Here BIRDAR™ was equipped with the redesigned antenna previously tested at Rome. The objectives of the Klamath Basin tests were to optimize radar operating parameters and determine the maximum detection range of the radar system. RF modulation frequency, RF bandwidth, and FFT size were among the parameters varied. A sample test matrix is displayed in table 3-1.

The radar was transported to the Lower Klamath National Wildlife Refuge and Tule Lake National Wildlife Refuge in an SUV. These locations, on the border between California and Oregon, were chosen because large populations of waterfowl were common (such as flocks of thousands of snow geese, which typically weigh 2.6 kg).

For testing at the Klamath Basin, the radar hardware was operated from the back of the SUV, as shown in figure 3-1, without the support trailer or laser range calibration equipment later used at DFW Airport. The antenna pointed out the back of the vehicle, with the display and controls accessible through the rear side doors. The long axis of the antenna was horizontal during these tests.

Testing was conducted on April 7 and 8, 2004 from about 6 am to 8 pm to capture virtually all potential bird movement. Several sites in the Klamath Basin were visited to acquire data. These are shown in figure 3-2.¹

TABLE 3-1. SAMPLE RADAR PARAMETER TEST MATRIX.

ΔF (Hz)	Mod Voltage (V)	Frame Time (ms)	Number of Angles	Angle Time (ms)	f_m (Hz)	R desired (m)	f_{IF} (calc) (Hz)	f_{IF} (Default) (MHz)	ΔR (m)	FFT Size	FFT Range (m)	Run
2.30E+08	5.000	108.504	60	1.808	588.7	4828	4.36E+06	5.00	0.652	8192	5342.61	A
1.15E+08	2.500	108.504	60	1.808	588.7	4828	2.18E+06	2.50	1.304	4096	5342.61	B
5.75E+07	1.250	108.504	60	1.808	588.7	4828	1.09E+06	1.25	2.609	2048	5342.61	C
2.30E+07	0.500	108.504	60	1.808	588.7	4828	4.36E+05	0.6	6.522	1024	6678.26	D
9.20E+06	0.200	108.504	60	1.808	588.7	4828	1.74E+05	0.6	16.304	512	8347.83	E
4.60E+06	0.100	108.504	60	1.808	588.7	4828	8.72E+04	0.6	32.609	512	16695.65	F
4.60E+06	0.100	108.504	60	1.808	588.7	4828	8.72E+04	0.6	32.609	256	8347.83	G
1.15E+08	2.500	60	60	1.0	1137	4828	4.21E+06	5.00	1.304	4096	5342.61	H
5.75E+07	1.250	60	60	1.0	1137	4828	2.10E+06	2.50	2.609	2048	5342.61	I
2.30E+07	0.500	60	60	1.0	1137	4828	8.42E+05	1.25	6.522	1024	6678.26	J
9.20E+06	0.200	60	60	1.0	1137	4828	3.37E+05	0.6	16.304	512	8347.83	K
4.60E+06	0.100	60	60	1.0	1137	4828	1.68E+05	0.6	32.609	512	16695.65	L
4.60E+06	0.100	60	60	1.0	1137	4828	1.68E+05	0.6	32.609	256	8347.83	M
5.75E+07	1.250	70	60	1.167	2130	4828	3.94E+06	5.00	2.609	2048	5342.61	N
2.30E+07	0.500	70	60	1.167	2130	4828	1.58E+06	2.50	6.522	1024	6678.26	O
9.20E+06	0.200	70	60	1.167	2130	4828	6.31E+05	0.6	16.304	512	8347.83	P
4.60E+06	0.100	70	60	1.167	2130	4828	3.15E+05	0.6	32.609	512	16695.65	Q
4.60E+06	0.100	70	60	1.167	2130	4828	3.15E+05	0.6	32.609	256	8347.83	R
5.75E+07	1.250	35	60	0.5833	2130	4828	3.94E+06	5.0	2.609	2048	5342.61	S
2.30E+07	0.500	35	60	0.5833	2130	4828	1.58E+06	2.5	6.522	1024	6678.26	T
9.20E+06	0.200	35	60	0.5833	2130	4828	6.31E+05	0.6	16.304	512	8347.83	U
4.60E+06	0.100	35	60	0.5833	2130	4828	3.15E+05	0.6	32.609	1024	33391.30	V
4.60E+06	0.100	35	60	0.5833	2130	4828	3.15E+05	0.6	32.609	512	16695.65	W
4.60E+06	0.100	35	60	0.5833	2130	4828	3.15E+05	0.6	32.609	256	8347.83	Y
2.30E+08	5.000	200	60	3.333	319.4	4828	2.36E+06	2.50	0.652	8192	5342.61	Z
1.15E+08	2.500	200	60	3.333	319.4	4828	1.18E+06	1.25	1.304	4096	5342.61	AA
5.75E+07	1.250	200	60	3.333	319.4	4828	5.91E+05	0.6	2.609	2048	5342.61	BB
2.30E+07	0.500	200	60	3.333	319.4	4828	2.36E+05	0.6	6.522	1024	6678.26	CC
9.20E+06	0.200	200	60	3.333	319.4	4828	9.46E+04	0.6	16.304	512	8347.83	DD
4.60E+06	0.100	200	60	3.333	319.4	4828	4.73E+04	0.6	32.609	256	8347.83	EE

Parameters to verify for each run: Mod voltage, f_m , f_{IF} , FFT Size

¹ Some of the material in this section comes from *A Report of Test Results of the 94 GHz Bird Detection Radar (BIRDAR™) at DFW Airport*, by Edwin E. Herricks, Jonathan R. B. Fisher, Joshua Markow, and Paul Antonik, December, 2004.



FIGURE 3-1. EXPERIMENTAL SETUP AT THE KLAMATH BASIN.



FIGURE 3-2. TEST LOCATIONS IN THE KLAMATH BASIN.

An effort was made to collect ground truthing information to provide verification of radar detections. However, it proved difficult for one person to create a written record, while simultaneously using binoculars for bird identification and checking the radar display to verify the detections. While the wildlife record had flaws, large numbers of large birds were observed at the Klamath as listed in table 3-2. Birds were seen as far as 2.1 km away and it appeared that the farthest detections did not represent the absolute upper detection limit of the radar. Typical wildlife scenes are depicted in figure 3-3.

TABLE 3-2. SOME MAJOR DETECTIONS AT THE KLAMATH BASIN TESTS.

Detection ID	Site	Date	Time	Duration	Bird Species/ Type	Number	Flock Type	Range (m)	Flight Direction
1	300	4/7	6:58	17	Snow geese	25	linear	200-300	NW
2	300	4/7	6:59	22	Snow geese	50	wide linear	200-350	NW
3	302	4/7	15:14	135	Snow geese	2000	large dense	350-1050	E
4	305	4/8	11:14	104	White-fronted geese	3000	large dense	1500-2100	E
5	306	4/8	19:20	30	Snow geese	1000	large dense	600-750	NW



Snow geese on lake



Snow geese in flight

FIGURE 3-3. SNOW GEESE DETECTED BY BIRDAR™ AT KLAMATH BASIN.

4. EL MIRAGE DRY LAKE BED TESTS

BIRDAR™ was next tested at El Mirage Dry Lake Bed near Adelanto, CA on August 24, 2004. figure 4-1 contains an aerial photograph of the area. The radar configuration consisted of a 575 mW transceiver that incorporates a receiver and low noise amplifier with a noise figure of 5.8 dB. The intermediate frequency (IF) amplifier has a fixed gain of 35 dB. The cutoff frequency of the IF amplifier was 500 KHz and the corresponding sampling frequency was 1 MHz. The RF sweep bandwidth was 65 MHz, corresponding to a spatial resolution of 2.3 m (7.6 ft). The sweep modulation frequency was 238 Hz.



FIGURE 4-1. EL MIRAGE DRY LAKE BED.

The BIRDAR™ system was evaluated with two antennas at El Mirage. The first had the original specification of 0.5-deg 3-dB beamwidth in one direction and 5-deg 3 dB beamwidth in the other. The 0.5 deg beam was swept over 30 degrees. The second antenna had a 2½-deg 3-dB beamwidth rather than 5 deg in the opposing direction. The smaller beamwidth gives a 6 dB improvement in two-way gain.

Two metal spheres of known radar cross section (RCS) were used as targets at El Mirage, namely 0.01 m² and 0.1 m² RCS. The spheres were attached one at a time to a kite string at a point between 50 and 100 ft below the kite. The kite was flown such that the spheres were approximately 75 to 100 ft above the ground. The antenna was mounted with the 30-deg scan vertical, i.e., the 0.5-deg beamwidth could resolve targets vertically and thus separate the sphere from the kite and the ground.

Pictures of the El Mirage trailer-mounted equipment and calibration sphere suspended from a kite are shown in figures 4-2 and 4-3, respectively.



FIGURE 4-2. 94 GHZ RADAR AS MOUNTED IN TRAILER WITH ANTENNA IN VERTICAL POSITION AT EL MIRAGE DRY LAKE BED.



FIGURE 4-3. KITE WITH METAL SPHERE SUSPENDED BELOW IT (IN BLACK CIRCLE). TAIL OF KITE IS BEHIND THE KITE AND NOT AT THE SAME ALTITUDE AS THE SPHERE.

The results of the sphere radar cross section measurement tests scaled with theory as described in table 4-1.

TABLE 4-1. EL MIRAGE TEST RESULTS.

Target Antenna	Maximum Range at Which Sphere was Visually Detected		Expected Percent Change in Range	Calculated Percent Change in Range
	0.01 m ² metal sphere	0.1 m ² metal sphere		
5-deg antenna	1 km	1.7 km	78	70
2½-deg antenna	1.4 km	2.4 km	78	71

The antenna gain change of 6 dB (when switching from the 0.5-deg x 5-deg to the 0.5-deg x 2½-deg antenna) should yield a 40 percent improvement in range for each metal sphere target. This was observed for the 0.01 m² and the 0.1 m² spheres.

Thus, the (Range)⁴ dependence of detection range with antenna gain and target RCS was verified for the BIRDARTM system. Accordingly, WaveBand concluded that the radar was operating properly and within specifications.

The correlation of sphere to bird flock detection range is difficult as there are no known (to our knowledge) RCS measurements of birds at W band. A summary of the available X-band bird RCS measurement information is given in table 4-2.

TABLE 4-2. INDIVIDUAL BIRD X-BAND RCS MEASUREMENT DATA FROM SEVERAL SOURCES.

Bird Type	RCS
Large bird	-20 dBm ²
Small birds (thrush, starling)	20 to 30 cm ²
Grackle	16 cm ²
Crows, gulls, geese, ducks	10 to 500 cm ²
Man	1.2 m ²

The RCS of birds is expected to be larger at W-band if a bird is modeled as a prolate spheroid, where the RCS increase is expected to exhibit a frequency dependence between that of a cylinder (f^4) and a sphere (f^0).²

While at the dry lake bed, we also demonstrated the capability of the radar to detect transmission wires such as electrical or telephone. The results of such a test are shown in figure 4-4 using the 2½-deg antenna.

² E. Knott, J. Shaeffer, M. Tuley, *Radar Cross Section*, 2nd Edition, Artech House, Boston, MA, 1993.

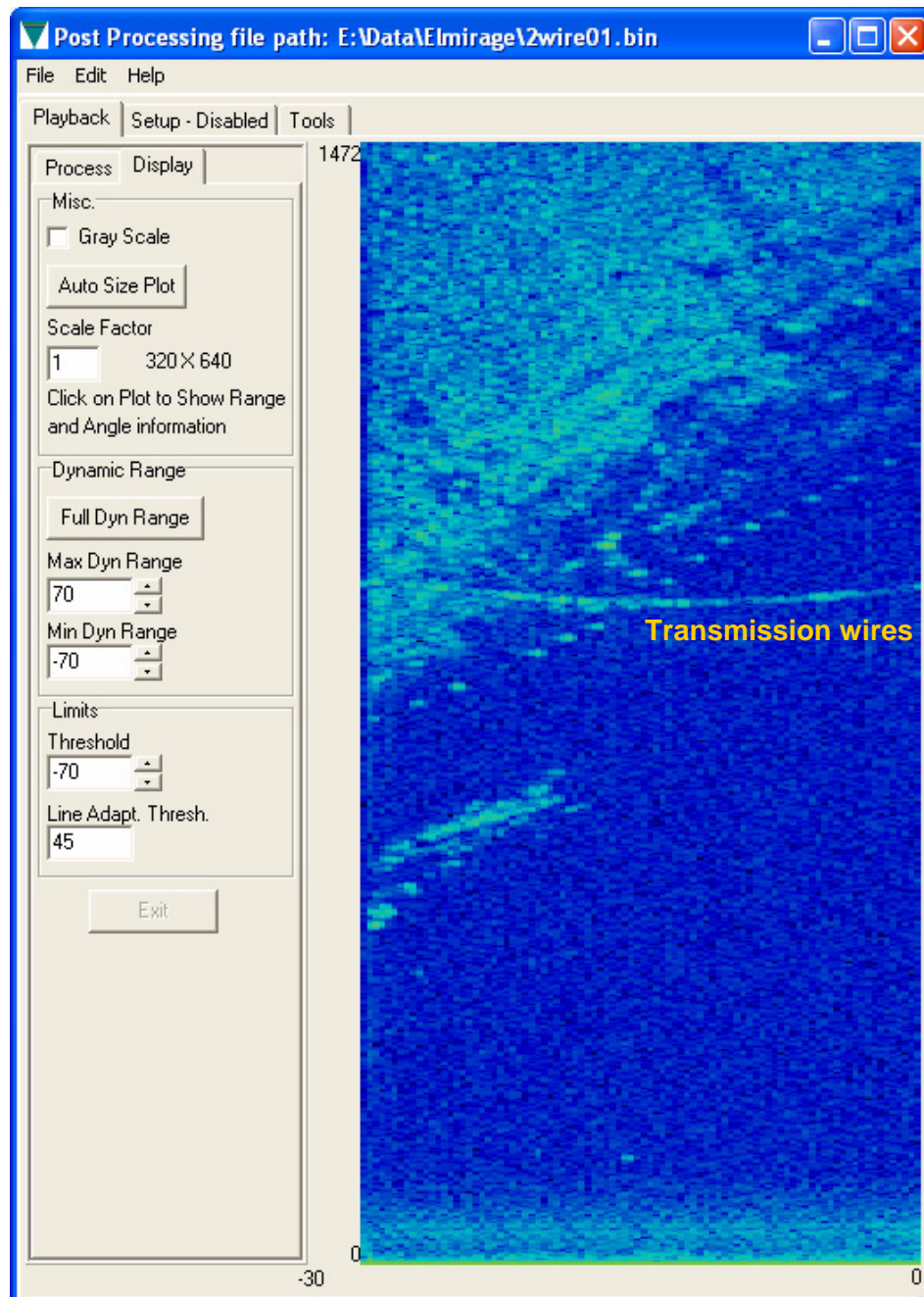


FIGURE 4-4. DETECTION OF TRANSMISSION WIRES AT EL MIRAGE DRY LAKE BED WITH 94 GHZ RADAR.

5. SALTON SEA TESTS

The next test sequence prior to the DFW Airport tests was conducted at the Salton Sea in California on August 26 and 27, 2004. This test used the same radar hardware and support trailer as at DFW Airport. The primary objective of these tests was to confirm the systems integration and operational consistency of the radar prior to deployment at DFW. At the Salton Sea, the

radar detected large numbers of large birds (such as snow geese and American white pelicans, which typically weigh 7 kg). Although downrange wildlife observations are unavailable for the Salton Sea trials, these data do provide useful information for estimating the radar's capabilities.³

WaveBand made several calls to the state and local land management personnel identified by the University of Illinois to determine the bird population available for detection in Southern California at this time of year. Large bird migrations are not expected until November through December. Local birds are present now, but not large size ones nor in great numbers. The wildlife managers at the Irvine Ranch Water District that overlooks Newport Bay and at the Salton Sea do not offer a great deal of encouragement in our quest for flocks of large birds at this time of year. The ranger at the State Recreation Area at the north end of the Salton Sea indicated that the best chance for locating birds is at farmers' fields some 20 to 30 miles east of the sea in the vicinity of Brawley and Niland and then only if the fields have been recently flooded.

Acting on the information obtained from the State Recreation Area ranger, WaveBand, accompanied by Jon Fisher, drove the trailer to the Salton Sea on Thursday August 26. Only the 2½-deg antenna was used in these tests. We were able to setup the trailer and radar at the Red Hill Marina on the southeast shoreline of the Sea in time to observe the evening bird activity (approximately 7 pm). The marina is denoted as Site 1 in figure 5-1. The test area is near Brawley, CA and its surrounding hay fields.

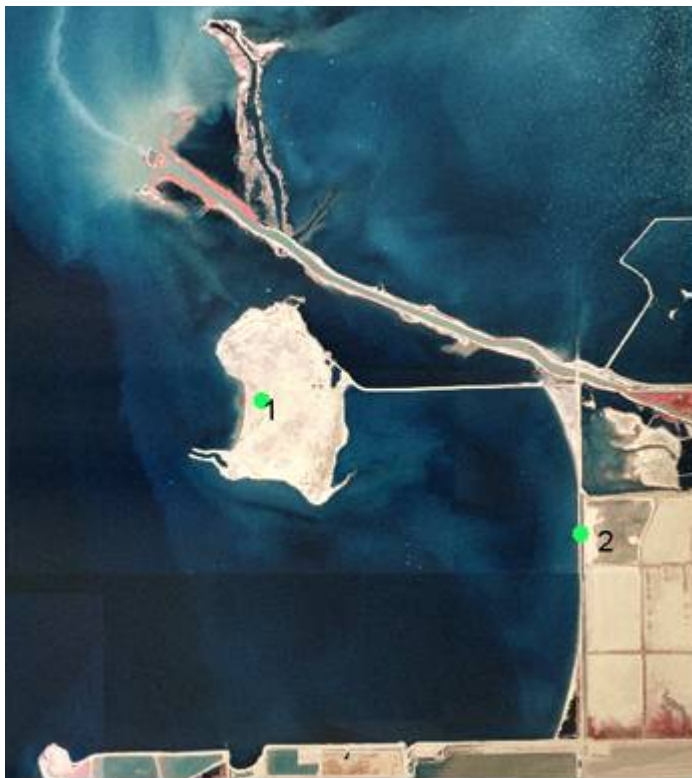


FIGURE 5-1. TEST LOCATIONS AT THE SALTON SEA.

³ *A Report of Test Results of the 94 GHz Bird Detection Radar (BIRDAR™) at DFW Airport*, Edwin E. Herricks, Jonathan R. B. Fisher, Joshua Markow, and Paul Antonik, December, 2004.

Figure 5-2 shows the trailer and radar setup. The long axis of the antenna was oriented horizontally during these tests. Some of the bird activity is illustrated in figure 5-3.



FIGURE 5-2. RADAR TRAILER SETUP ALONG SHORE OF SALTON SEA NEAR RED HILL MARINA ON EVENING OF AUGUST 26, 2004. VIEW OF RADAR IS TOWARD THE SALTON SEA.



FIGURE 5-3. EVENING BIRD ACTIVITY – SALTON SEA AUGUST 26, 2004.

During the evening test, a bird was detected at 1.6 km from the radar as shown in figure 5-4. The bird was identified by the bird-like signature and movement observed on the radar screen as it was too distant to be observed visually. The bird detection activity from the Salton Sea tests is summarized in table 5-1.

The following morning at about 5:30 am, the trailer was setup at a site further from the shoreline on a pullout along the road that leads to the marina, shown as Site 2 in figure 5-1. Figure 5-5 illustrates this setup. Figure 5-6 shows the typical early morning bird activity.

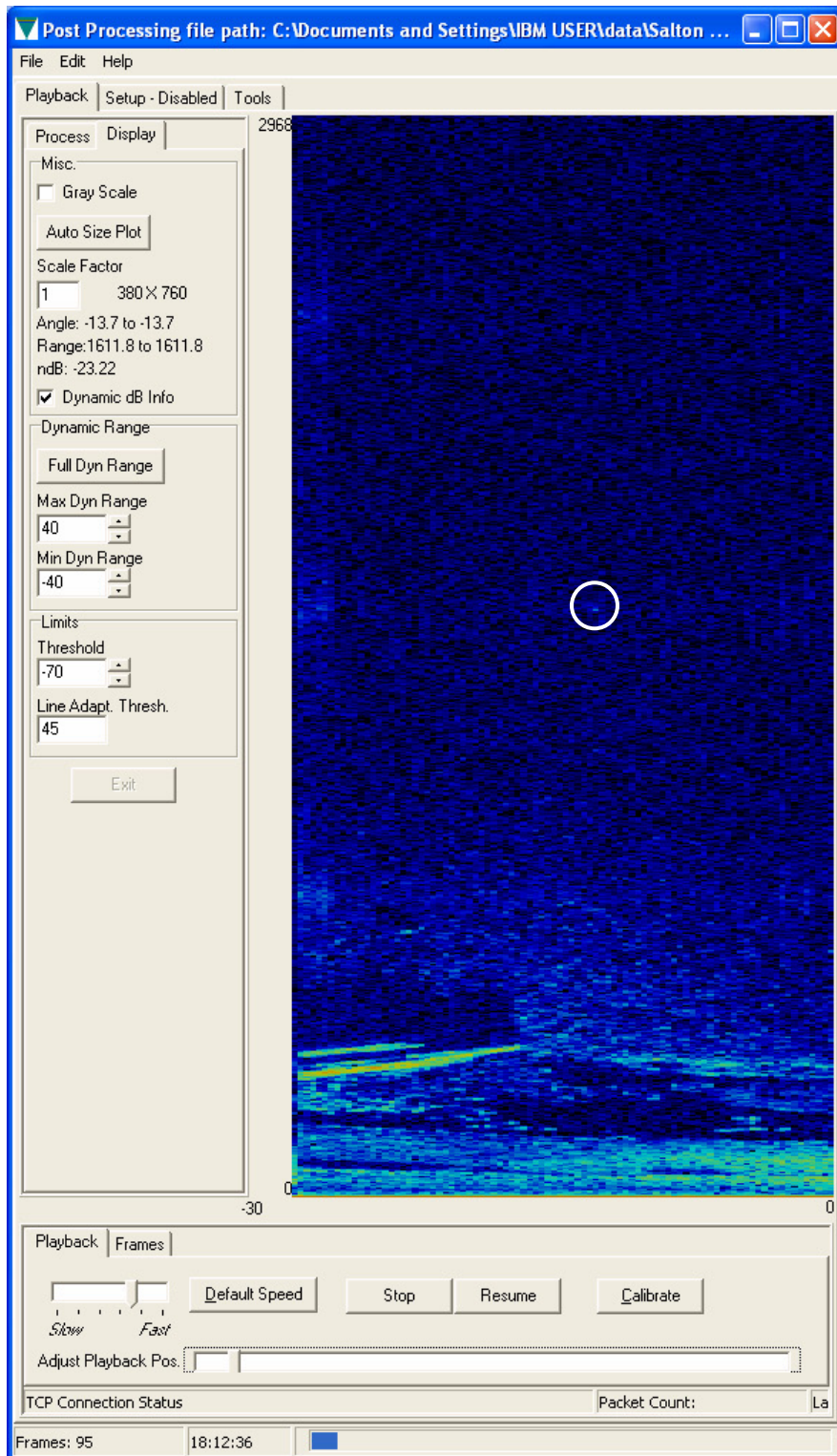


FIGURE 5-4. RCS OF INDIVIDUAL BIRD DETECTION AT 1.6 KM OVER SALTON SEA EVENING OF AUGUST 26, 2004.

TABLE 5-1. SOME MAJOR DETECTIONS AT THE SALTON SEA TEST.

Detection ID	Site	Date	Time	Duration	Bird Species/ Type	Number	Flock Type	Range (m)	Flight Direction
1	1	8/26	18:13	55	Pelican	2	n/a	1250-1600	NE
2	1	8/26	18:25	140	Pelican	1	n/a	1300-2050	NE
3	2	8/27	6:07	100	Unidentified flock		thick linear	1400-1700	S
4	2	8/27	6:20	15	Pelican	1	n/a	2000	N
5	2	8/27	6:31	25	Unidentified geese	100	2 small flocks	2450-2650	W



FIGURE 5-5. RADAR TRAILER SETUP ALONG ROAD LEADING TO RED HILL MARINA AND SALTON SEA ON MORNING OF AUGUST 27, 2004. VIEW OF RADAR IS TOWARD THE SALTON SEA.



FIGURE 5-6. TYPICAL EARLY MORNING BIRD ACTIVITY – SALTON SEA AUGUST 27, 2004.

These morning observations included individual bird sightings at 2 and 2.3 km and a flock sighting at 2.6 km from the radar as indicated in figures 5-7 through 5-9. The flock sighting was

observed when the trailer was turned about 90 degrees to view birds flying toward the Sea from the hay fields.

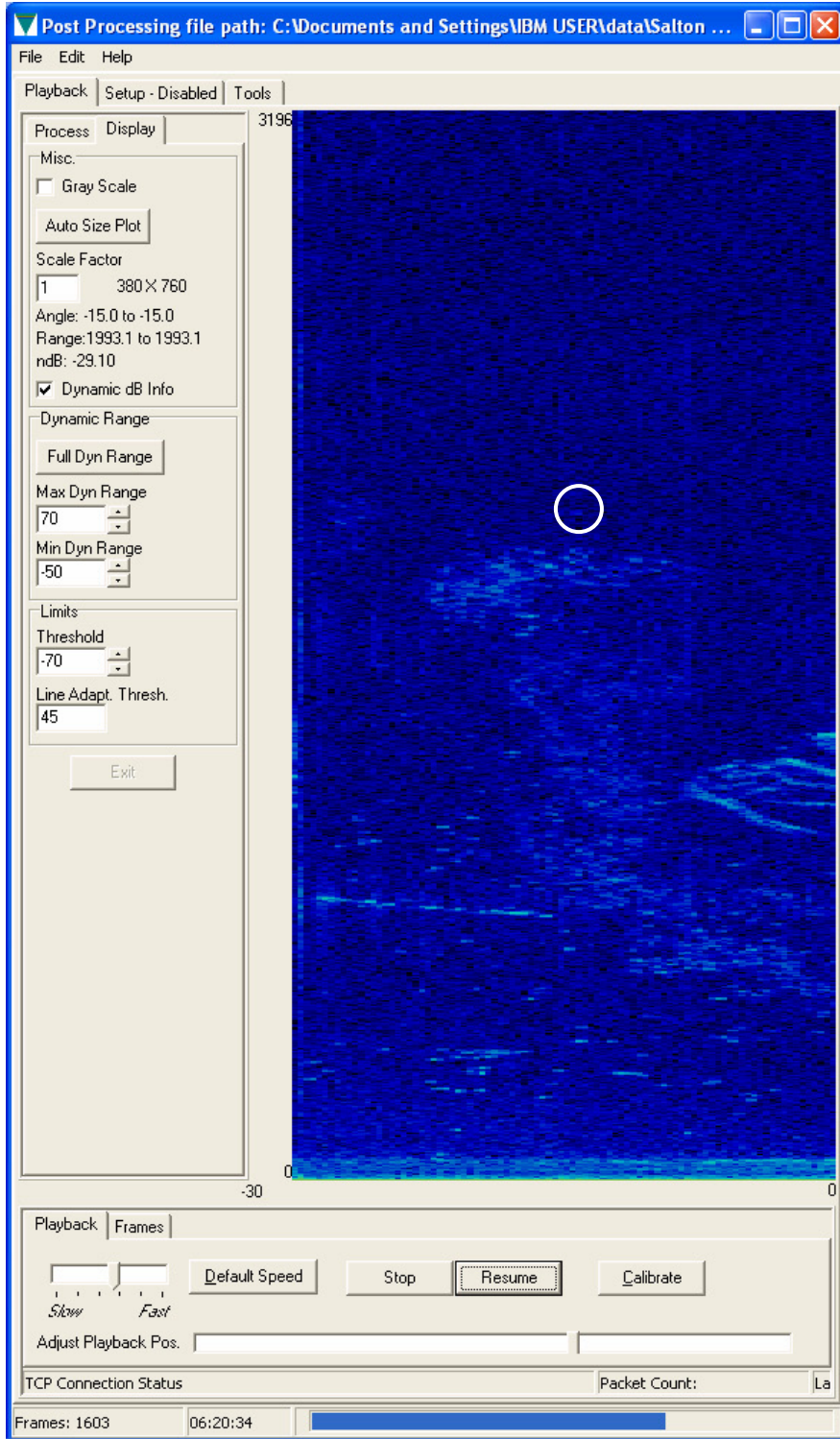


FIGURE 5-7. RCS OF INDIVIDUAL BIRD DETECTION AT 1.9 KM OVER SALTON SEA MORNING OF AUGUST 27, 2004.

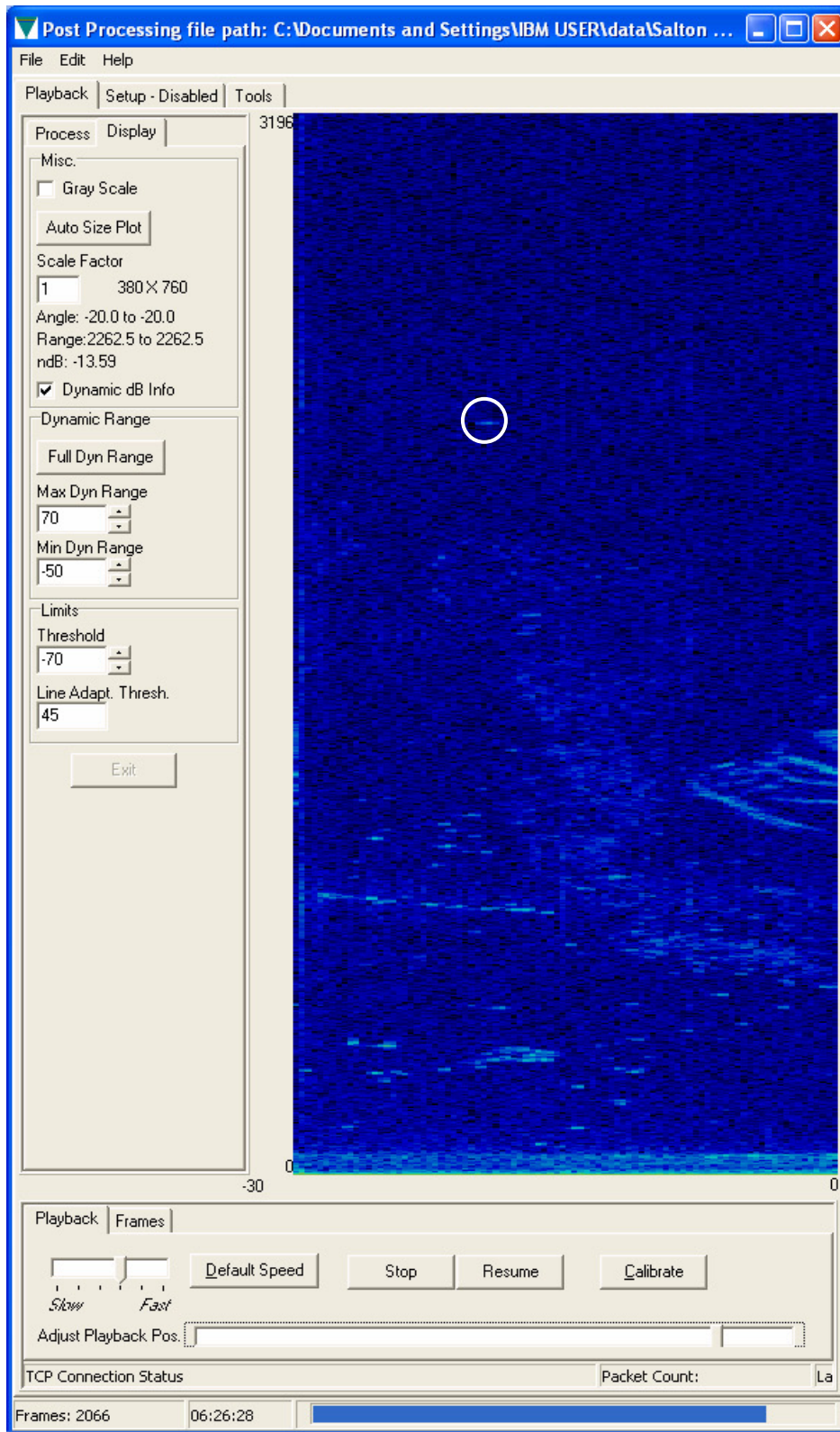


FIGURE 5-8. RCS OF INDIVIDUAL BIRD DETECTION AT 2.3 KM OVER SALTON SEA MORNING OF AUGUST 27, 2004.

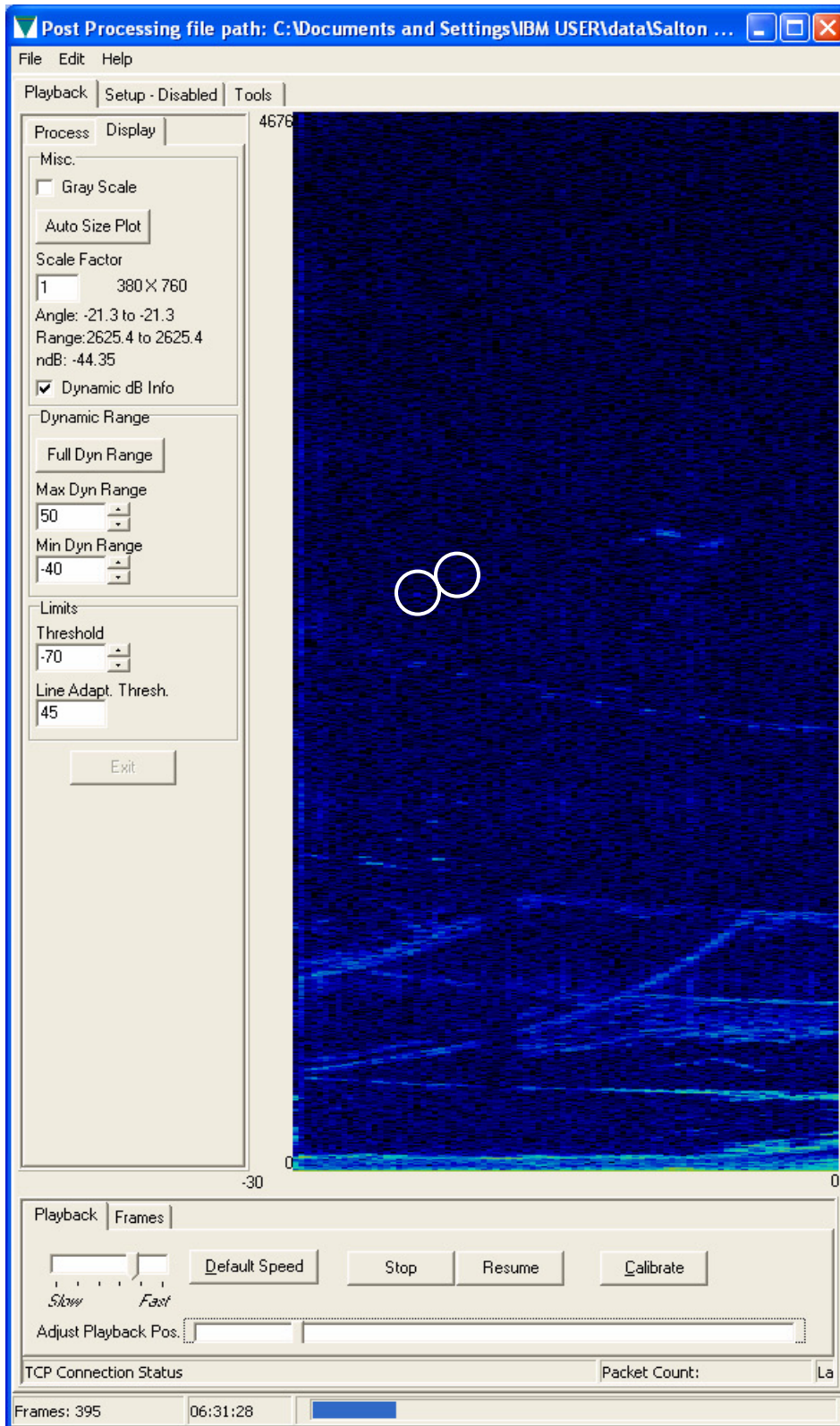


FIGURE 5-9. RCS OF BIRD FLOCK DETECTION AT 2.6 KM. BIRDS WERE FLYING TOWARD SALTON SEA MORNING OF AUGUST 27, 2004.

6. BOLSA CHICA BIRD RESERVE TESTS

A final series of tests and performance evaluations was conducted at the Bolsa Chica Bird Reserve in Huntington Beach, CA before conducting a readiness review for the Dallas tests. The nearby Huntington Beach location was used to verify that calibration and test procedures were repeatable and adequate for establishing the detection range capabilities of the radar.

The radar in its final configuration as mounted in the University of Illinois trailer was towed to Bolsa Chica on three different days to perform morning, afternoon, and evening calibration runs against trihedral retroreflector targets mounted on a tripod. Bird targets of opportunity were also detected.

A map showing the location of the Bolsa Chica Bird reserve and wetlands photograph are shown in figures 6-1 and 6-2. The trailer with BIDAR™ looking out the rear window at a corner reflector target on the shore is shown in figure 6-3.

The results of these tests demonstrated that the radar operation was stable since the magnitude of the reflector return signals were constant when the reflectors were placed at the preselected locations.

Based on the preceding series of tests, the FAA in conjunction with the Air Force, University of Illinois, and Waveband decided that the radar was operating and performing satisfactorily and that we should proceed with the Dallas tests.

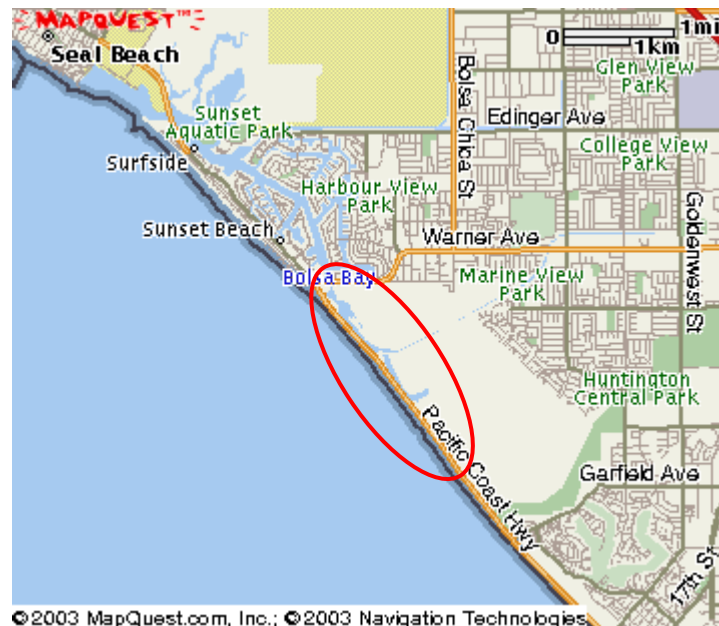


FIGURE 6-1. BOLSA CHICA BIRD RESERVE LOCATION, HUNTINGTON BEACH, CA.



FIGURE 6-2. GULLS AND CORMORANTS FLYING OVERHEAD AT BOLSA CHICA BIRD RESERVE, HUNTINGTON BEACH, CA JUST BEFORE SUNRISE.



(a) BIRDAR™ on rotating mount in trailer.



(b) Corner reflector target setup at shoreline later in the day.

FIGURE 6-3. RADAR SETUP AND CALIBRATION CONFIGURATION AT BOLSA CHICA BIRD RESERVE.

7. DFW AIRPORT TESTS

The primary purpose of the DFW tests was to demonstrate consistent radar performance in detecting flocks of large birds. However, at the time of year the DFW tests were performed, migrations of large bird populations were not present at the airport. Therefore, the radar detections were limited to birds of opportunity, which included individual small and medium sized birds and flocks of small birds.

A summary of the test sites, data acquisition procedures, and major findings from the DFW Airport tests is found in a separate report prepared for the FAA and AFRL: *A Report of Test Results of the 94 GHz Bird Detection Radar (BIRDAR™) at DFW Airport*, by Edwin E. Herricks, Jonathan R. B. Fisher, Joshua Markow, and Paul Antonik, December, 2004. A table with the major findings from the DFW and other tests is described in the next section.

The test plan for the DFW tests is found in Appendix B. The test protocol included using a laser rangefinder to measure the range to the trihedral retroreflectors. This procedure provided radar calibration information. Figure 7-1 shows the laser rangefinder alongside the trailer that housed the radar and the corner reflector calibration target placed in the far field of the radar.



(a) Laser rangefinder total station used to measure distance to calibration targets.



(b) Trihedral retroreflectors in far field of radar.

FIGURE 7-1. RADAR CALIBRATION AT DFW AIRPORT.

Figure 7-2 shows the radar operator at the radar console inside the trailer. The antenna and transceiver are mounted such that the antenna is scanning in the vertical direction in this particular run. The top row on the equipment rack contains one of two radar signal monitors on the left and the video monitor (on the right) that displays the image seen by the camera boresighted with the antenna. The second row of equipment consists of the azimuth pointing controls and a VCR. The equipment shelf on the bottom contains the second radar signal monitor, power supplies, waveform generator, and the PC radar signal processor and controller. The radar data are initially stored on a hard drive that is part of the PC. The data are transferred to a DVD at the end of a day's testing.

Testing at DFW Airport was a great success in that the radar functioned perfectly throughout the tests and was able to detect birds of opportunity at ranges that provided data to substantiate the extrapolation of future radar designs to the detection of large bird flocks at 3 miles.

The FAA-issued press release describing the DFW BIRDAR™ tests and DFW test coverage from the Chicago Tribune are contained in Appendix C.



FIGURE 7-2. RADAR OPERATOR AT CONSOLE INSIDE TRAILER.

8. RADAR PERFORMANCE SUMMARY

A summary of the demonstrated detection performance of the 94 GHz BIRDAR™ during the Klamath Basin, Salton, Sea, El Mirage, and DFW Airport tests is given in table 8-1. The table contains the results from the several bird detection tests and a radar calibration test using metal spheres of known radar cross section. The target detections reported in table 8-1 were made by a human observer observing the radar return signals on a computer monitor.

TABLE 8-1. DEMONSTRATED RANGE DETECTION PERFORMANCE OF BIRDAR™ AT DFW AIRPORT, KLAMATH FALLS, SALTON SEA, AND EL MIRAGE DRY LAKE BED (WITH HUMAN OBSERVER FOR TARGET DETECTION).

Test Location	Radar Configuration	Target	Detection Range (km)
DFW	94 GHz 0.5 x 2.5 deg ant	Blackbird flocks	1.2 to 1.3
DFW	94 GHz 0.5 x 2.5 deg ant	Raptors	1.2
Klamath Falls	94 GHz 0.5 x 5 deg ant	Snow geese	2.1
Salton Sea	94 GHz 0.5 x 2.5 deg ant	Pelicans	1.6 to 2
Salton Sea	94 GHz 0.5 x 2.5 deg ant	Geese	2.3 to 2.6
Dry Lake Bed	94 GHz 0.5 x 2.5 deg ant	0.01m ² metal sphere	1.4
Dry Lake Bed	94 GHz 0.5 x 2.5 deg ant	0.1m ² metal sphere	2.4

9. LESSONS LEARNED

From the point of view of radar design, the primary lesson learned from the extended series of tests conducted at Bolsa Chica Bird Reserve, Klamath Falls, Salton Sea, and DFW Airport is

that increased SNR is needed to detect flocks of large birds at the desired 3 mile range when automatic target detection is implemented.

Other lessons learned are:

- Radar detection range can be fairly accurately estimated based on a SNR calculation when the radar design parameters are known.
- Bird radar cross section (RCS) at 94 GHz is not accurately known and can only be estimated.
- Based on measurements to date with the 94 GHz BIRDAR™, it appears that flocks of large birds have an RCS between 0.01 and 0.1 m².
- Limited available millimeter-wave power and atmospheric absorption losses at 94 GHz may lead to other frequencies, such as 35 GHz, being explored for future BIRDAR™ operation.
- At the output power levels tested, 94 GHz radar operation does not interfere with the functioning of airport sensors and other equipment.
- Rather extensive calibration procedures that eliminate ground bounce are needed to get an absolute radar calibration.

10. NEED FOR MODIFIED RADAR DESIGNS TO MEET AUTOMATIC DETECTION RANGE GOAL OF 3 MILES

As a result of these tests and evaluations, WaveBand developed modified radar designs that can *automatically* detect flocks of large birds at ranges as far as 3 miles and within the glide slope of departing and arriving aircraft. Two potential operating frequencies were analyzed: 35 and 94 GHz. The 35 GHz system operates over greater distances, primarily because of increased millimeter-wave power that is commercially available at this frequency. The 35 GHz design exhibits a signal-to-noise ratio of 16.6 dB at 3 miles, which is more than adequate to support automatic target detection at that range. The 94 GHz design exhibits a signal-to-noise ratio of 15 dB at 1 mile and a signal-to-noise ratio of 0 dB at ranges of 2.5 miles and less (adequate for human in the loop bird flock detection). These results are based on detailed design and operating parameters given later in tables 11-3 and 11-4.

Table 10-1 shows the predicted detection ranges for the improved 35 and 94 GHz radars with human and automatic target detection options as extrapolated from the data in table 8-1 and with a target whose radar cross section equals 0.03 m². For 35 GHz, the maximum range for human target detection of flocks of large birds is approximately between 11 and 12 km, while for 94 GHz it lies between 3.7 and 4 km. For automatic target detection, the corresponding ranges are between 4.7 and 5 km and 1.6 and 1.7 km. The maximum range for human target detection is based on a signal-to-noise ratio (SNR) of 0 dB, while the maximum range for automatic target detection is conservatively based on a SNR of 15 dB. These values are calculated using the analysis presented in other sections of this proposal. The confidence in the predicted detection ranges is high as the range is extrapolated from the test results of table 8-1 and improvement factors based on known phenomena.

TABLE 10-1. PREDICTED RANGE DETECTION PERFORMANCE OF IMPROVED 94 GHZ AND 35 GHZ RADARS WITH HUMAN (SNR = 0 DB) AND AUTOMATIC TARGET DETECTION (SNR = 15 DB).

Radar Configuration	Test Data Baseline	Range Improvement Factor**	Predicted Detection Range with SNR = 0 dB (km)	Predicted Detection Range with SNR = 15 dB (km)
94 GHz 0.5 x 1.25 deg ant	DFW raptors (1.2 km)	1.6	1.9	0.8
94 GHz 0.5 x 1.25 deg ant	Salton Sea geese (2.3 km)	1.6	3.7	1.6
94 GHz 0.5 x 1.25 deg ant	Modeled 0.03m ² RCS target	1.6	4	1.7
35 GHz 1.08 x 1.25 deg ant	DFW raptors (1.2 km)	4.86	5.8	2.5
35 GHz 1.08 x 1.25 deg ant	Salton Sea geese (2.3 km)	4.86	11.2	4.7
35 GHz 1.08 x 1.25 deg ant	Modeled 0.03m ² RCS target	4.86	12	5

* The procedure for calculating the Range Improvement Factor listed in table 2 is based on the equation for SNR that appears in the Modeled Detection Range section of this proposal. The Range Improvement Factor is equal to the fourth root of the ratio of the calculated values of SNR for the modified radars over the SNR for the 94 GHz radar used at DFW Airport. This factor is independent of the absolute value of range. For example, the new SNR for the 94 GHz radar is calculated using the parameters in table 11-4. The ratio is formed as the [New SNR/DFW 94 GHz SNR = 6.6 (independent of range)] and the fourth root of that value is found and used as the Range Improvement Factor = 1.6. At 35 GHz, the new SNR is calculated using the parameters in table 11-3. The corresponding SNR ratio = 558, with a Range Improvement Factor = 4.86.

The Predicted Detection Range with SNR = 15 dB is equal to the Predicted Range for 0 dB reduced by a factor equal to the fourth root of 15 dB or 2.37.

11. RADAR DESIGN AND PERFORMANCE CONSIDERATIONS FOR BIRDAR™ WITH AUTOMATIC DETECTION FEATURE

11.1 Range Resolution Cell and Number of Range Bins

First we consider the original BIRDAR™ design having the design parameters shown in table 1-2.

The range resolution ΔR of the radar is given by

$$\Delta R = c/2(\Delta F) = 3 \times 10^8/[2(230 \times 10^6)] = 0.65 \text{ m}, \quad (11-1)$$

where c = speed of light and ΔF = RF modulation frequency.

To gather data over a 3 mile (4.8 km) range requires $4800/0.65 = 7385$ range bins.

The number of range bins is typically set equal to the next higher value that lies above this number as calculated from a power of 2. In this case, that number is 8192 range bins.

11.2 Time Bird Remains in a Range Resolution Cell

Noncoherent integration time is dependent on the time the bird targets spend in a range resolution cell and the frame rate (i.e., the antenna drum rotation rate). As will be shown below, the range resolution cell is smaller than the resolution calculated from the 3 dB antenna beamwidth. Thus, the range resolution controls the number of frames that can be noncoherently integrated as birds will remain in a range resolution cell for less time than they will in an antenna beamwidth limited resolution cell. A frame is defined as the time for one revolution of the antenna drum.

The time for a bird to remain in a resolution cell is found as follows.

If a bird flies at $20 \text{ mi/hr} = 32.2 \text{ km/hr} = 0.00894 \text{ km/s} = 9 \text{ m/s}$, the bird will remain in the 0.65 m range cell for $0.65/9 = 0.072 \text{ s}$. If a bird flies at $30 \text{ mi/hr} = 48.2 \text{ km/hr} = 0.0134 \text{ km/s} = 13.4 \text{ m/s}$, the bird will remain in the 0.65 m range cell for $0.65/13.4 = 0.048 \text{ s}$. The range resolution cell limits the integration time as the antenna resolution cell dimension formed by the 0.5 deg antenna beamwidth is larger, equal to

$$\begin{aligned} \text{Az resolution cell dimension} &= (\text{Az 3dB beamwidth})(\text{Range})\pi/180 = (0.5)(4.8)(3.14)/180 \\ &= 0.04186 \text{ km} \approx 42 \text{ m at a range of 4.8 km.} \end{aligned} \quad (11-2)$$

Thus, a bird remains in the antenna resolution cell for $42/9 = 4.67 \text{ s}$ when the bird flies at 20 mi/hr (9 m/s).

11.3 Transmitted Waveform

Two types of waveforms are generally used in frequency modulated continuous wave (FMCW) radars. The waveform shown in figure 11-1a, which has been used in all BIRDAR™ radars to

date, consists of a frequency upsweep in which the frequency changes linearly with time over a specified bandwidth ΔF . The waveform in figure 11-1b contains both an upsweep and a downsweep frequency component. This waveform allows the Doppler frequency shift and hence the speed of the target to be calculated as described later. The symbol f_m represents the RF modulation frequency.

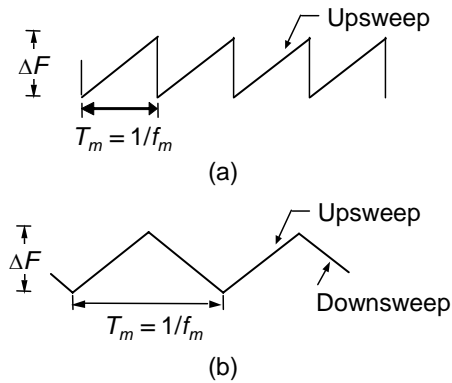


FIGURE 11-1. TRANSMITTED WAVEFORMS: (A) UPSWEEP COMPONENT ONLY. (B) UPSWEEP AND DOWNSWEEP COMPONENTS.

11.4 RF Modulation Frequency

Case 1: Transmitted waveform with upsweep component only

If the antenna beamwidth is 0.5 deg and the total angle scanned is 30 deg, a minimum of 60 resolution cell positions is needed to scan the 30 deg sector. If over sampling by a factor of 1½ or 2 is desired, e.g., to produce sharp imagery for the human eye to analyze, then 90 or 120 cell positions are required. The RF modulation period T_m is related to the drum rotation speed and the number of cell positions by

$$T_m' = \text{Time for 1 revolution of drum/number of cell positions.} \quad (11-3)$$

Accordingly, for 60 cell positions and for a drum rotation speed of 10 rev/s,

$$T_m' = 0.1/60 = 16.6 \times 10^{-4} \text{ s.} \quad (11-4)$$

The above value of T_m' is decreased by approximately 10 percent to account for the time needed for the transmitted waveform to begin the next upsweep or downsweep in frequency. Thus

$$T_m = 0.9T_m' = 14.9 \times 10^{-4} \text{ s or} \quad (11-5)$$

$$f_m = 1/T_m \approx 669 \text{ Hz.} \quad (11-6)$$

Case 2: Transmitted waveform with upsweep and downsweep components

When the transmitted waveform has upsweep and downsweep components, the RF bandwidth excursion ΔF occurs in half the time as before since both an upsweep and downsweep must be

transmitted for each position of the antenna resolution cell. Thus, for the example cited in Case 1, the upswEEP and downswEEP each occur during an interval

$$T_m/2 = 7.4 \times 10^{-4} \text{ s} \quad (11-7)$$

By definition, the RF modulation frequency remains the same as in Case 1 equal to

$$f_m = 1/T_m = 1/(2 \times 7.45 \times 10^{-4}) \approx 669 \text{ Hz.} \quad (11-8)$$

11.5 Noncoherent Integration of Radar Returns Over Several Frames

To derive the number of frames that can be noncoherently integrated, we consider the antenna drum rotation speed or frame time and the length of time a bird remains in a range resolution cell.

For a drum rotation rate of 10 rev/s, each azimuth cell is revisited every 0.1 s. Therefore, no more than 1 radar return can be noncoherently integrated during the 0.072 s a bird flying at 20 mi/h remains in a range resolution cell. Similarly, no more than 1 radar return can be noncoherently integrated during the 0.048 s a bird flying at 30 mi/h remains in a range resolution cell.

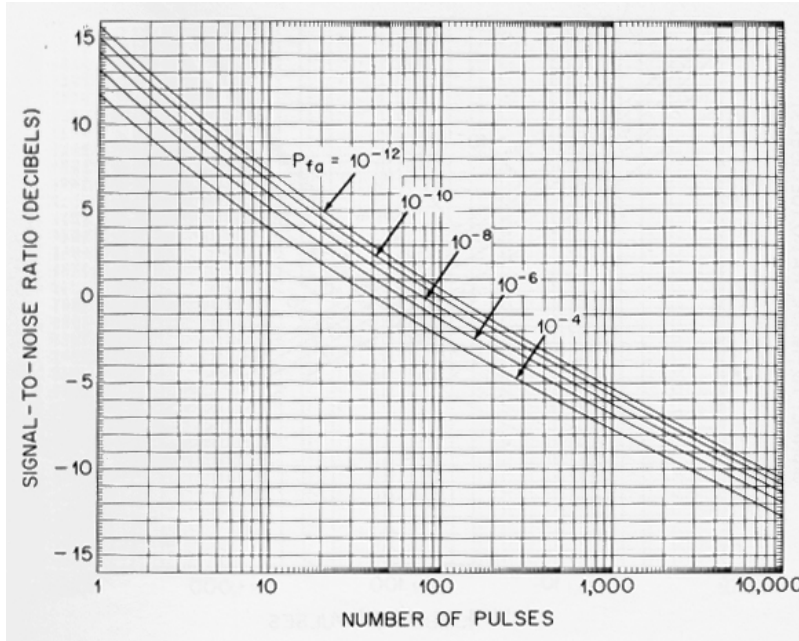
11.6 Noncoherent Frame Integration as a Function of Detection and False Alarm Probabilities

The detection probability (P_d) curves in figure 11-2 for non-fluctuating targets indicate that approximately 40 returns are needed to achieve a detection probability of 0.90 at a SNR = 0 when the false alarm probability (P_{fa}) is 10^{-4} with noncoherent integration. SNR = 0 dB is selected as the benchmark for entering the detection probability curves based on the 94 GHz radar detection results from DFW Airport, Salton Sea, and Klamath Falls as this appears to be the lower limit for SNR when human detection of flying birds was observed. Figure 11-3 shows that more than 1,000 returns are needed to reach a $P_d = 0.90$ when the target behaves as a Swerling 1 fluctuating model and the SNR = 0.

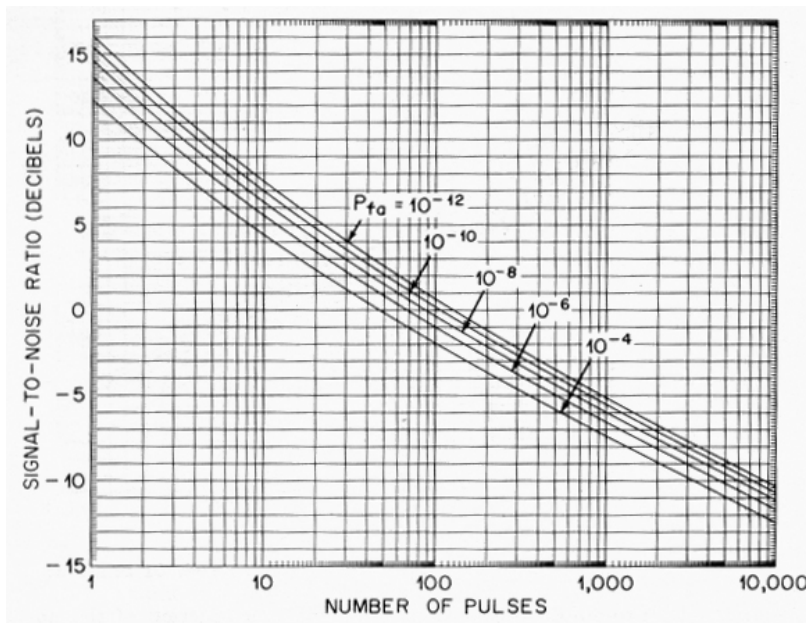
It appears that moving bird targets do not behave as non-fluctuating objects, but may not present as severe a detection challenge as a Swerling 1 target. Nevertheless, noncoherent integration would require a number of returns greater than 40 and perhaps less than 1,000. Thus, noncoherent integration appears to be impractical by itself to increase the detection range of the radar used at DFW for bird flock detection at 3 miles because of the speed at which birds potentially fly and the practical design limits of the radar (e.g., available output power, noise figure, atmospheric attenuation, and antenna and waveguide losses).

However, noncoherent integration, to whatever extent possible, does offer some advantages. Noncoherent integration sums the radar returns and divides the sum by the number of returns N . This process reduces the variance of the noise and the variance of the signal plus noise by a factor proportional to N , but keeps their mean values the same as shown in figure 11-4. (Ref: L.A. Klein, *Millimeter-Wave and Infrared Multisensor Design and Signal Processing*, Artech House, Norwood, MA, 1997.) Noncoherent integration is beneficial in making a signal easier to

detect when the SNR is greater than zero. Therefore, when applicable, noncoherent integration may be useful for enabling automatic target detection. Another way of interpreting the beneficial effects of noncoherent integration is through the reduction in Type 1 and Type 2 errors that result. This is explained further in figure 11-5.

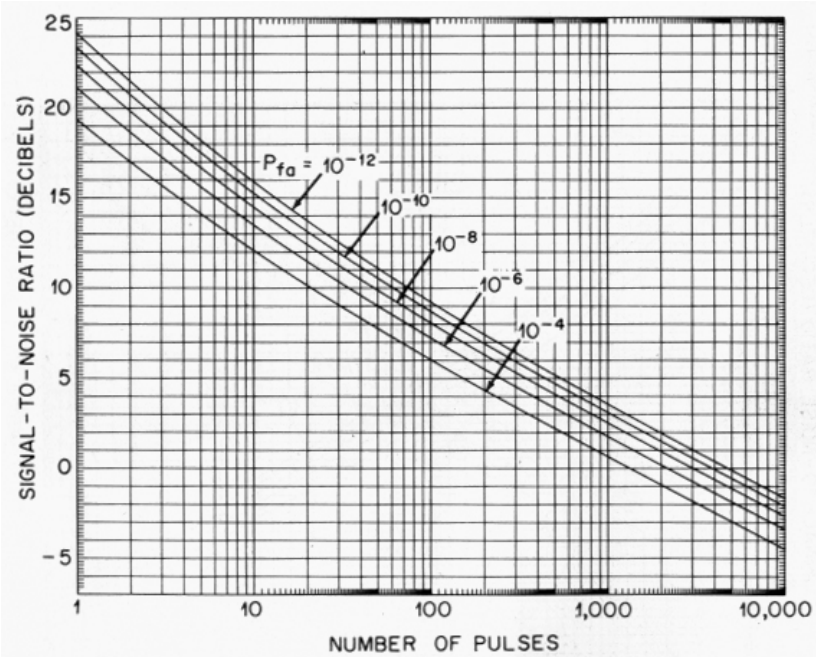


$$P_d = 0.90$$

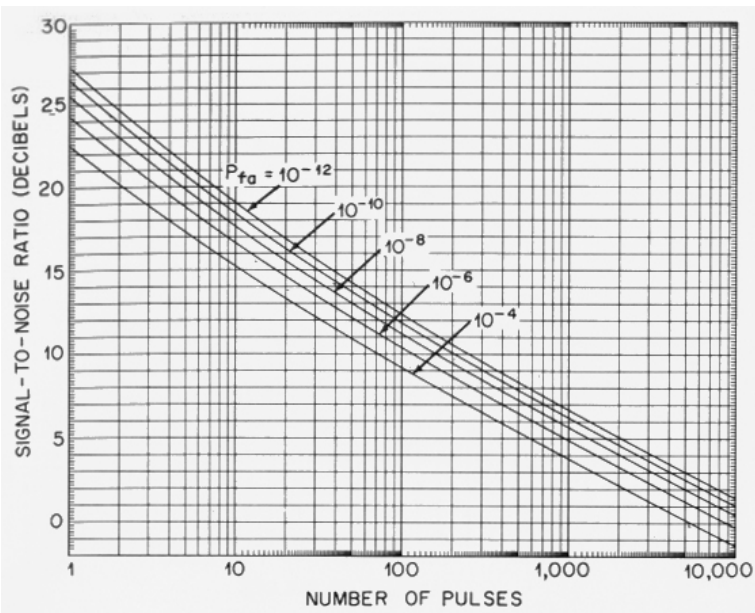


$$P_d = 0.95$$

FIGURE 11-2. SNR FOR DETECTION PROBABILITIES OF 0.90 AND 0.95 FOR NON-FLUCTUATING TARGETS (SOURCE: M. SKOLNIK, *RADAR HANDBOOK*, MCGRAW-HILL BOOK COMPANY, NY, 1970).



$P_d = 0.90$



$P_d = 0.95$

FIGURE 11-3. SNR FOR DETECTION PROBABILITIES OF 0.90 AND 0.95 FOR SWERLING 1 FLUCTUATING TARGETS (SOURCE: M. SKOLNIK, *RADAR HANDBOOK*, MCGRAW-HILL BOOK COMPANY, NY, 1970).

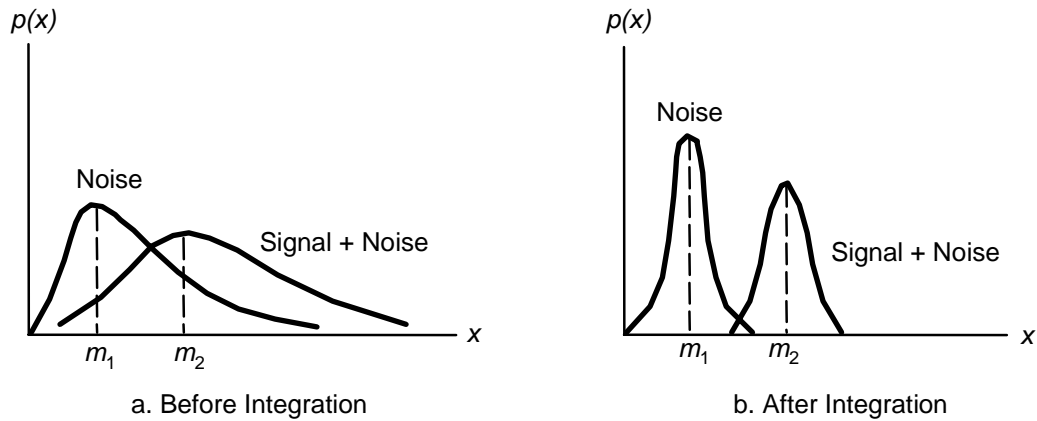


FIGURE 11-4. NONCOHERENT VIDEO INTEGRATION OF INDEPENDENT SIGNAL SAMPLES SHOWING REDUCTION IN VARIANCE OF NOISE AND SIGNAL PLUS NOISE. (SOURCE: L.A. KLEIN, *MILLIMETER-WAVE AND INFRARED MULTISENSOR DESIGN AND SIGNAL PROCESSING*, ARTECH HOUSE, NORWOOD, MA, 1997).

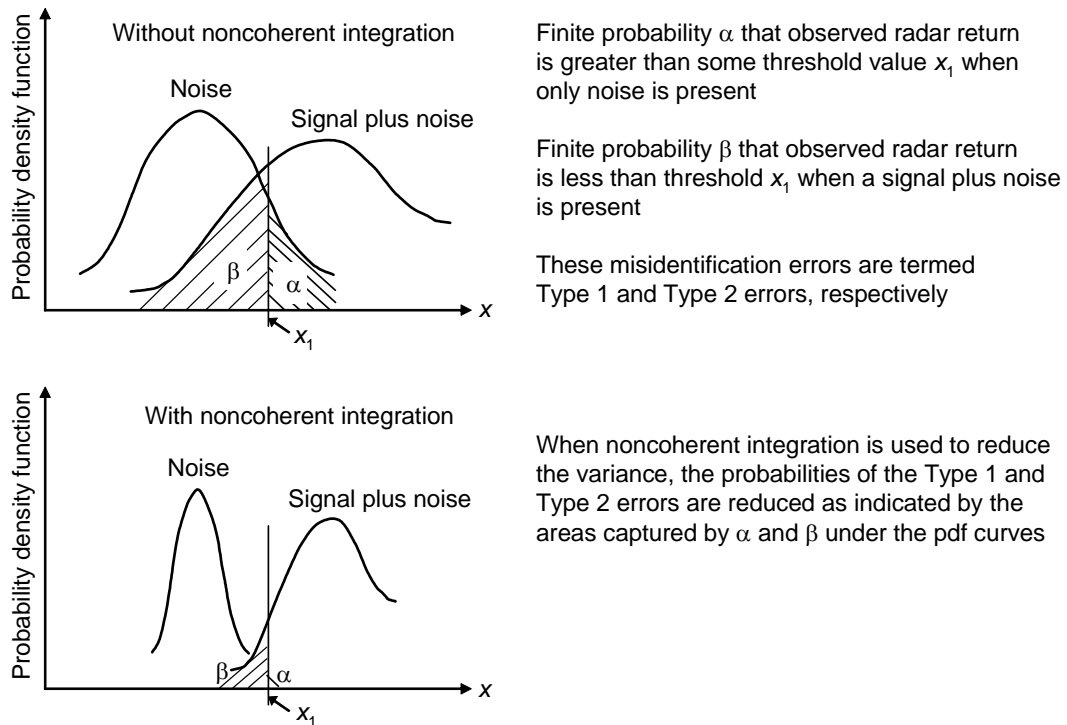


FIGURE 11-5. TYPE 1 AND TYPE 2 TARGET CLASSIFICATION ERRORS ARE REDUCED BY NONCOHERENT INTEGRATION AS A RESULT OF THE DECREASE IN VARIANCE OF THE NOISE AND SIGNAL PLUS NOISE. (SOURCE: L.A. KLEIN, *SENSOR AND DATA FUSION: A TOOL FOR INFORMATION ASSESSMENT AND DECISION MAKING*, SPIE PRESS MONOGRAPH 138, BELLINGHAM, WA, JUNE 2004).

11.7 Radar Range Equation Expressed as Signal-to-Noise Ratio

The detection range of a radar for bird detection can be determined by examining the equation for SNR assuming that detection is noise limited. This will be true when detecting birds against a sky background. The SNR equation is given by

$$\text{SNR} = \frac{P_t G_t G_r \lambda^2 \sigma}{(4\pi)^3 R^4 k_B T_0 B F_n L L_{wg}} G_{imrej} G_{FFT}, \quad (11-9)$$

where P_t = transmitted power, G_t, G_r = transmitted, received antenna gain at 3 dB points, λ = wavelength corresponding to transmitted frequency, σ = radar cross section (RCS) of target object, R = range to target, k_B = Boltzmann's constant = 1.38×10^{-23} J/K, T_0 = temperature of receiver assumed equal to 290K, B = IF noise bandwidth, F_n = noise figure of receiver, L = combined FFT window, signal processing, and atmospheric losses, L_{wg} = waveguide connection losses, G_{imrej} = gain from image band rejection, and G_{FFT} = gain from FFT processing.

When the aperture is uniformly illuminated, antenna gain G may be expressed in terms of the solid angle captured by the beam as

$$G = 9.84/(\theta_a \theta_e), \quad (11-10)$$

where θ_a, θ_e are the azimuth and elevation 3 dB beamwidths, respectively. *In practice, ohmic, feed, and spillover losses reduce the gain calculated from this expression.* (Ref. J.V. DiFranco and W.L. Rubin, *Radar Detection*, Prentice Hall, NJ, 1968.)

The IF noise bandwidth B is computed from the RF modulation bandwidth ΔF , RF modulation frequency f_m , maximum range to target R_M , and speed of light c as

$$B = \max[f_{IF}] = 2 \Delta F f_m R_M/c \quad (11-11)$$

when the transmitted waveform consists of an up-sweep frequency signal as illustrated in figure 11-1a. This waveform was used in all BIRDARTM tests to date, including the DFW Airport tests. The symbol f_{IF} represents the instantaneous value of the IF frequency.

When the transmitted waveform contains both an up-sweep and down-sweep component as shown in figure 11-1b, the IF noise bandwidth is given by

$$B = \max[f_{IF}] = 4 \Delta F f_m R_M/c. \quad (11-12)$$

The waveform in figure 11-1b is proposed for the improved BIRDARTM as it will allow moving target indicator (MTI) performance to be enhanced by supporting retention of small SNR bird returns while rejecting signals due to noise and stationary objects.

FFT windowing loss was set equal to 1.74 dB based on the digital Hamming filter loss (Ref. N. Levanon, *Radar Principles*, John Wiley and Sons, NY, 1988). Signal processing loss was

estimated as 2 dB, one-way 94 GHz atmospheric absorption as 0.3 dB/km, and 94 GHz waveguide loss as 2 dB.

The other parameters in the SNR equation are defined in table 1-2 for the original 94 GHz BIRDAR™ design and table 1-3 for the BIRDAR™ design used at the Salton Sea and DFW.

11.8 Modeled Detection Range

The predicted detection range for the original 94 GHz BIRDAR™ design (having radar parameters shown in table 1-2) with human interpretation of the radar imagery was ≈ 2.9 km against a flock of large birds with assumed RCS of 0.03 m^2 . This detection range prediction is equal to the range at which the SNR is zero as shown by the upper curve in figure 11-6.

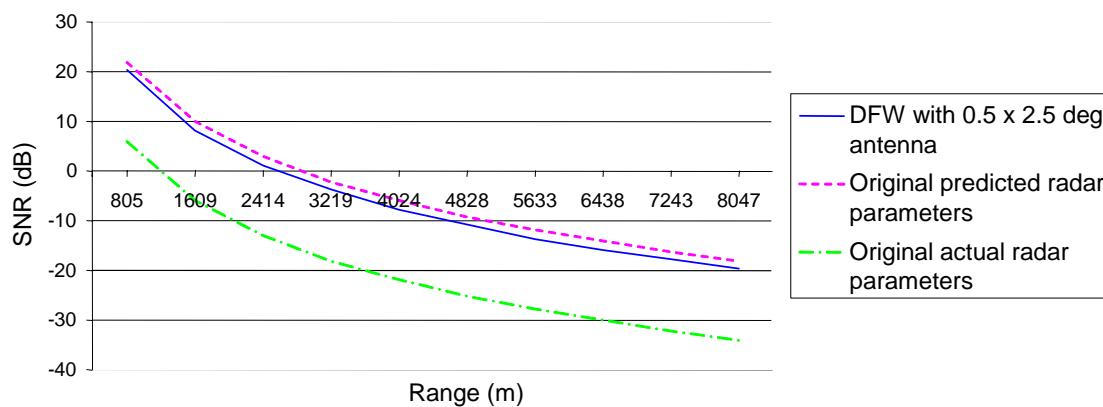


FIGURE 11-6. 94 GHZ BIRDAR™ SNR FOR ORIGINAL AND DFW AIRPORT RADAR CONFIGURATIONS ASSUMING BIRD FLOCK TARGETS WITH $\text{RCS} = 0.03\text{M}^2$.

The gain and loss budget used in Eq. 11-9 for the SNR is shown in table 11-1 as an example of the SNR calculation for the prediction of the original 94 GHz BIRDAR™ performance at $R = 3.2$ km. The -2 dB net SNR in the table is the same as that shown by the upper curve in figure 11-6 when $R = 3.2$ km.

The predicted detection range was subsequently reduced to ≈ 1.2 km ($\text{SNR} = 0$ on lower curve in figure 11-6) when actual antenna gains and FFT windowing, signal processing, atmospheric absorption, and waveguide losses were included.

Using the 0.5 by 2.5 deg antenna, increased power of 575 mW, reduced IF bandwidth to limit noise, and realistic losses (these radar parameters are shown in table 1-3) predicts a detection range for a flock of large birds of 2.5 km corresponding to a $\text{SNR} = 0$. The confidence in achieving this detection range with a human observer is higher than with the original 94 GHz radar design parameters because of the improved estimates of the design and operating parameters that are incorporated into the SNR equation. The SNR curve for these parameters is illustrated by the middle curve in figure 11-6 drawn with the solid line.

Extrapolation of the detection results at DFW to large birds, i.e., Canada geese, appears to support the 2.5 km detection range forecast. At DFW, flocks of small birds and single medium

sized raptors were detected by human observers as far as 1.2 km away. The medium sized hawks and vultures typically weigh 1 to 1.5 kg, while the large Canada geese the radar was designed to detect at 4.8 km weigh up to 6.6 kg. If the RCS is proportional to bird mass, then Canada geese should be detectable at ranges between $(6.6/1.0)^{0.25} \times 1.2 \text{ km} = 1.9 \text{ km}$ and $(6.6/1.5)^{0.25} \times 1.2 \text{ km} = 1.7 \text{ km}$ with the DFW radar. (The $\frac{1}{4}$ power exponent comes from the fourth power dependence of SNR on range as shown in Eq. 11-9.) However, this calculation appears overly pessimistic as flocks of geese were detected at the Salton Sea and Klamath Falls at ranges of 2.1 to 2.6 km. *The Salton Sea and Klamath Falls results are more in line with the predicted detection range of 2.5 km.*

TABLE 11-1. SNR CALCULATION FOR ORIGINAL 94 GHZ BIRDAR™ DESIGN.

Parameter	Positive Contribution (dB)	Negative Contribution (dB)
P_t		4
G_t	38	
G_r	38	
λ^2		50
σ		15
$(4\pi)^3$		33
R^4		140
$k_B T_0$	204	
B		67
F_n		6
L		3
L_{wg}		0
G_{imreg}	0	
G_{FFT}	36	
Subtotals	316	318
Net SNR		-2 dB

11.9 Reduced Drum Rotation Speed and Spatial Integration

The detection range of the radar deployed at DFW Airport was potentially increased through spatial integration implemented by decreasing the modulation frequency and drum rotation speed. The analysis that supports this conclusion is described below.

Spatial integration creates an effective dwell period when the bird is in the 2.3 m range cell (Table 1-3) as compared to the dwell time when the bird is in the original 0.65 m range cell (Table 1-2). Therefore, a pseudo dwell factor of as much as $2.3/0.65 = 3.5 = 5.4 \text{ dB}$ could be present to enhance the SNR through the increased size of the range cell. Another way to describe this effect is through the increased power that is delivered to the target as a result of the increased dwell time. This results in an increase in SNR as described by DiFranco and Rubin.

Still another way of viewing the results of spatial integration is in terms of noncoherent integration that could arise if the drum speed could be made sufficiently fast. In this case, a large number of returns could be noncoherently integrated to achieve the same SNR as with the longer dwell period. However, this method could require faster signal processors and drum speeds beyond present capabilities and would offer no improvement in SNR over that obtained with the slower drum speed and spatial integration.

11.10 Antenna Configuration to Reduce Ground Return

To reduce signals received from ground clutter, WaveBand proposes to mount the antenna with the long axis vertically. The fast scan from the drum rotation will be in the vertical direction over 6 degrees. To ensure sufficient azimuth coverage, a stepper motor will be used to scan the horizontal direction over ± 15 degrees. This antenna configuration is illustrated in figure 11-7.

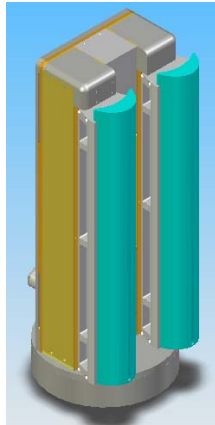


FIGURE 11-7. TWO DIMENSIONAL ANTENNA SCANNING CONCEPT.

11.11 Radar Designs for Automatic Target Detection

Signal-to-noise ratio improvement

In order to implement automatic target detection, a SNR of at least 15 dB is needed. This is based on the detection probability curves of figures 11-2 and 11-3 that show a detection probability of 0.9 to 0.95 for SNR of 15 to 20 dB and false alarm probability = 10^{-4} for non-fluctuating and Swerling 1 fluctuating targets.

In order to achieve SNR = 15 dB at a 3 mile range with a flock of large bird targets, we examined the design options that could be realistically used for a 35 and 94 GHz radar. The major improvements at 35 GHz arise from coherent operation, increased transmitted power, reduction in the larger antenna resolution beamwidth to $1\frac{1}{4}$ degrees, decreased noise figure, decreased waveguide losses to approximately 1 dB, and decreased atmospheric losses. Table 11-2 lists the one-way atmospheric absorption values at 35 and 94 GHz.

TABLE 11-2. ONE-WAY ABSORPTION (REF. N.C. CURRIE AND C.E. BROWN, PRINCIPLES AND APPLICATIONS OF MILLIMETER-WAVE RADAR, ARTECH HOUSE, NORWOOD, MA, 1987).

Frequency (GHz)	Absorption (dB/km)
35	0.05
94	0.3

A potential drawback to 35 GHz operation could be interference with existing FAA or airport equipment. An early task in the proposed development plan for the automatic bird detection radar calls for discussing and evaluating this risk with FAA and airport personnel.

The major improvements at 94 GHz come from coherent operation, increased power to 2 W CW, and increased antenna gain by 6 dB (two way) from a reduction in the larger resolution beamwidth to 1¼ degrees. A potential limitation of the high power 94 GHz approach is the more limited lifetime of the 2 W transmitter source that was postulated as it is not solid state.

RF modulation frequency

The antenna rotation speed and modulation frequency analysis is illustrated in figure 11-8 for the 35 GHz antenna parameters.

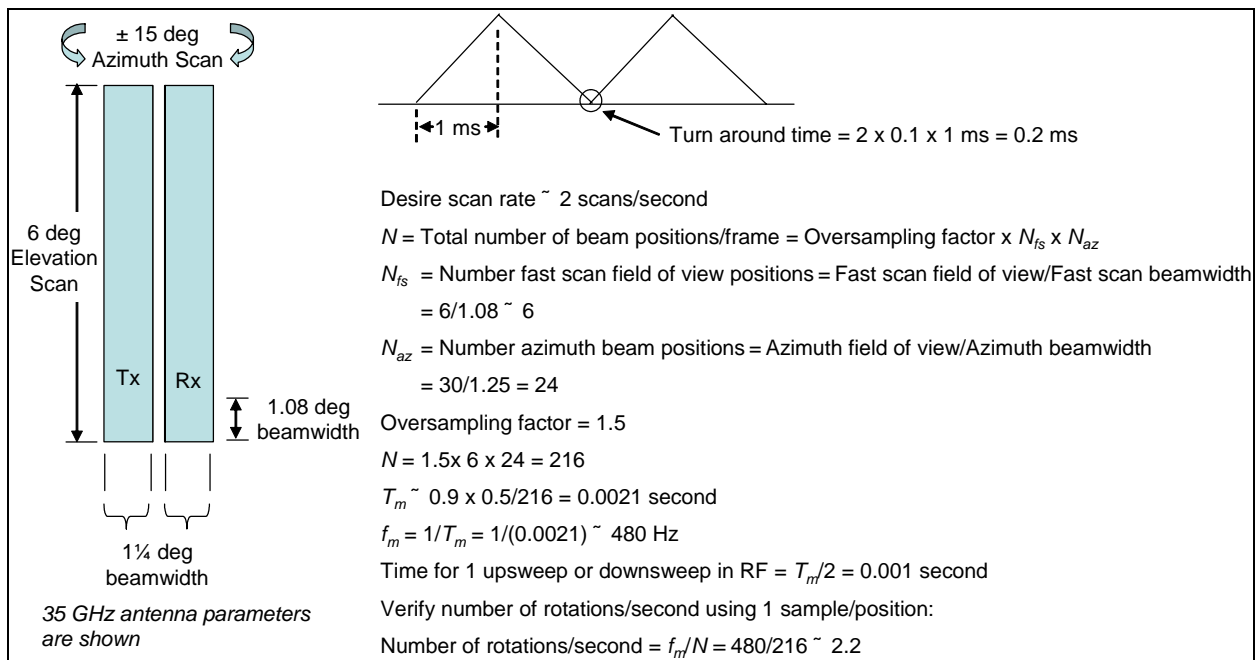


FIGURE 11-8. ANTENNA ROTATION SPEED AND MODULATION FREQUENCY ANALYSIS.

To enable spatial integration, we desire an antenna scan rate of about 2 scans/s. When the transmitted waveform has an upswEEP and a downswEEP, the RF modulation period is given by

$$T_m = 0.9 \times \text{Time for 1 revolution of drum}/(\text{number of cell positions/frame}). \quad (11-13)$$

The number of beam positions per frame N is equal to

$$N = \text{Oversampling factor} \times N_{fs} \times N_{az}, \quad (11-14)$$

where

$$N_{fs} = \text{number of fast scan field of view positions} = \text{Fast scan field of view} / \text{Fast scan beamwidth and}$$

$$N_{az} = \text{number of azimuth beam positions} = \text{Azimuth field of view} / \text{Azimuth beamwidth.}$$

For the 35 GHz radar parameters postulated for the bird detection radar shown in table 11-3, which assumes a vertically oriented antenna drum,

$$N_{fs} = (6)/1.08 = 5.56 \approx 6, \quad (11-15)$$

$$N_{az} = 30/1.25 = 24,$$

and

$$N = 1.5 \times 6 \times 24 = 216$$

when the oversampling factor = 1.5.

Therefore, the RF modulation period is

$$T_m \approx 0.9 \times 0.5 / (216) = 0.0021 \text{ s.} \quad (11-16)$$

By definition, the RF modulation frequency is equal to

$$f_m = 1/T_m \approx 480 \text{ Hz.} \quad (11-17)$$

At 35 GHz, the time for one up-sweep or one down-sweep in frequency (including turn around time) is

$$T_m/2 = 0.001 \text{ s.} \quad (11-18)$$

For the 94 GHz radar parameters postulated for the bird detection radar shown in table 11-4,

$$N_{fs} = (6)/0.5 = 12, \quad (11-19)$$

$$N_{az} = (30)/(1.25) = 24, \quad (11-20)$$

and

$$N = 1.5 \times 12 \times 24 = 432. \quad (11-21)$$

TABLE 11-3. 35 GHZ BIRDAR™ DESIGN PARAMETERS.

Parameter	Value
Center frequency	35 GHz
Waveform	Sawtooth in support of Doppler MTI processing
Azimuth beamwidth	1.08 degrees
Elevation beamwidth	1.25 degrees
Antenna gain (transmit and receive, each)	36 dB
Antenna polarization	Horizontal (when fast scan is in vertical direction)
Total losses (FFT window, signal processing, atmospheric, waveguide)	5.5 dB
Fast scan field of view	6 degrees
Fast scan time function	Linear, true continuous
Fast scan speed	≈ 2 scans per second
Azimuth field of view	30 degrees
Beam positions/frame	216
Output power	10 W CW
Noise figure	3 dB with low noise amplifier
IF bandwidth	2 MHz
RF modulation bandwidth	65 MHz
RF modulation period $T_m/2$	1 ms
Image band rejection	-3 dB in noise
IF processing	4K FFT (4K utilized giving 36 dB processing gain)
Displayed range cells	Up to 4K per azimuth beam
Range cell size	7.5 ft (2.3 m)
Target radar cross section	0.0015 m ² for individual birds 0.03 m ² for bird flocks

Therefore, the RF modulation period is

$$T_m \approx 0.9 \times 0.5 / (432) = 0.001 \text{ s.} \quad (11-22)$$

and

$$f_m = 1/T_m \approx 1 \text{ kHz.}$$

At 94 GHz, the time for one upswEEP or one downswEEP in frequency (including turn around time) is

$$T_m/2 = 0.5 \text{ ms.} \quad (11-23)$$

TABLE 11-4. IMPROVED 94 GHZ BIRDAR™ DESIGN PARAMETERS.

Parameter	Value
Center frequency	94.3 ± 0.5 GHz
Waveform	Sawtooth in support of Doppler MTI processing
Azimuth beamwidth	0.5 degree
Elevation beamwidth	1.25 degrees
Antenna gain (transmit and receive, each)	39 dB
Antenna polarization	Horizontal (when fast scan is in vertical direction)
Total losses (FFT window, signal processing, atmospheric, waveguide)	9 dB
Fast scan field of view	6 degrees
Fast scan time function	Linear, true continuous
Fast scan speed	≈ 2 scans per second
Azimuth field of view	30 degrees
Beam positions/frame	432
Output power	2 W CW
Noise figure	6 dB with low noise amplifier
IF bandwidth	4 MHz
RF modulation bandwidth	65 MHz
RF modulation period $T_m/2$	0.5 ms
Image band rejection	-3 dB in noise
IF processing	4K FFT (4K utilized giving 36 dB processing gain)
Displayed range cells	Up to 4K per azimuth beam
Range cell size	7.5 ft (2.3 m)
Target radar cross section	0.0015 m ² for individual birds 0.03 m ² for bird flocks

Noise bandwidth

The noise bandwidth is given by

$$B = \max[f_{IF}] = 4 \Delta F f_m R_M/c. \tag{11-24}$$

Thus, at 35 GHz

$$B = (4)(65 \times 10^6)(480)(4800)/(3 \times 10^8) \approx 2 \text{ MHz}. \tag{11-25}$$

At 94 GHz,

$$B = (4)(65 \times 10^6)(1000)(4800)/(3 \times 10^8) \approx 4.2 \text{ MHz}. \tag{10-26}$$

Noncoherent integration

As discussed in Section 11.6, noncoherent integration can be used to reduce the variance of the noise and signal plus noise if the antenna drum rotation rate, range cell resolution, and bird speed allow. The benefit would be in increasing the probability of correctly classifying returns as belonging to flying birds and differentiating them from noise.

However, the radar revisits each azimuth cell every 0.5 second when the drum rotation rate is 2 rev/s. Since a bird remains in a range resolution cell for 0.172 to 0.256 s as shown in table 11-5, noncoherent integration is not possible.

TABLE 11-5. MAXIMUM NUMBER OF RETURNS NONCOHERENTLY INTEGRATED IN A 2.3 M RANGE RESOLUTION CELL WHEN THE RF MODULATION OCCURS OVER $T_M/2 = 2$ MS AND BIRDS FLY AT SPEEDS OF 20 AND 30 MI/H.

Bird Speed	Time in 2.3 m Cell
20 mi/h (9 m/s)	0.256 s
30 mi/h (13.4 m/s)	0.172 s

Radar performance summary

Figure 11-9 shows the SNR as a function of range for detection of flocks of large birds with the proposed 35 and 94 GHz radars. In support of automatic target detection, the 35 GHz radar achieves a SNR of 15 dB at ranges up to 5.2 km, while the 94 GHz design achieves SNR equal to 15 dB at ranges of 1.7 km and less. At 4.8 km (3 mi), the SNR for the 35 GHz radar is 16.6 dB, more than adequate for automatic target detection. The corresponding SNR for the 94 GHz radar is -2.7 dB. With a human in the loop for target detection, the 35 GHz radar supports detection at 12 km (assuming human detection occurs with SNR as low as 0 dB), while the improved 94 GHz radar supports human detection up to approximately 4 km.

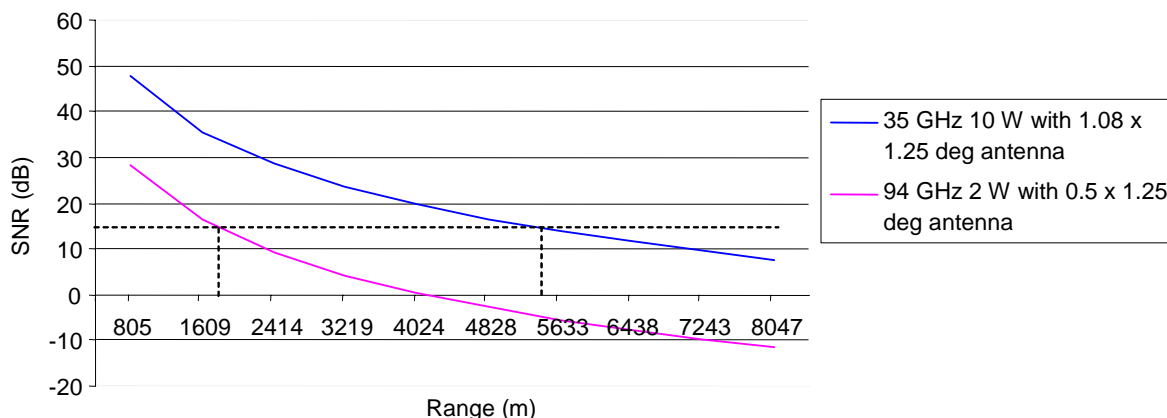


FIGURE 11-9. SNR FOR PROPOSED 35 AND 94 GHz BIRDAR™ RADARS ASSUMING BIRD FLOCK TARGETS WITH RCS = 0.03M².

11.12 Improved Moving Target Indicator Algorithm

Another proposed improvement to operation of the bird detection radar is the incorporation of an improved MTI algorithm in the eventual 35 or 94 GHz radar. Currently, BIRDARTM implements MTI by subtracting an average background computed from 10 frames of data from the current frame of data. The frames that represent the stationary background are acquired during time periods when there is no bird activity. In this way, radar returns from stationary objects are subtracted from the current real-time image data. The resulting MTI data represent only moving objects, presumably birds. The MTI data are then overlaid on a GIS map of the local airport area to display the regions of bird activity in a meaningful manner. A threshold is set to limit MTI signals that arise from noise from being applied to the map overlay process. The drawback with the threshold limit is that low amplitude MTI signals from valid moving objects, i.e., birds, may be discarded along with the noise. The improved MTI technique described in the next paragraph eliminates this disadvantage.

The improved MTI is based on a calculation of the Doppler frequency or speed of the moving objects. This technique is enabled by transmitting a sawtooth waveform that contains an up and down frequency sweep as illustrated in figure 11-1b.

The algebra that describes the calculation of the Doppler frequency shift is illustrated in figure 11-10. The Doppler MTI operates by calculating the difference in frequencies that arise between the transmitted and received frequencies during the upsweep and downsweep periods at a given time. The time difference Δt between transmission and reception of a corresponding signal is proportional to the specific range at which a target object is located.

11.13 Coherent Receiver Design and Signal Demodulation

Figures 11-11 and 11-12 describe the recommended approach for implementing a coherent superheterodyne transceiver through the use of two intermediate frequencies (IFs), digitization of the final 60 MHz IF signal, and digital down conversion to inphase (I) and quadrature (Q) baseband digital signals. The I and Q signals are treated as the real and imaginary components of a complex signal. A complex fast Fourier transform (FFT) of the I and Q signal is performed to generate the complex spectra of the signal. Performing an FFT on a real signal sequence results in a complex spectrum with half the number of points that are in the real array. However, performing a complex FFT on a complex signal, such as produced by I and Q down conversion, results in an FFT that has the same number of points as in the complex signal array. Therefore, performing an FFT on a complex signal array produces a factor of two increase in SNR as compared with performing an FFT on a real number signal array (as is the case in the DFW 94 GHz radar).

The signal source in the superheterodyne transceiver of figure 11-11 is a 4 GHz YIG oscillator. Its frequency is modulated by the triangular wave to generate the linear frequency modulated (LFM) signal. The LFM signal is mixed with the 90 GHz local oscillator (LO) signal to translate the frequency up to 94 GHz. The 90 GHz LO is generated by frequency multiplying the 15 GHz dielectric resonance oscillator (DRO) output by a factor of six.

or cosine lookup tables is eliminated. The operation of the circuit is straightforward and the outputs can be derived using basic trigonometric identities.

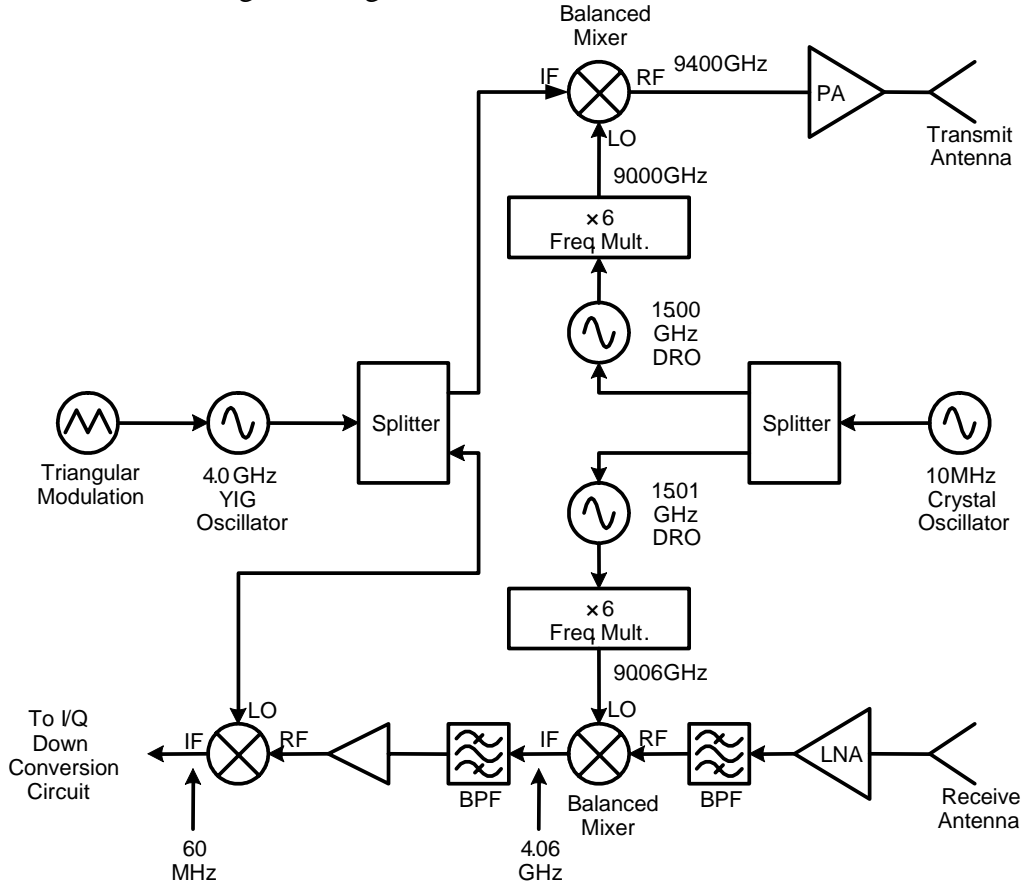


FIGURE 11-11. SUPERHETERODYNE TRANSCEIVER.

In summary, the advantages of the proposed quadrature demodulation technique are:

- Elimination of DC offset and I and Q gain/phase imbalance characteristic of analog demodulation techniques.
- Elimination of manual adjustments and calibrations.
- Insensitivity to temperature variations.
- Elimination of susceptibility to low frequency interference and noise.
- Implementation of quadrature local oscillators through a simple sequence of ones, zeros, and minus ones.
- Elimination of additional analog down conversion.
- Simple design and easy to build phase locked loop (PLL) circuit to generate the sampling clock.

Thus, there are no inherent difficulties in the quadrature demodulation approach.

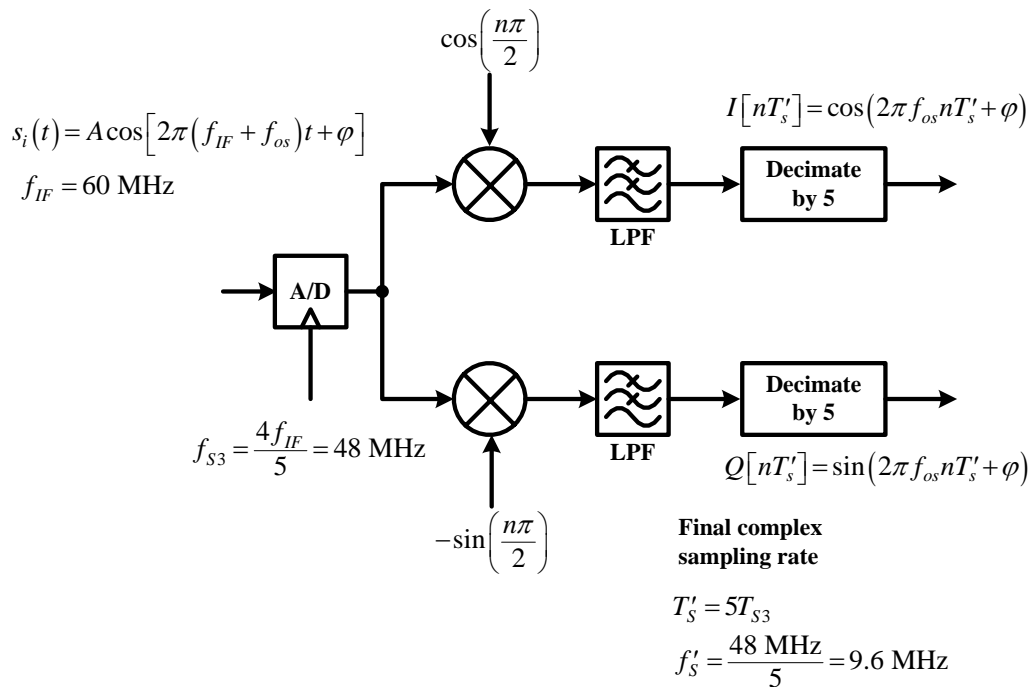


FIGURE 11-12. QUADRATURE DEMODULATION USING DIRECT IF SAMPLING AND DIGITAL I AND Q.

12. BENEFIT SUMMARY

To summarize, the benefits of either of the proposed 35 and 94 GHz BIRDAR™ designs are:

- Increased detection range for flocks of large birds, the primary wildlife threat to aircraft safety.
- Support of automatic target detection through increased SNR.
- Improved moving target indicator performance allowing display of birds with smaller SNR return signals on GIS airport maps.
- Direct calculation of bird speeds from Doppler signal processing enabled by enhanced sawtooth transmitted waveform.
- Potential algorithm development to classify birds by their wing flap spectrum.
- Computer operating system with real time interrupts to support enhanced radar control and signal processing.
- Simplified user interface that identifies magnitude and location of bird collision threats.
- Generation of manufacturing plan and drawings for field-deployable BIRDAR™.

13. DEVELOPMENT AND DEMONSTRATION SCHEDULE

The 3-year BIRDAR™ development and test schedule is shown in figure 13-1.

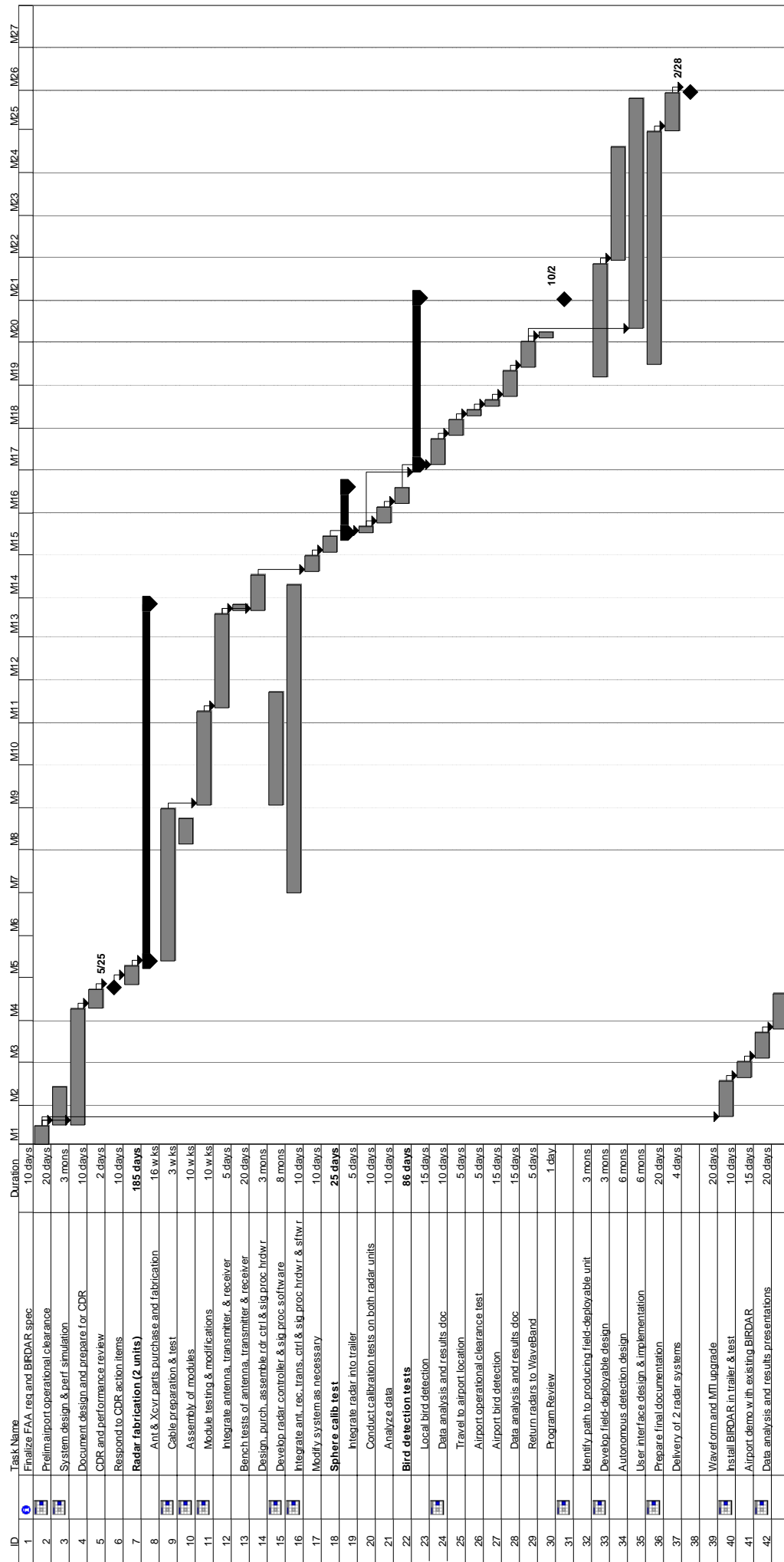


FIGURE 13-1. BIRDAR™ DEVELOPMENT AND DEMONSTRATION SCHEDULE.

13.1 Task Summary by Year

The first year (FY 2005) tasks address the following objectives:

- Maintenance of program momentum through demonstration of BIRDAR™ (DFW model) at Chicago O'Hare Airport.
- Implementation of improved moving target indicator algorithm.
- Finalization of FAA requirements and BIRDAR™ specification.
- Conducting Critical Design Review.
- Risk reduction through tasks that include design, build, and test of antenna and coherent receiver and performance reviews with the FAA and AF.
- Commencing path to operational certification by developing a Unix or other real-time operating system for the radar and signal processing software.

Second year (FY 2006) tasks address:

- Continue on path to operational certification through development of real-time data display software.
- Design, build, and test of radar controller and signal processor hardware.
- Integration and test of real-time operating system and radar controller hardware.
- Integration of antenna, transceiver, signal processor hardware, and control and data processing software into a fully operational radar system.
- Modification of hardware and software as necessary as a result of laboratory and local field tests.
- Maintenance of program momentum through demonstration of BIRDAR™ (DFW model) at another airport, possibly JFK in New York City.
- Show path to field-deployable and autonomously operating radar system by preparing manufacturing plan for BIRDAR™.

Third year (FY 2007) tasks include:

- Demonstration of adapted radar system performance in CA through two series of tests.
- Modification of University of Illinois trailer to accommodate new radar.
- Demonstration of adapted radar system at an airport to be selected.
- Conducting tests required for eventual certification for use of BIRDAR™ at airports.
- Continuation of path to field-deployable and autonomously operating radar system by developing final drawings and specifications.
- Delivery of two BIRDAR™ radars and all required documentation.

APPENDIX A: 94 GHz BIRD DETECTION RADAR FIELD TEST PLAN

*Development of a 94 GHz Radar System for Dedicated Bird
Detection at Airports and Airfields*

Agreement Number F30602-02-2-0119

Prepared by

WaveBand Corporation
17152 Armstrong Avenue
Irvine, CA 92614

The logo for WaveBand Corporation, featuring the text "WWW WAVEBAND" in white on a black rectangular background, which is centered over a larger, light brown square.

for

Air Force Research Laboratory, Rome, NY
and FAA Technical Center, Atlantic City, NJ



October 30, 2003

Preface

This appendix contains the test specifications and plans developed for the field tests to be conducted at the Air Force Research Laboratory at Rome, NY and at John F. Kennedy (JFK) International Airport in Jamaica, NY. The data gathered at the Air Force Research Laboratory will quantify the performance of the 94 GHz radar used for detecting birds at airports and airfields using a tethered metalized balloon as a radar target of known radar cross section. Upon satisfactory calibration of the radar and verification of its performance, the radar will be transported to JFK Airport, where it will be used to detect birds and track their movements.

It is anticipated that some of the test plans will be modified as the field tests proceed. These changes will be incorporated into the Test Plan and Test Results Report at the end of the test period.

TABLE OF CONTENTS

LIST OF FIGURES	55
LIST OF TABLES	56
A. TEST OBJECTIVES	57
B. RADAR DESCRIPTION	57
C. AIR FORCE RESEARCH LABORATORY TESTS	59
D. JFK AIRPORT TESTS	63
E. DAILY ACTIVITIES SCHEDULE	65
F. WEATHER, BIRD, AND RADAR DATA SHEET	66
G. DATA RECORDING AND ANALYSIS	66
H. SECURITY FOR THE TEST SITE	66
APPENDIX: EQUIPMENT AND FACILITIES PROVIDED BY AIR FORCE RESEARCH LABORATORY	70

LIST OF FIGURES

FIGURE 1.	94 GHz FMCW TRANSCEIVER WITH A LOW PHASE NOISE RF SOURCE AND LOW NOISE AMPLIFIER RECEIVER.....	58
FIGURE 2.	94 GHz FMCW TRANSCEIVER PHOTOGRAPH SHOWING THE PRINCIPAL RADAR COMPONENTS.	58
FIGURE 3.	TRANSCEIVER AND ANTENNA DIMENSIONS AND WEIGHT.	59
FIGURE 4.	TRIHEDRAL RETROREFLECTOR.	61
FIGURE 5.	BERGIN BASIN SITE AT END OF RUNWAY 13R.....	63
FIGURE 6.	OUTFALL 10 SITE ALONG RUNWAY 13R (NEAR ENVIRONMENTAL SERVICES TRAILER).....	63
FIGURE 7.	RUNWAY 4L – 22R SITE.	64
FIGURE 8.	ZULU SITE.....	64
FIGURE 9.	FALCON USED TO CHASE BIRDS FROM VICINITY OF RUNWAYS AT JFK AIRPORT.	65
FIGURE A.1.	PORTABLE ELECTRICAL GENERATOR SPECIFICATIONS.....	70
FIGURE A.2.	TEST TRAILER.....	71
FIGURE A.3.	TRAILER DIMENSIONS.....	72
FIGURE A.4.	SPHERICAL RADAR CALIBRATION TARGET SUSPENDED FROM BALLOON.....	72

LIST OF TABLES

TABLE 1.	94 GHz MMW IMAGING RADAR SPECIFICATIONS (NOMINAL).	57
TABLE 2.	TRIHEDRAL RETROREFLECTOR AND SPHERICAL REFLECTOR DIMENSIONS FOR 0.1, 1, 5, 10, 100, AND 500 SQUARE METERS ($F = 94$ GHz).	61
TABLE 3.	MINIMUM HEIGHT FOR SUSPENDING RADAR CALIBRATION TARGETS.	62
TABLE 4.	DAY 1 ACTIVITIES LIST FOR JFK BIRD DATA ACQUISITION.	66
TABLE 5.	SUCCEEDING DAY ACTIVITIES LIST FOR JFK BIRD DATA ACQUISITION.	66
TABLE 6.	WEATHER, BIRD, AND RADAR DATA SHEETS.....	67
TABLE A.1.	RADAR CROSS SECTIONS OF AF RESEARCH LABORATORY SPHERICAL CALBRATION TARGETS.....	73

94 GHZ BIRD DETECTION RADAR FIELD TEST PLAN

A. TEST OBJECTIVES

1. The objectives of the tests at the Air Force Research Laboratory at Rome, NY are to:
 - i. Ensure that the radar can detect and track targets at distances commensurate with those needed for bird detection at airports and airfields,
 - ii. Display their movement on the monitor, and
 - iii. Calibrate the output of the radar using targets of known radar cross section.

The calibration targets will be metal or metalized spheres of known cross section suspended from a tethered balloon. The targets will be located in the far field of the radar antenna. Visible spectrum (video) imagery of the tests will be recorded as part of the documentation of the tests.

2. If inclement weather (e.g., rain, fog) is present, the calibration tests and the measurement of radar performance under these conditions will be made, if possible.

B. RADAR DESCRIPTION

Table 1 lists the radar specifications. A block diagram of the prototype radar unit is shown in Figure 1 and a photograph of it in figure 2. Its dimensions are shown in figure 3. New models of the transceiver and antennas will be used for the Air Force Research Laboratory and JFK Airport tests; however, the dimensions will be about the same as those shown in figure 3.

TABLE 1. 94 GHZ MMW IMAGING RADAR SPECIFICATIONS (NOMINAL).

Parameter	Value
Operating frequency	94.3 GHz \pm 0.5 GHz
RF modulation bandwidth	230 MHz
Azimuth beamwidth	0.5 deg
Elevation beamwidth	5 deg
Antenna gain	38 dB
Antenna polarization	Horizontal (when antenna is vertical)
Azimuth scan range	30 deg (-20 to +10)
Azimuth scan time function	Linear true continuous
Azimuth scan speed	10 frames per second
Elevation adjustment range	30 deg
Weight (antenna & T/R module)	25 lb
Transmitter output power	430 mW CW
IF bandwidth	5 MHz (3 dB)
Noise figure	6 dB (SSB)
Dynamic signal range	82 dB until A/D converter saturates
Angles/Frame	60 at 10 frames per second
Range samples/Azimuth sweep angle	8,192 range cells/angle at 10 MHz sampling rate
FFT size	8,192 points (36 dB processing gain)

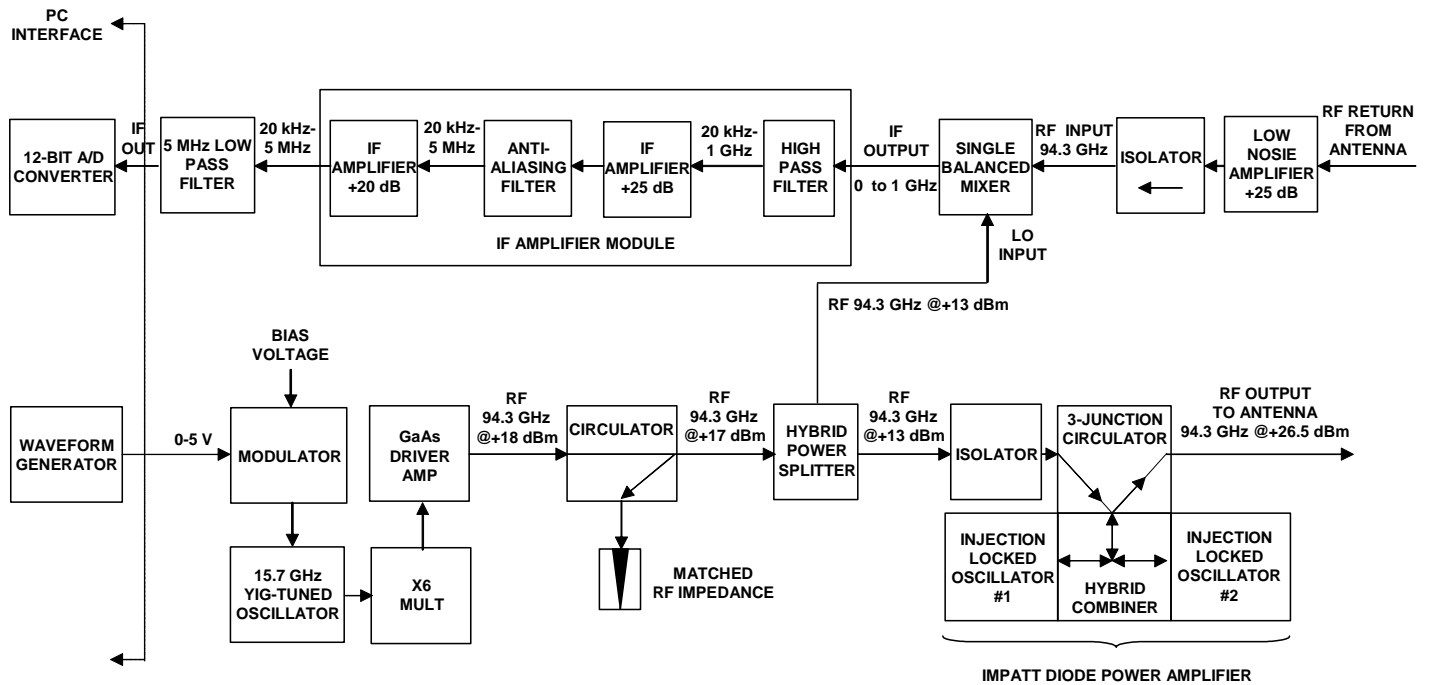


FIGURE 1. 94 GHz FMCW TRANSCEIVER WITH A LOW PHASE NOISE RF SOURCE AND LOW NOISE AMPLIFIER RECEIVER.

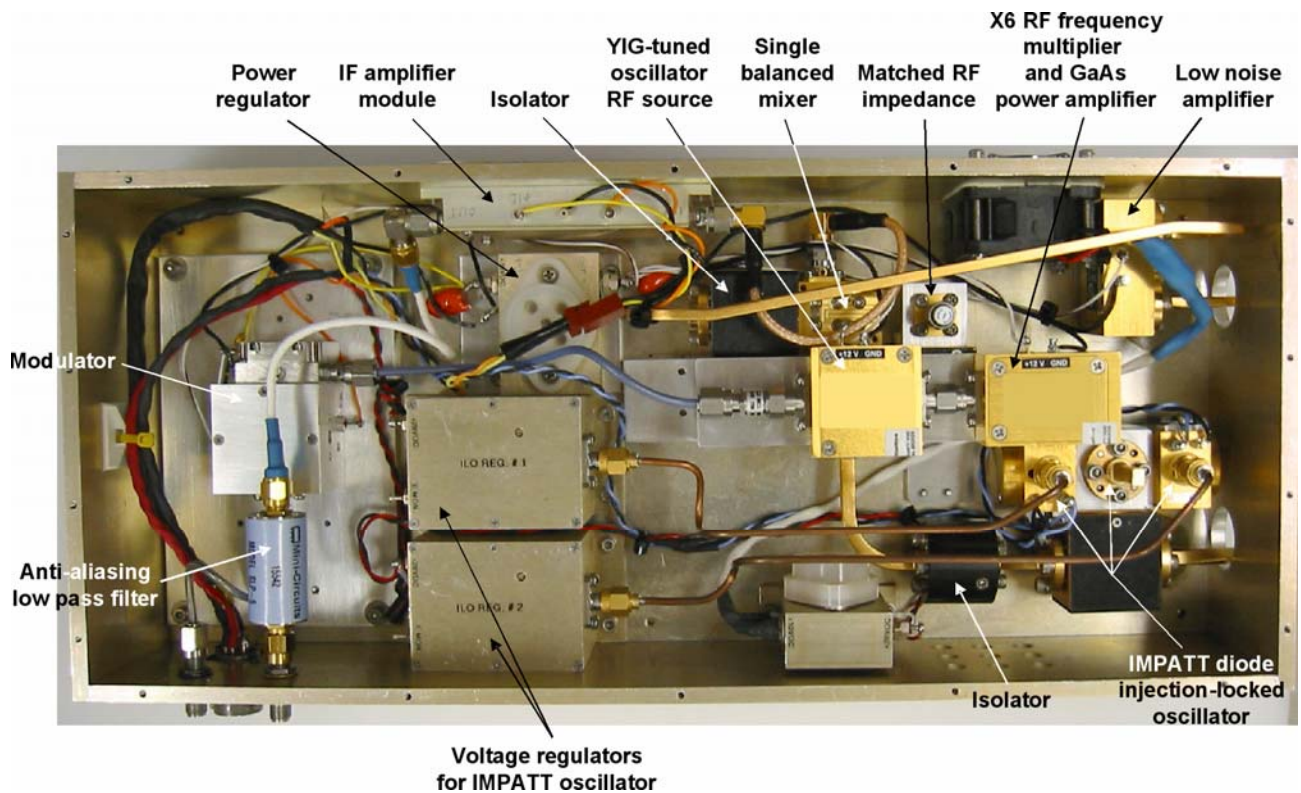


FIGURE 2. 94 GHz FMCW TRANSCEIVER PHOTOGRAPH SHOWING THE PRINCIPAL RADAR COMPONENTS.

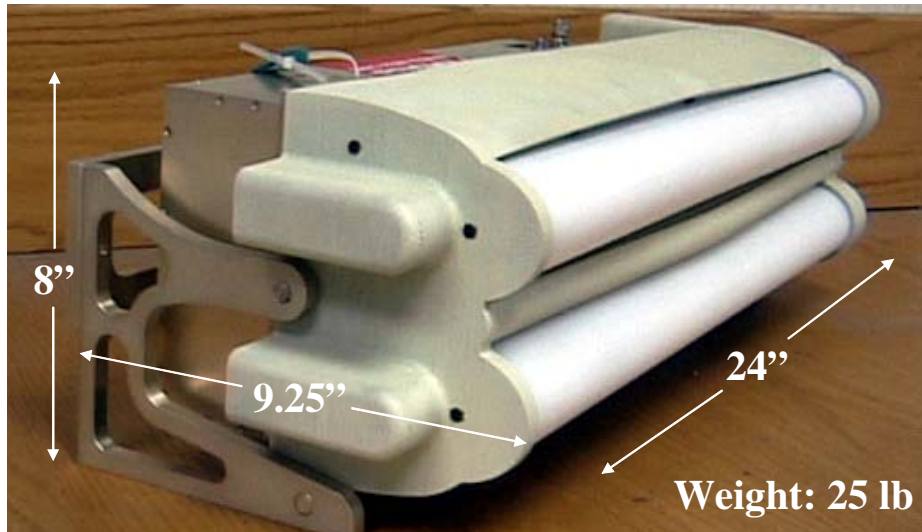


FIGURE 3. TRANSCIEVER AND ANTENNA DIMENSIONS AND WEIGHT.

C. AIR FORCE RESEARCH LABORATORY TESTS

1. The Laboratory expressed a willingness to purchase some specialized test equipment required for the test. These items include a digital camera and recorder, modification of a truck or trailer in which the radar will be mounted (including perhaps a radome structure on the roof), an external 115 VAC power generator that provides a true sine wave output (output current requirement is no more than 6 amps at equipment startup and may be less with the MMIC solid state 94 GHz output amplifier), calibration targets, and a distance measuring device (such as a laser radar) for determining the distance to the calibration targets.

2. The radar and data recording equipment will be mounted in an enclosure (trailer or motorized van or truck). The enclosure will serve multiple functions: protect the equipment and personnel from inclement weather, support collection and recording of radar data by means of an integrated radome, provide a window through which visible spectrum imagery (boresighted with the radar) can be collected, and provide an interface to power for operating the equipment. The enclosure may contain generators (which will be operated outside the enclosure) and power conditioning equipment, such as uninterruptible power supplies. Other test equipment that may be located in the enclosure includes a time code generator, video recording device for the radar-boresighted imagery, and equipment racks.

The radar system includes its own power supplies that operate from 115 VAC; a computer to control the radar, data acquisition, and data processing; and an uninterruptible power supply that incorporates a battery backup.

The appendix contains pictures and specifications for some of the equipment provided by the Air Force Research Laboratory.

3. As a result of discussions with Laboratory personnel, it was decided to mount the radar antenna and transceiver on the roof of the enclosure. The Laboratory will attempt to attach a

rotating platform to the roof of the enclosure, on which the radar can be placed so that it can be positioned to search particular areas of interest that may not be in its nominal scan area due to the orientation of the trailer as parked at the test area. The power and signal cables that connect the radar to power supplies and the radar signal processor computer will be routed through an opening in the roof of the enclosure. Eventually (i.e., in time for the Dallas-Ft. Worth Airport tests in Spring 2004) a radome will be designed and purchased by WaveBand to fit over the roof-mounted radar assemblies.

4. The recommended radar end-to-end calibration scheme utilizes spherical reflectors of known radar cross section attached to tethered balloons suspended in the atmosphere. The radar is then pointed in the direction of the reflector. This technique has the advantage of minimizing the clutter return, which is zero from the sky in clear weather. The only interfering signal using this procedure should be from receiver noise. Spherical reflectors having radar cross sections of 0.1 and 1 square meter at 94 GHz are recommended for calibrating the radar. Larger spherical reflectors can be used if they can be easily manufactured and suspended in the atmosphere while attached to the tethered balloons. A coarse calibration using trihedral retroreflectors can be made by mounting the retroreflectors on a pole of small radar section at a high enough height to minimize ground return.

The calibration procedure involves several steps, including:

1. Pointing the radar at the sky and measuring the return;
2. Pointing the radar at the tethered balloon without a spherical reflector attached and measuring the return;
3. Pointing the radar at the tethered balloon with a spherical reflector of known size attached and measuring the return;
4. Repeating Step 3 several times for each of the different value reflectors available.

The radar cross section σ of a trihedral retroreflector is given by

$$\sigma = (4\pi l^4)/(3\lambda^2) \quad (1)$$

where l is the length of the edge of the trihedral as shown in figure 4.

The radar cross section of a spherical reflector is given by

$$\sigma \approx \pi r^2 \quad (2)$$

when the radius of the reflector is greater than the wavelength transmitted by the radar, i.e., $2\pi r/\lambda \gg 1$, and where r is the radius of the sphere and $\lambda = 0.0032$ m.

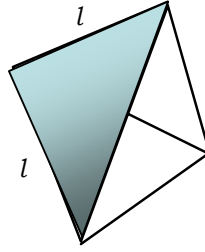


FIGURE 4. TRIHEDRAL RETROREFLECTOR.

Table 2 gives the dimension l of trihedral retroreflectors and the radius r of spherical reflectors of 0.1, 1, 5, 10, 100, and 500 square meters at 94 GHz.

The reflectors or other targets should be in the far field of the radar, which is the distance R given by

$$R = 2L^2/\lambda \quad (3)$$

where L is the length of the antenna aperture, here equal to 20 in (0.51 m). With these dimensions, $R = 533$ ft (163 m).

TABLE 2. TRIHEDRAL RETROREFLECTOR AND SPHERICAL REFLECTOR DIMENSIONS FOR 0.1, 1, 5, 10, 100, AND 500 SQUARE METERS ($F = 94$ GHz).

Radar Cross Section (m ²)	Length of Side l (in)	Radius r of spherical reflector (in)
0.1	0.88	7.02
1	1.56	22.21
5	2.33	49.67
10	2.77	70.24
100	4.92	222.12
500	7.36	496.68

5. Precipitation in the form of rain, fog, and snow may affect the operation of the 94 GHz radar. The radar will be operated in these conditions as they arise to determine their effect, if any, on the performance of the radar. Local weather reports and any available weather bureau data will be used to quantitatively and qualitatively characterize the weather conditions.

6. The minimum height at which the spherical calibration targets should be suspended in the atmosphere is given in table 3 as a function of slant range R from the radar. These heights are based on the 5-degree elevation beamwidth of the antenna and an assumption that the return from ground clutter will be negligible if the minimum height is calculated using an elevation angle that is at least three times the elevation beamwidth. Thus, the minimum height h is given by

$$h = R \sin 15. \quad (4)$$

TABLE 3. MINIMUM HEIGHT FOR SUSPENDING RADAR CALIBRATION TARGETS.

Range R (ft)	h (ft)
0	0.00
500	129.41
1,000	258.82
1,500	388.23
2,000	517.64

7. Data accumulation times should be kept to a maximum of 5 to 10 minutes to limit the stored file to a manageable size for later analysis. Data can be downloaded to a DVD or an external hard drive at the end of each data acquisition period or the end of the day.

D. JFK AIRPORT TESTS

Test sites will be selected from among the four identified at JFK Airport in July 2003. These are listed below:

1. Bergen Basin at end of Runway 13R (western airport boundary). Jamaica Bay runs parallel to Runway 13R.
2. Outfall 10 along Runway 13R near 10,000 ft runway mark. There is an environmental service trailer at this site.
3. Runway 4L – 22R at end of runway. Laughing gulls and terns are found near this location.
4. At ZULU, ILS Z, 4R Z.

All of these sites require that an auxiliary AC power source be made available. The sites are shown in figures 5 – 8.



FIGURE 5. BERGIN BASIN SITE AT END OF RUNWAY 13R.



FIGURE 6. OUTFALL 10 SITE ALONG RUNWAY 13R (NEAR ENVIRONMENTAL SERVICES TRAILER).



FIGURE 7. RUNWAY 4L – 22R SITE.



FIGURE 8. ZULU SITE.

The radar antenna will be mounted either horizontally to electronically scan in azimuth or vertically to scan in elevation, depending on the objective of the test and the location of the birds.

An airport official is needed to escort test personnel to and from the site. This function can be performed by the biologist who will assist in the identification of bird species.

Imagery recorded by a video camera and the notes of a biologist will be used to assist in the identification of bird species. Notes may be in written form or on voice recordings. If the falcons used to scare other birds away from airport runways are at JFK Airport during the radar

tests, the falcons will be released as part of a controlled experiment to calibrate the radar against known bird species. Figure 9 shows one of the bird-chasing falcons sitting on a perch in the back of a pickup truck on airport property.



FIGURE 9. FALCON USED TO CHASE BIRDS FROM VICINITY OF RUNWAYS AT JFK AIRPORT.

Radar and video data will be recorded during periods in which migrating or permanent resident birds at the airport are active, for example at early morning and twilight hours.

A means of independently measuring the distance to the birds is needed. This may be done by identifying known land or water masses on which or above which the birds are located and referring to maps or other documents that have the appropriate distances noted. Alternatively, a low power laser radar or other distance measuring device may be used to determine the distance to the bird targets. Airport maps and other documents showing distances to bird locations and other prominent features will be supplied by the appropriate airport department.

Once several independent measurements of distance to targets are made, the distance as measured by the radar may be substituted for the distance measured by the independent measuring device (assuming the radar distance measure agrees with the distance measured by the independent device within an agreed upon accuracy).

E. DAILY ACTIVITIES SCHEDULE

A schedule of activities for each day of data acquisition will be prepared by the Project Engineer with the assistance of the biologist. Sample activities lists are given in table s 4 and 5 for Day 1 and succeeding days of testing, respectively. This list will be finalized during a meeting with the biologist and other airport staff on or before the first day of tests. Table 5 will be used as a model

for data acquisition activities at all test sites at JFK Airport. It is anticipated that at least two test sites will be used to acquire bird data. The data acquisition times assume that birds are most active at dawn and late afternoon or early evening twilight.

TABLE 4. DAY 1 ACTIVITIES LIST FOR JFK BIRD DATA ACQUISITION.

Time	Event
0800	Planning meeting at Laura’s office
0930	Meet escort in front of Laura’s building
1000	Arrive at Test Site 1 and setup equipment
1100	Begin data acquisition – sample run
1300	Lunch
1400	Return to site and continue data acquisition into twilight and evening hours
1900	Conclude tests for day
2000	Transfer data files to CD or DVD and review plans for following day

TABLE 5. SUCCEEDING DAY ACTIVITIES LIST FOR JFK BIRD DATA ACQUISITION.

Time	Event
0500	Meet at main gate or Laura’s building for escort
0530	Begin data acquisition at Test Site 1
0800	Break for breakfast and data analysis
1530	Return to site and continue data acquisition into twilight and evening hours
1900	Conclude tests for day
2000	Transfer data files to CD or DVD and review plans for following day

F. WEATHER, BIRD, AND RADAR DATA SHEET

A data sheet will be prepared by the Project Engineer with the assistance of the biologist and other team members to provide the information noted in table 6. Weather information will be obtained from the airport operations center or other appropriate airport organization.

G. DATA RECORDING AND ANALYSIS

Radar data will be recorded on the hard drive of the radar signal processor computer and transferred to a DVD, CD-ROM, or an external hard drive at the end of each test period or each day, depending on the size of the data files and the storage capacity of the hard drive on which the data is stored during the data acquisition periods. Data acquisition times should be kept to a maximum of 5 to 10 minutes to keep the stored data files to a manageable size for later analysis.

H. SECURITY FOR THE TEST SITE

Provisions will be made by airport personnel to secure the trailer, van, or truck and equipment from burglary and vandalism.

APPENDIX: EQUIPMENT AND FACILITIES PROVIDED BY AIR FORCE RESEARCH LABORATORY





HONDA
One Word Says It All!

CompanyInfo
Lawn&Garden
Generators&Pumps
Snowblowers
DealerLocator
Brochure
Accessories
Owner'sManuals
SiteMap
Contact




Generators

Hand Held
EU1000
EU2000

Economy
EN2500
EG2500
EG3500
EG5000

Deluxe
EB3000
EM3500
EM5000
EX5500
EM6000
ES6500
EB12D

Super Quiet Inverter
EU1000
EU2000
EU3000

AVR
EX4500
EX5500
EB12D

Industrial/Commercial
EB3000
EB3500
EG3500
EB5000
EG5000
EB6500

Generators Choosing a Generator Compare Generators Wattage Calculator Convert to Home Use Generator Safety Generator Operation	Generator Models Hand Held Economy Deluxe Super Quiet Industrial/Commercial RV	Water Pumps Choosing a Pump Compare Pumps Storage/Priming Tips Pump Terminology Pump Theory/Design Troubleshooting Guide	Water Pump Mode General Purpose Construction Submersible
---	---	---	--

<p>Super Quiet Generator EU3000</p>  <p style="text-align: center;">Click on image to zoom</p>	<table border="1" style="width: 100%; border-collapse: collapse;"> <tr> <th colspan="2" style="text-align: left;">Specifications</th> </tr> <tr> <td style="width: 25%;">Engine</td> <td>6.5 HP, Single Cylinder, Overhead Valve, Air Cooled</td> </tr> <tr> <td>Displacement</td> <td>196 cc</td> </tr> <tr> <td>AC Output</td> <td>120V 3000W max.(25A) 2800W rated (23.3A)</td> </tr> <tr> <td rowspan="2">Receptacles</td> <td>20A 125V Duplex NEMA Plug Number: 5-20P</td> </tr> <tr> <td>30A 125V Locking Plug NEMA Plug Number: L5-30P</td> </tr> <tr> <td>DC Output</td> <td>12V, 144W (12A)</td> </tr> <tr> <td>Starting System</td> <td>Recoil, Electric</td> </tr> <tr> <td>Fuel Tank Capacity</td> <td>3.4 gallons</td> </tr> <tr> <td>Run Time on One Tankful</td> <td>7.2 hrs. @ rated load 20 hrs. @ 1/4 load</td> </tr> <tr> <td>Dimensions (L x W x H)</td> <td>25.8" x 18.9" x 22.4"</td> </tr> <tr> <td>Noise Level</td> <td>58 dB @ rated load 49 dB @ 1/4 load</td> </tr> <tr> <td>Dry Weight</td> <td>134 lbs.</td> </tr> </table>	Specifications		Engine	6.5 HP, Single Cylinder, Overhead Valve, Air Cooled	Displacement	196 cc	AC Output	120V 3000W max.(25A) 2800W rated (23.3A)	Receptacles	20A 125V Duplex NEMA Plug Number: 5-20P	30A 125V Locking Plug NEMA Plug Number: L5-30P	DC Output	12V, 144W (12A)	Starting System	Recoil, Electric	Fuel Tank Capacity	3.4 gallons	Run Time on One Tankful	7.2 hrs. @ rated load 20 hrs. @ 1/4 load	Dimensions (L x W x H)	25.8" x 18.9" x 22.4"	Noise Level	58 dB @ rated load 49 dB @ 1/4 load	Dry Weight	134 lbs.
Specifications																										
Engine	6.5 HP, Single Cylinder, Overhead Valve, Air Cooled																									
Displacement	196 cc																									
AC Output	120V 3000W max.(25A) 2800W rated (23.3A)																									
Receptacles	20A 125V Duplex NEMA Plug Number: 5-20P																									
	30A 125V Locking Plug NEMA Plug Number: L5-30P																									
DC Output	12V, 144W (12A)																									
Starting System	Recoil, Electric																									
Fuel Tank Capacity	3.4 gallons																									
Run Time on One Tankful	7.2 hrs. @ rated load 20 hrs. @ 1/4 load																									
Dimensions (L x W x H)	25.8" x 18.9" x 22.4"																									
Noise Level	58 dB @ rated load 49 dB @ 1/4 load																									
Dry Weight	134 lbs.																									
<p>Features & Benefits</p> <ul style="list-style-type: none"> Honda Overhead Valve Engine Lightweight and Compact High Quality, Stable and High Power Output Quiet Operation Low Fuel Consumption Parallel Operation Capability Oil Alert[®] Electronic Ignition Simultaneous AC/DC use Electronic Circuit Breakers Fuel Meter Inverter (Computer Friendly) USDA-Qualified Spark Arrestor/Muffler Fully Enclosed for Quieter Operation EcoThrottle™ (load dependent operation) Battery Standard 2 Year Residential Warranty 1 Year Commercial Warranty 																										
<p>Options</p>																										

FIGURE A.1. PORTABLE ELECTRICAL GENERATOR SPECIFICATIONS.



FIGURE A.2. TEST TRAILER.

GPR Trailer

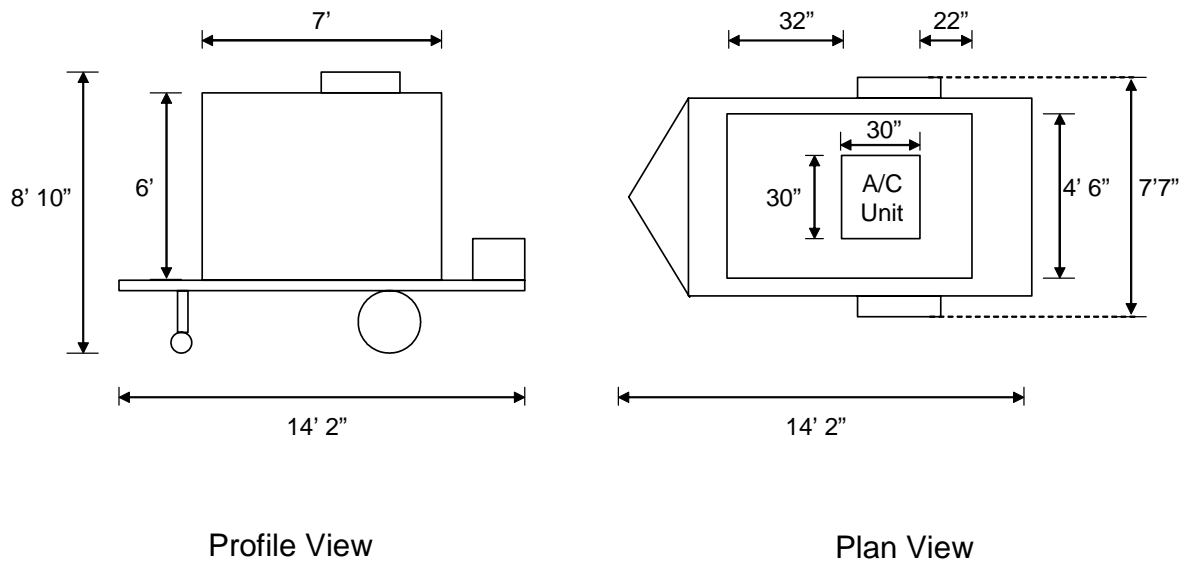


FIGURE A.3. TRAILER DIMENSIONS.



FIGURE A.4. SPHERICAL RADAR CALIBRATION TARGET SUSPENDED FROM BALLOON.

TABLE A.1. RADAR CROSS SECTIONS OF AF RESEARCH LABORATORY SPHERICAL CALIBRATION TARGETS

Diameter of spherical target	Radar Cross Section (m²)	Radar Cross Section (dBsm)
1 meter	0.785	-1.05
14 inches	0.099	-10.03
4.75 inches	0.011	-19.42

**APPENDIX B: PROTOCOL FOR FIELD TESTING OF THE 94 GHZ BIRD
DETECTION RADAR AT THE DFW AIRPORT**

TEA - Agreement Number F30602-02-2-0119

WWW.WAVEBAND



August 13, 2004

A. TEST DATES

Tests will be conducted for a period of two weeks. Start date is August 30, 2004.

B. TEST OBJECTIVES

The objectives of the tests at DFW Airport are to:

- iv. Ensure that the radar can detect and track bird targets at distances commensurate with those needed for bird detection at airports and airfields,
- v. Display their movement on the monitor, and
- vi. Display the bird targets on a computer containing a GIS.

This test will also be used as a bird radar demonstration for interested government personnel.

C. PREPARATION AND PRE-TESTS VERIFICATION

1. Preparation

Radar and data recording equipment will be installed into the trailer provided by the University of Illinois. The trailer provides a 7' x 16' enclosed workspace. Access to the trailer workspace is through a door on the starboard side; double swing doors provide access to the rear of the trailer where the radar is mounted. A 3,000W generator provides the primary power through a 20 amp service in the trailer through which lights and internal and external electrical outlets function. The rear door of the trailer has an auxiliary transparent plastic window. The plastic is of two types. One side of the plastic window is ½-in plexiglass to facilitate visual observation of birds using cameras. The other side is 1/8-in polycarbonate selected to be transparent to energy transmitted by the radar. An awning has been mounted over the rear of the trailer to minimize solar heating in the trailer. Equipment racks, desk, and bench space are provided in the trailer. An 11,000 BTU air conditioner unit provides cooling. The trailer serves multiple functions: protect the radar control and data recording equipment and personnel from inclement weather, serve as a platform on which to mount the radar and its protective enclosure, and provide an interface to field generated or commercial power for operating the equipment.

The radar system operates from the 115 VAC power source. In addition to the radar antennas, transmitter, and receiver, the radar system contains a computer to control the radar parameters and provide data acquisition and data processing; a power distribution module; video camera and S-VHS video recorder; azimuth position rotator and control; and compass and inclinometer measuring devices.

The radar is mounted in the trailer on the equipment racks. Jacks provide trailer stability, which level and stabilize the trailer for radar operation. A three axis adjustment on the equipment racks provides fine adjustment of radar orientation. The racks will accommodate the radar with the long dimension of the antenna in either the vertical or horizontal direction.

The video camera is boresighted with the radar antenna. Its horizontal field of view has been adjusted to correspond to the radar scan angle of 30 degrees. The radar antenna elevation beamwidth of either ± 2.5 degrees or ± 1.25 degrees has been marked on the monitor to facilitate correlation between radar imagery and the field of view captured by the video camera.

Test support equipment includes radio communication devices, tools, personal conveniences, and a distance measurement device to provide accurate distance measurement to 3,500 m with an error of less than 1 cm and accurate angle measurement for elevation determination.

2. Pretests and Verification

A number of pretests will be conducted prior to the radar system and trailer leaving California for DFW. The pretests will ensure that the radar and all associated equipment are functioning properly. These tests will be conducted at sites selected by WaveBand. Testing will consist of:

- a. Calibration tests – calibration tests will be conducted with aluminum spheres and trihedral retroreflectors of known radar cross section (RCS).
- b. Bird detection and verification tests – after integration of the radar and display equipment into the trailer, bird detection tests will be conducted at one or more sites. Additional verification tests will be conducted using model airplanes flown at various speeds and distances from the radar.

Calibration Tests

Calibration tests will follow the protocol below:

1. The trailer with mounted radar will be moved to the site selected for gathering radar calibration data. The trailer will be leveled and stabilized, generator set up, and power and voltage levels verified.
2. The radar detection area (i.e., field of view) will be verified. This will involve placement of trihedral retroreflectors in the expected field of view of the radar at a minimum distance of 500 feet from the radar. The retroreflectors will be left in place for the test sequence to provide reference locations to alert the operators to any change in orientation of the radar or trailer during the test.
3. The first set of calibration tests will use trihedral retroreflectors with 107 m^2 and 658 m^2 RCS. The retroreflectors will be placed at varying distances and elevations from the radar. Distance to the retroreflectors will be marked with a visible cone, numbered to be consistent with calibration measurements. Pertinent parameters from the radar setup screen will be noted on the data sheet before starting the data acquisition run. Following radar calibration, the distance to each measurement point will be verified using the total station. Cones will also be placed under retroreflectors used for elevation measurement

testing. Elevation will be determined by establishing an angle from the radar to the target. Elevation will be calculated using the measured distance.

4. The second set of calibration tests will use aluminum spheres with 0.01 m^2 and 0.1 m^2 RCS. They will be attached and flown from a kite controlled from a moving vehicle driving away from the radar at slow speed. The speed will be sufficient to keep the kite with attached sphere airborne. Data will be recorded as the vehicle increases the distance from the radar from 500 feet to 2 miles or further or until a signal is no longer received by the radar. Pertinent parameters from the radar setup screen will be noted on the data sheet before starting the data acquisition run.
5. All data from the test will be verified using the radar post-processor software while the calibration targets are still setup and one electronic backup copy of the data will be made when the test sequence is completed.

Bird Detection Verification Tests

A series of tests will be conducted to verify and evaluate the capability of the radar to detect and recognize moving and stationary bird targets. This testing will follow the protocol below:

1. The trailer will be moved to the test site and Steps #1 – #3 of the Calibration Test Protocol will be repeated.
2. Bird detection verification tests will be opportunistic, using the radar to detect birds within the range of the radar. In these tests, the recommended personnel will include two members capable of bird identification. One identification specialist should be in the trailer, assisting radar test personnel; the second identification specialist should be down range, placed to facilitate the observation and identification of birds at long distances from the radar. As in the calibration tests, full observations will include marking of target distance from the radar and determination of target elevation. Data recording protocols should include a time stamp on both radar data files and video records. Communication between the radar location and downrange will be by radio communication. In the verification tests, data from at least 10 small, 10 medium, and 10 large birds should be obtained (assuming the opportunistic bird detection conditions allow). Because detection verification tests will be opportunistic, verification testing may require multiple deployments of the radar at different locations.
3. Following all testing a final verification will be made following Steps #1 – #3 of the Calibration Test Protocol.
4. All data from the test will be verified using the radar post-processor software while the calibration targets are still setup and one electronic backup copy of the data will be made when the test sequence is completed.

D. DFW AIRPORT TEST LOCATIONS

A number of test sites have been identified as shown in table 1. Priorities and bird types have been established by airport personnel and the FAA Center of Excellence. Site selection will be based on visual observations at the time of testing. Detailed test site maps are shown in Appendix One. Modeled radar angular field of views are shown in Appendix Two. Preliminary radar test locations are shown in figure 1.

TABLE 1. DFW TEST IDENTIFICATION.

Site #	Radar Azimuth	Priority	Bird Type	Comment
1	355 degrees	1	Blackbirds	
2	355 degrees	3	Blackbirds, Starlings & Hawks	
3	175 degrees	2	Hawks & Pigeons	
4				Not Used
5	355 degrees	6	Blackbirds, Starlings & Hawks	
6	175 degrees	4	Egrets & Hawks	
7	310 degrees	5	Egrets & Seagulls	Subject to Approval
8	175 degrees	7	Blackbirds & Hawks	Subject to Approval

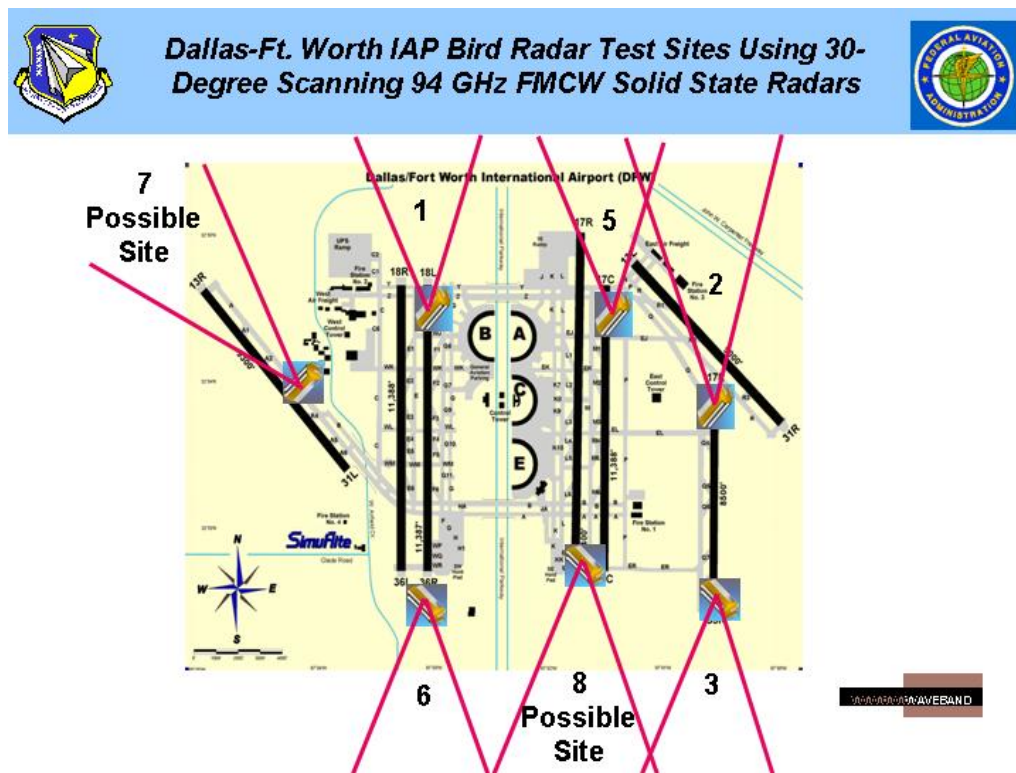


FIGURE 1. PRELIMINARY RADAR TEST LOCATIONS.

E. DAILY ACTIVITIES SCHEDULE

On the first day of the testing, WaveBand and FAA COE personnel will meet with airport officials to discuss and review testing activities.

Please meet at 7:30 AM at the following airport location:

A typical schedule of daily activities is as follows:

Time	Event
0445	Meet at main gate or airport official's building for escort
0545	Begin data acquisition at selected Test Site
1000	Break for brunch and data analysis
1530	Return to site and continue data acquisition into twilight and evening hours
2100	Conclude tests for day
2200	Transfer data files to CD or DVD and review plans for following day

F. TEST PROCEDURES

1. Overall

The primary objective of the DFW testing is to evaluate the radar in an airport operational environment and determine utility in recognizing hazards created by birds and other wildlife. (If this is indeed true, then radar calibration tests pursey may not be needed or are secondary to the primary purpose of the tests.) Testing of the radar will occur at multiple sites over time periods appropriate to bird activity. In this protocol, a test is a single objective evaluation conducted to provide the needed data for radar evaluation. With this definition, multiple tests can be performed on any day and it is expected that multiple daily tests will be conducted during the evaluation period.

Based on present planning, at least two tests will be conducted at the dawn or dusk period, and two tests during periods of high level aircraft utilization. Other testing will be conducted to determine the effect of topographic shadowing, optimum location to detect greatest hazards to aircraft movement, and additional calibration and detection/recognition of bird targets. Each test will have a stated specific objective (Stating this objective should be included in the protocol detailed below).

This protocol for DFW testing recognizes:

- Location selection will be made based on test objectives.
- Detection of bird targets will be opportunistic, depending on the natural movement of birds on and around the AOA.

Each test will adhere to the following protocol:

1. The trailer with mounted radar will be moved to the site selected for the test. The trailer will be leveled and stabilized, generator set up and power and voltage levels verified. A WAAS enabled GPS measurement will be made to establish the location of the trailer. This measurement will be made at the hitch of the trailer. Location will be verified by reference to maps or the DFW GIS. In addition to location, the orientation/bearing of the trailer axis will be recorded.
2. The radar detection area will be verified for that location. This verification will involve placement of retroreflectors in the expected radar field of view at a minimum distance of 500 feet from the radar. All distance measurements will be verified with retroreflectors, which will be left in place for the test session to provide reference locations to detect any change in orientation of the radar or trailer during the test. Other measurements that give the radar orientation are the azimuth, compass, and pitch values that can be recorded from the rotator on which the radar is mounted (when it scans in the horizontal direction) and the instruments mounted on the radar.
3. Radar testing will include target calibration and opportunistic bird detection. In these tests, the optimum personnel team will utilize two members for radar operation and two to three members for bird identification. One radar operation team member will operate the radar and the other will coordinate with target and downrange personnel. The bird identification team will include one identification specialist in the trailer, assisting radar test personnel and one or two identification specialists at downrange locations to facilitate the observation and identification of birds at long distances from the radar. As in the calibration tests, data and information recording will include marking of target distance from the radar and determination of target elevation. Detection protocols will include a time stamp on both radar data files and video records. Communication between radar location and downrange personnel will be by radio. Any needed escorts and radio frequency allocations will be provided by DFW personnel.
4. Following all testing at a site, a final calibration will be made before trailer movement using the trihedral retroreflectors. In this calibration a 100 square meter retroreflector will be placed at a known distance in excess of 500 feet from the radar and the radar return signal will be recorded.
5. All data acquired during the test will be verified using the radar post-processor software and multiple electronic copies of the data will be created as described in Section 4b.

2. Verification of Proper Radar Operation

A means of independently determining proper functioning of the radar before and after test sessions and the accurate measuring of the distance to the birds is required. Establishing proper radar operation for each test will consist of placing retroreflectors at a fixed distance from the radar and measuring the return signal from these reflectors. Measuring the distance to birds can be accomplished by identifying known land or water masses on which or above which the birds are located and using existing GIS resources or reference to maps or other documents that have the appropriate distances noted. When possible, markers will be placed at points of bird

observations and measurements will be made to those markers from the radar. Airport maps and other documents showing distances to bird locations and other prominent features will be used. Once a sufficient number of independent measurements of distance to targets are made, a radar coverage map will be developed based on landmarks or identified targets and the distance as measured by the radar may be substituted for the distance measured by the independent measuring device.

3. Radar Field of View

The field of view of the radar will be determined for each test location and verified at the beginning and the end of each test session. Radar corner reflectors will be the primary means of marking field of view, although it is also possible to use vehicles, landscape features, or other means to verify that the radar is detecting known objects in the far field of the antenna. If possible, cones will be used to mark the limits of the radar field of view.

4. Data Acquisition

- Overall
Data sheets will be prepared by the Project Engineer with the assistance of the biologist and other team members to provide the information noted in Appendix Three. For each test, a brief narrative will be prepared to describe the test objective, test location, general test conditions, and all records of test protocol calibration and verification measurements. Data sheets will also contain the names and location of all computer files generated during the test.
- Radar data
During each test, efforts will be made to minimize the length of files. An initial recommendation is made to limit individual test times to approximately 10 to 15 minutes, after which files will be written to a data storage device. Backup copies of all data will be made either during the data acquisition period or after a test session is completed. Before the start of each data acquisition run or test, a file name for the test data will be created with the following format: number of the test site, 2-digit hour representing the start time of the test, and 2-digit minute corresponding to the start time of the test. For example, the file name S10545 represents data collected at Test site 1 beginning a 5:45 AM. All data files for a particular test session (i.e., Site 1, September 2 AM) will be stored in a folder containing the test date, site number, and AM or PM designation. At the end of each test, a digital file will be created that contains a catalogue of test or run files with a brief description of the contents of each file. This catalogue file, with test data, will be written to an archive DVD or DVD set, which will become a part of the permanent record for each test.
- Video and Audio Recording
Video and audio recordings made during each test will be digitized and files will be transferred to the archive DVD.

- **Observation Records**

The test data sheet will also provide a summary of all other observations made during the test. Observation records will be made on a standardized form used by all observers. This form will contain the name of the observer, the observer's location in relation to the radar, and any observations made during the test. All observations will be time stamped with time measurement synchronized with radar time stamps. It is expected that independent records of bird movement will be maintained by each observer. The objective of these observations is to establish species and movement paths of all birds in the radar field of view. These forms will also provide a record of all calibration measurements made downrange. The information on the forms will be entered into an Excel spreadsheet by the person who entered the information on the paper form.

In addition to records of visual observations, downrange observers will be in radio contact with radar test personnel to provide real-time observation data that will be used to verify radar detection capability. Observers will provide information species, number, direction of travel, distance from radar, and time interval for moving birds. These observations will be recorded in and become part of the permanent record of each test.

5. Radar Data Transfer, Data Integration, Data Display

All test data will be recorded, initially to high capacity portable digital storage drives, and then DVDs. All processed data will also be stored with processed data files named with a convention that will refer to individual tests. It is expected that radar test data will be processed by Center of Excellence personnel, with the assistance of WaveBand, and displayed with a spatial resolution appropriate to the radar field of view. Test data will also be processed for use in the DFW GIS developed by the Center of Excellence.

For users, Data Display is a critical end-product component of the system. Expected visitors during testing will be shown the overall system, but the user-friendliness of the data display will be key to future uses and applications of the system.

RESOURCES NEEDED

LOGISTICS AND PERSONNEL				
ITEM	Needed From	POC	Duration	Comment
Test trailer placement	DFW Support WaveBand COE	Jim Hewitt Robert Mino	At test initial test location and all subsequent locations.	General sequence of testing should be established prior to initial testing to provide lead time for any specific preparations needed for tests.
Escort to test site	DFW support	Jim Hewitt	Beginning and end of daily tests	Can be performed by an airport biologist who can also assist in the identification of bird species.
Radar calibration on-site	Test team DFW support	Robert Mino Jim Hewitt	At each test site	Need to position corner reflectors in far field of radar and verify proper radar operation
Bird Identification	DFW Support Local Ornithologists	Jim Hewitt Ed Herricks	All tests	
FAA Approval	FAA-Regional Office	Rick Compton Cell #	Fall of 2004	At the minimum test sites 1 thru 6, and possibly 7 and 8

USEFUL NUMBERS –

Paul Antonik (U.S. Air Force)	Work	315-330-7057	Cell
Rick Compton (FAA DFW)	Work	817-222-5608	Cell
Jon Fisher (U of Illinois)	Work	217-244-1109	Cell (217) 649-0778
James Hewitt (DFW Airport)	Work	(972) 574-8736	Cell (214) 277-3861
Edwin Herricks (U of Illinois)	Work	217-333-0997	Cell (217) 840-5348
Michel Hovan (FAA)	Work	609-485-5552	Cell (609) 505-2093
Larry Klein (Waveband Co.)	Work	949-253-4019, Ext 106	Cell (714) 356-2275
Robert Mino (Waveband)	Work	949-253-4019, Ext 110	Cell (310) 795-4496

MATERIALS AND OTHER ITEMS				
ITEM	Needed From	POC	Duration	Comment
Video recording	WaveBand U.S. Air Force	Larry Klein Paul Antonik	When birds are present	
Distance Measurement	COE WaveBand	Jon Fisher Larry Klein	For each test site	Total station
Method to determine the Field of View at test sites	WaveBand	Larry Klein	For each new positioning of the radar antenna	<ul style="list-style-type: none"> • Traffic cones • Corner reflectors • Vehicle permitted on perimeter road
Radios	COE and DFW	Jon Fisher Jim Hewitt	Needed during each test	Frequency allocation and range
Maps	COE and DFW	Jon Fisher Jim Hewitt	Provided prior to testing	
Field data sheets	WaveBand and COE	Ed Herricks Larry Klein	Developed prior to testing and available for all tests	

DETAILED TEST SITE LOCATIONS – From DFW maps

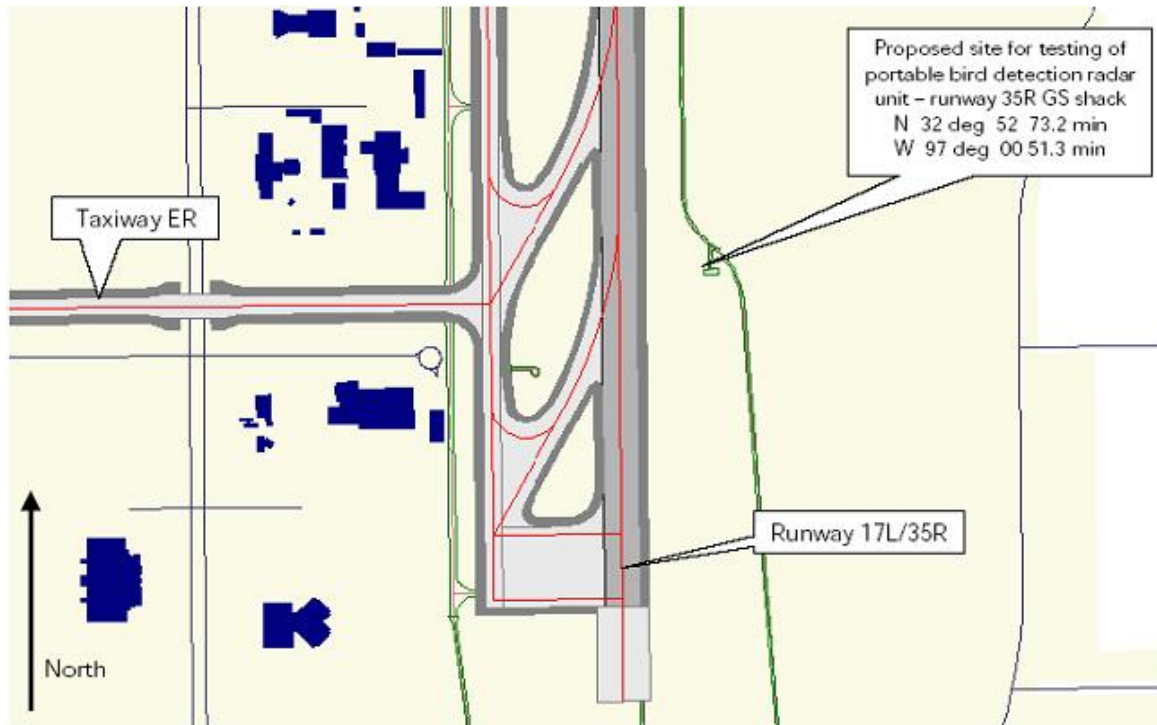
Site 1.



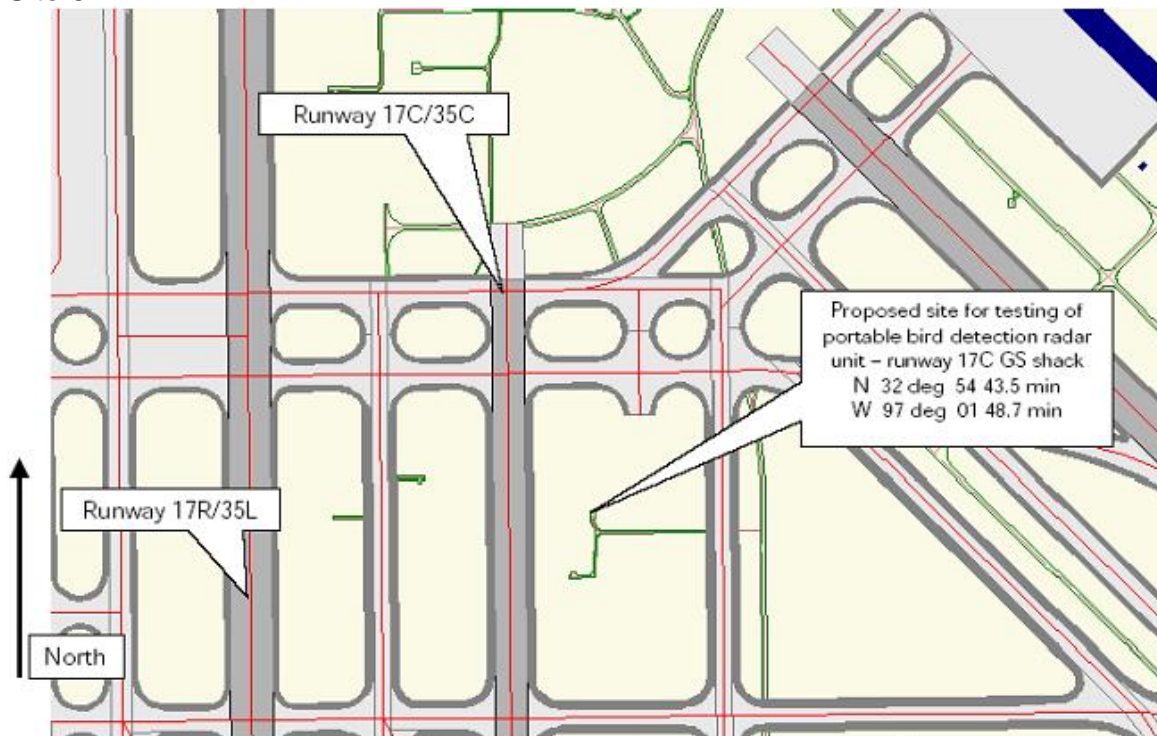
Site 2.



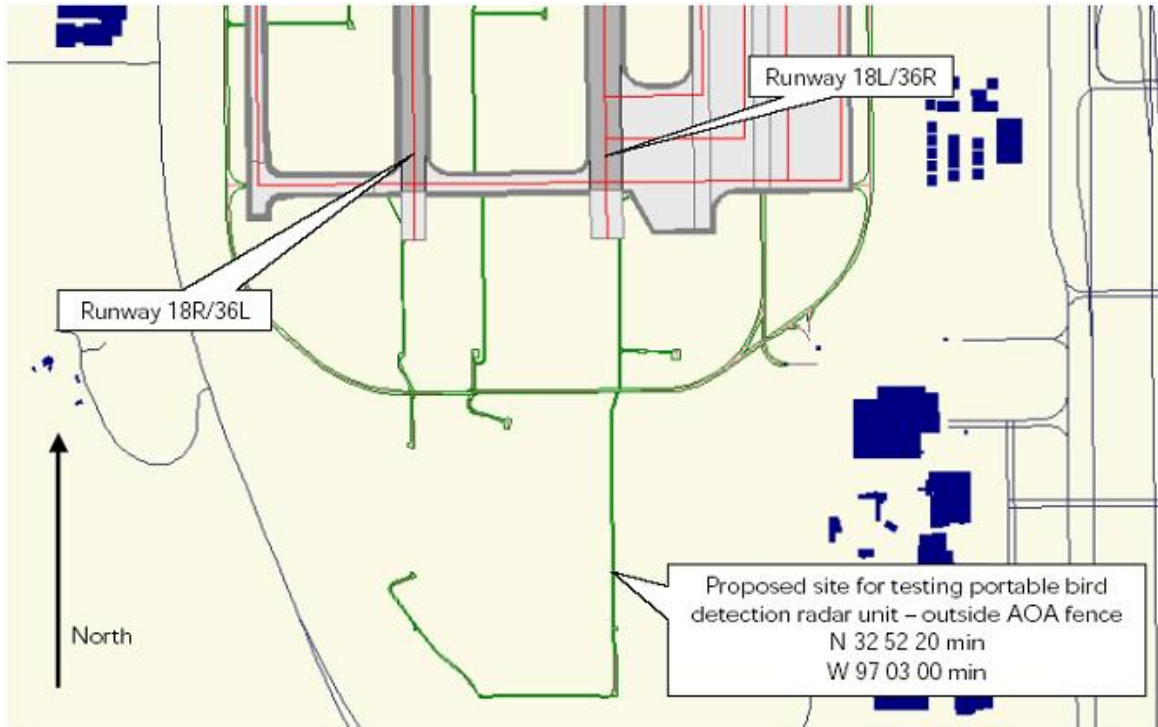
Site 3.



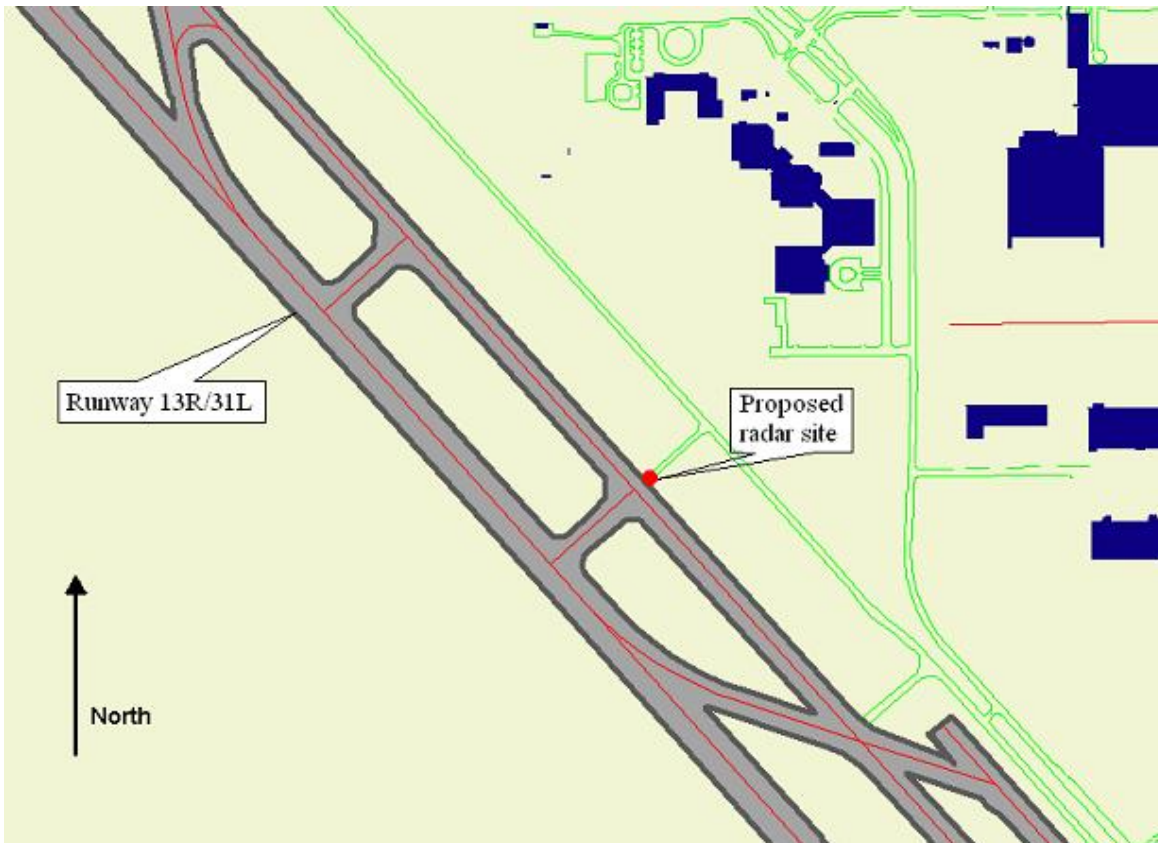
Site 5.



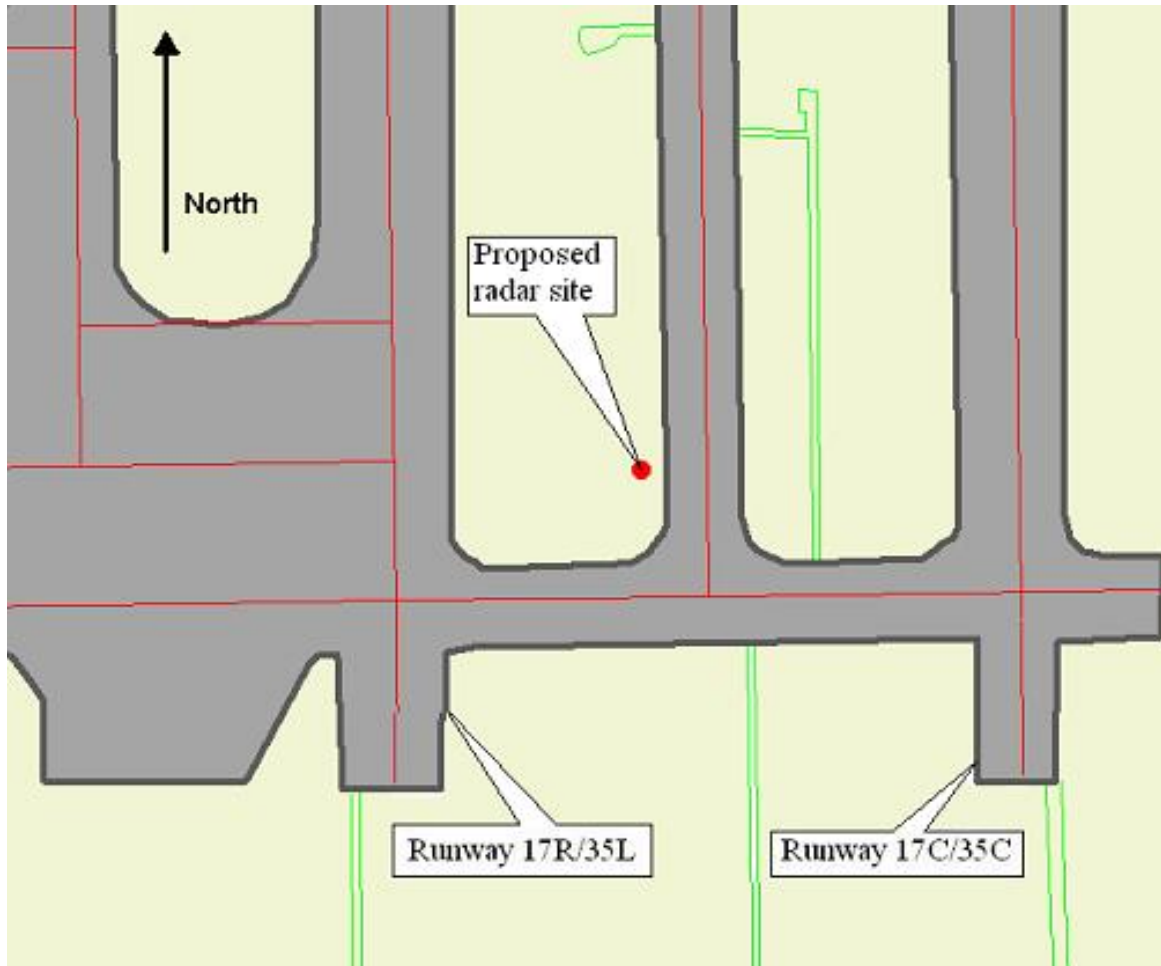
Site 6. <WE SHOULD UPDATE THE LOCATION MAP FOR SITE 6 ONCE WE CLARIFY EXACTLY WHERE IT SHOULD BE>



Site 7.

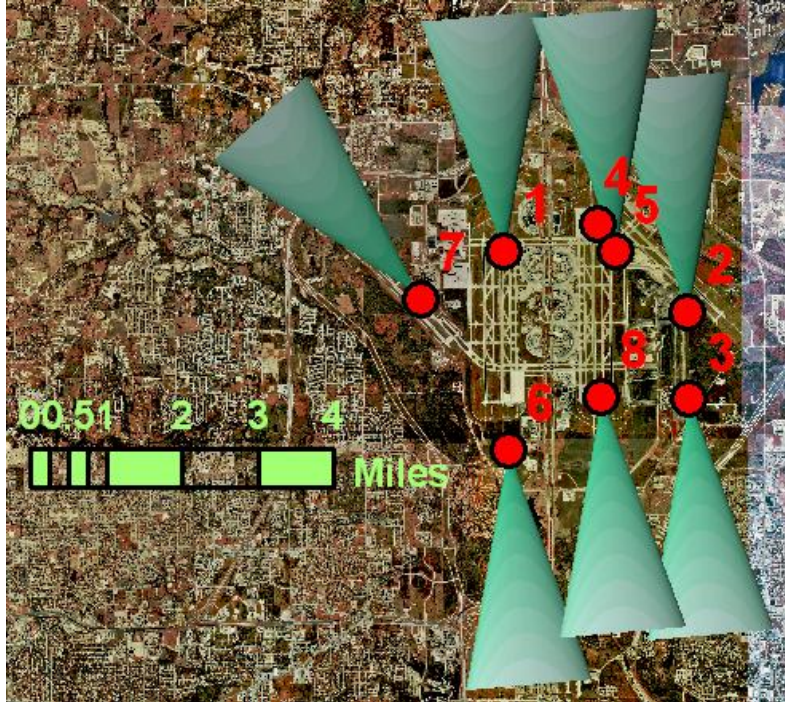


Site 8.



Radar angular field of views

Radar Coverage for Horizontal Orientation.



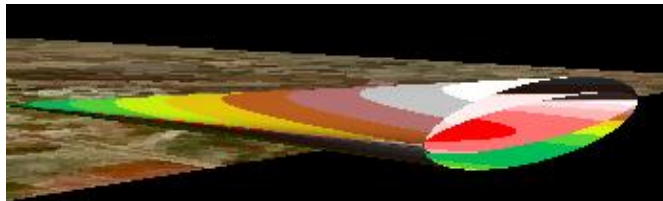
Radar Coverage for Vertical Orientation, 5 degree beamwidth.



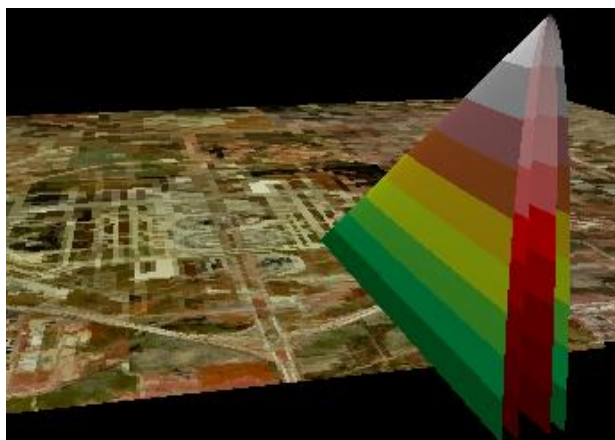
Radar Coverage for Vertical Orientation, 2.5 degree beamwidth.



3D View of Radar Coverage from Site 1: Horizontal Orientation. 2.5 degree cone is shown within 5 degree cone.



3D View of Radar Coverage from Site 1: Vertical Orientation. 2.5 degree cone is shown within 5 degree cone.



RADAR DESCRIPTION

TABLE 2. 94 GHZ MMW BIRD DETECTION RADAR SPECIFICATIONS (NOMINAL).

Parameter	Value
Operating frequency	94.3 GHz \pm 0.5 GHz
RF modulation bandwidth	65 MHz
Range resolution	2.3 meters (7.6 feet)
Azimuth beamwidth (when large antenna dimension is horizontal)	0.5 deg
Elevation beamwidth	5 deg or 2.5 deg
Antenna gain	36 dB
Antenna polarization	Vertical (when large antenna dimension is horizontal)
Azimuth scan range (Frame)	30 deg (–30 to 0)
Azimuth scan time function	Linear true continuous
Azimuth scan speed	4 frames per second
Elevation adjustment range	30 deg
Weight (antenna & T/R module)	30 lb
Transmitter output power	575 mW CW
IF bandwidth	0.5 MHz (3 dB)
Noise figure	6 dB max (SSB)
Dynamic signal range	82 dB until A/D converter saturates
Angles/Frame	90
Range samples/Azimuth resolution angle	4,096 range cells/0.5-deg angle at 1 MHz sampling rate
FFT size	4,096 points (33 dB processing gain)